2015

Impacts of the Three-Dimensional Oceanic Thermal Structure and Translation Speed on Tropical Cyclogenesis and Intensity Fluctuations during the 2005 North Atlantic Hurricane Season

Jordan Vick Pino
Louisiana State University and Agricultural and Mechanical College

IMPACTS OF THE THREE-DIMENSIONAL OCEANIC THERMAL STRUCTURE AND TRANSLATION SPEED ON TROPICAL CYCLOGENESIS AND INTENSITY FLUCTUATIONS DURING THE 2005 NORTH ATLANTIC HURRICANE SEASON

A Thesis

Submitted to the Graduate Faculty of the
Louisiana State University and
Agricultural and Mechanical College
in partial fulfillment of the
requirements for the degree of
Master of Science

in

The Department of Geography and Anthropology

by
Jordan Vick Pino
B.S., Louisiana State University, 2013
December 2015

ACKNOWLEDGMENTS

I must thank several people who contributed to the successful completion of this thesis. First, I would like to acknowledge my co-advisor, Dr. Robert Rohli, who provided me with unending support throughout my undergraduate and graduate careers at Louisiana State University. His dedication and attention to detail have inspired me to become a better graduate student and researcher. Dr. Nan Walker, also my co-advisor, had a large impact on the researcher I have become today. She provided me with a position at the Earth Scan Laboratory back when I was an undergraduate student and, over the course of our time working together, became a great mentor and friend. Without my time at the lab, I would have not gained the knowledge needed to complete this thesis. Dr. Jill Trepanier also has my thanks for all her great advice and myriad of information about hurricanes and the R programming language. Her friendly attitude and easy-going personality made the writing of this thesis a less difficult task.

Mr. Chet Pilley, my supervisor while at the Earth Scan Laboratory, was also instrumental along the way. His patience and helpfulness with data visualization, analysis, and computer programming made this thesis feasible. I cannot thank him enough. Also, I would be remiss if I did not thank Mr. Alaric Haag for his willingness to offer advice on computer programming without hesitation, and Mr. Ambrose Bordelon for his support and helpfulness during my undergraduate and graduate time at the lab.

Special thanks are due to Dr. Gustavo Goni for graciously providing the dataset utilized in this thesis and to Mr. Ricardo Domingues for preparing the dataset and promptly answering my email inquiries. Last, but certainly not least, I would like to acknowledge my family and friends who have offered me more support than I could have ever imagined. Thank you all very much.

TABLE OF CONTENTS

LIST OF TABLES

LIST OF FIGURES

LIST OF ABBREVIATIONS

AOML	Atlantic Oceanographic and Meteorological Laboratory
AVISO	Archiving, Validation, and Interpretation of Satellite Oceanographic Data
CCEs	Cold-core eddies
D26	Depth of the 26°C isotherm (m)
ETOPO1	1 arc-minute global relief model
EX	Extratropical cyclone
GMT	Generic Mapping Tools
H1	Saffir-Simpson scale category 1 hurricane (*i.e.*, $U_{10} \geq 33$ m s^{-1})
H2	Saffir-Simpson scale category 2 hurricane (*i.e.*, $U_{10} \geq 43$ m s^{-1})
H3	Saffir-Simpson scale category 3 hurricane (*i.e.*, $U_{10} \geq 50$ m s^{-1})
H4	Saffir-Simpson scale category 4 hurricane (*i.e.*, $U_{10} \geq 58$ m s^{-1})
H5	Saffir-Simpson scale category 5 hurricane (*i.e.*, $U_{10} \geq 70$ m s^{-1})
HPP	Hurricane Heat Potential
HURDAT	HURricane DATabase
LO	Low-pressure
NGDC	National Geophysical Data Center
NHC	National Hurricane Center
numpy	numerical python
RMS	Radius of maximum winds
SSTs	Sea surface temperatures (°C)
TD	Saffir-Simpson scale tropical depression (*i.e.*, $U_{10} \leq 17$ m s^{-1})
TCHP	Tropical cyclone heat potential

U_{10}	Wind speed (m s^{-1}; 10 m above surface)
U_h	Translation speed (m s^{-1})
WCEs	Warm-core eddies

ABSTRACT

Tropical cyclones are some of the most devastating natural phenomena on the planet. While it has long been recognized that sea surface temperature is an important factor in the evolution of tropical cyclones, it is limited due to its two-dimensional nature. This research seeks to investigate the role of the three-dimensional oceanic thermal structure and translation speed (U_h) on the cyclogenesis and intensity fluctuations of these powerful storm systems. This investigation utilized two main data sets: (1) depth of the 26°C isotherm (D26) which indicates the depth (or volume) of the warm water layer, and (2) hourly-interpolated wind speed (U_{10}) and translation speed (U_h). These two data sets were used to complete an along-track analysis of 23 named tropical systems during the 2005 North Atlantic basin hurricane season. A more detailed analysis of five of the season's major storms ($U_{10} \geq 50$ m s^{-1}; Dennis, Emily, Katrina, Rita, and Wilma) was undertaken to determine whether D26 and U_h for these major storms played a role in their attainment of major status.

Results suggest that the condition of the underlying three-dimensional oceanic thermal structure played a role in the cyclogenesis and intensity fluctuations. U_h was also found to be a likely factor in the intensification and weakening processes by affecting the amount of time a storm spent over the ocean. Oceanic mesoscale features such as warm- and cold-core eddies, coupled with U_h, are likely to influence storm intensity by providing either abundant or insufficient oceanic heat content. Specifically, warm-core eddies were found to be especially important for the rapid intensification of major storms. These storms were found to pass either in close proximity or directly over these eddies, triggering intensification. The minimum D26 value for tropical storm cyclogenesis was found to be 23.5 m, and for hurricanes (category 1) it was 36.8 m. The surface area of the North Atlantic basin over which these minimum thicknesses of

the surface warm layer occur was found to expand and then contract over the season (1 June – 30 November), reaching a peak in August and September. Linear regression models suggest that major storms, most notably category 5, appear to be influenced more by along-track D26 and U_h than weaker storms.

CHAPTER 1: INTRODUCTION

1.1 Background

Tropical cyclones are some of the most powerful and destructive storm systems on the planet. These storms can inflict substantial damages to life and property, as seen during the 2005 North Atlantic basin hurricane season, which caused over USD $100 billion in damages and over 1,700 deaths (Beven *et al*., 2008). Tropical cyclones are defined as closed, warm-cored atmospheric circulation systems that form and obtain energy over the ocean's warmest waters via enthalpy fluxes (Emanuel, 1986; 2003). They form in seven basins throughout the world, with each basin having its own predefined "season."

The formation or "cyclogenesis" of tropical cyclones requires a number of prerequisite conditions, some of which include: an initial atmospheric disturbance, weak vertical wind shear, abundant atmospheric moisture, and most importantly, sea surface temperatures (SSTs) of approximately 26° – 27°C (Palmén, 1948; Byers, 1974; Elsner and Kara, 1999). Tropical cyclones rarely form equatorward of 5° N or 5° S latitude, due to the relatively weak Coriolis effect near the equator (Emanuel, 2003). Once conditions are in place, cyclogenesis and further intensification can occur as the developing system travels over warm oceanic waters. However, they can and do weaken despite being over warm waters when atmospheric conditions are not ideal (Emanuel, 2003). Once these storms move onshore, they can cause strong winds, storm surge, tornadoes, and inland flooding. All of these hazards threaten life and property, thus highlighting the need for a more complete understanding of tropical cyclones.

It has been widely accepted that high SSTs (*i.e.*, waters $\geq$ 26°C) are a prerequisite for the formation and maintenance of tropical systems. However, perhaps of greater importance is the oceanic thermal structure during the system's lifespan. The skin temperature is only part of this thermal structure, as these warm oceanic waters must extend deep into the water column to

provide sufficient latent heat in the form of evaporated water to energize a major storm.

This research seeks to investigate the role of the three-dimensional oceanic thermal structure on the formation and intensification of tropical systems. The depth of the 26°C isotherm (D26), a proxy for oceanic heat content, is particularly valuable to understand as it relates to tropical cyclones, because its depth indexes the volume of water from which sufficient energy exists to promote the development of a tropical cyclone. In addition, the important impact of translation speed (U_h), or propagation speed, is also investigated in detail.

1.2 Research Questions

This research seeks to analyze the role of the three-dimensional oceanic thermal structure and U_h on the cyclogenesis and intensity fluctuations of tropical cyclones. It focuses on the 2005 North Atlantic basin hurricane season – the most active season of the 120 or more years of reliable instrumental record. Also, in an attempt to gain an understanding of the required D26 for the formation of tropical storms and hurricanes (category 1), a threshold value is found for both. A statistical analysis is performed using regression models to use along-track D26 and U_h to explain the variation in wind speed (U_{10}) of storms during the season. This research will investigate the following specific questions:

1.) What effect do along-track D26 and U_h have on U_{10} for storms during the 2005 North Atlantic basin hurricane season?

2.) What is the threshold D26 value (*i.e.*, the minimum depth of the warm near-surface layer) required for tropical cyclones to achieve tropical storm and hurricane status (category 1) in the 2005 North Atlantic basin hurricane season?

3.) How did the area of the ocean basins covered by D26 values exceeding these thresholds vary spatially and temporally throughout the course of the 2005 season (1 June – 30 November)?

4.) Can along-track D26 and U_h explain the variation in U_{10} of storms during the 2005 North Atlantic basin hurricane season using single/multiple linear regression models?

1.3 Study Area

This research focuses on the North Atlantic basin, which encompasses the Atlantic Ocean (Figure 1.1a), Caribbean Sea (Figure 1.1b), and the Gulf of Mexico (Figure 1.1c).

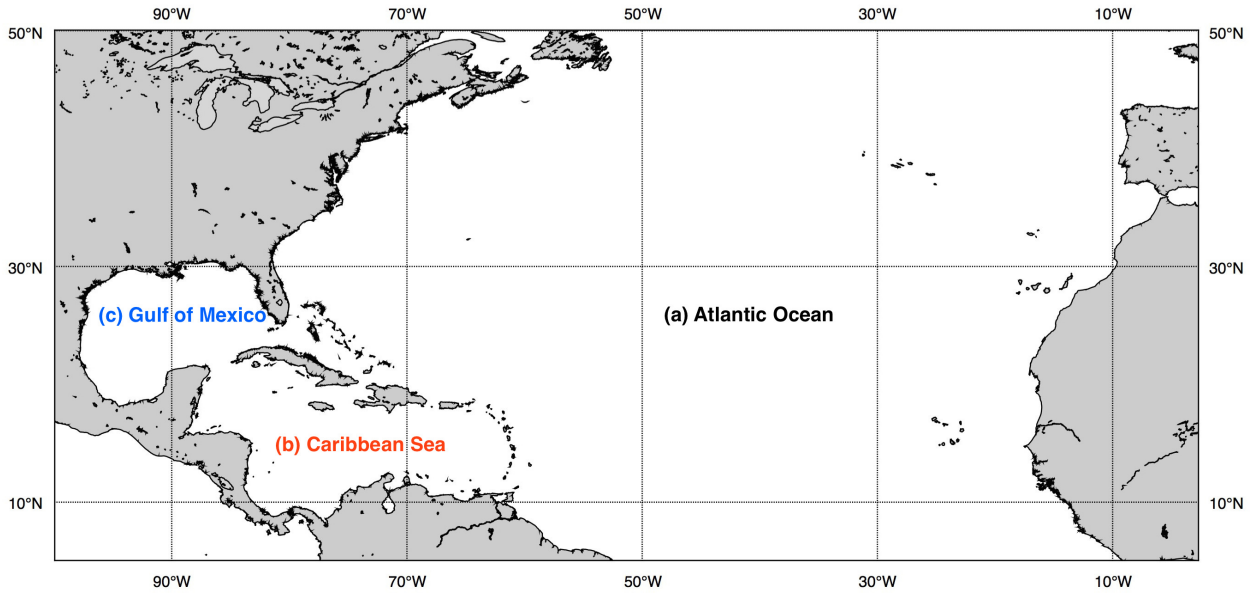

Figure 1.1: Map of study area with bodies of water labeled.

1.3.1 2005 North Atlantic Basin Hurricane Season

The 2005 North Atlantic basin hurricane season was the most active on record (Foltz and McPhaden, 2006; Lea and Saunders, 2006), with a total of 28 named systems (27 tropical and 1 subtropical). Of those systems 27 were tropical in nature, 15 achieved hurricane status (*i.e.*, $U_{10} \geq$ 33 m s^{-1}), 7 achieved major status (*i.e.*, $U_{10} \geq$ 50 m s^{-1}) and 3 reached category 5 status on the

Saffir-Simpson scale (*i.e.*, $U_{10} \geq 70$ m s^{-1}; Beven *et al*., 2008; Figure 1.2). This season also had the greatest number of major (category 3 +, $U_{10} \geq 50$ m s^{-1}) storms (Dennis, Katrina, Rita, and Wilma) to make landfall in the United States in one season (Lea and Saunders, 2006). In addition to being one of the most active seasons on record, the 2005 North Atlantic basin hurricane season was one of the deadliest, with Hurricane Katrina causing 1,575 deaths in Louisiana alone (Boyd, 2011).

Many studies have investigated the cause of the extreme activity during the season, which runs from 1 June – 30 November. Several of these have attributed the activity to the unusually high SSTs during the majority of the season (Virmani and Weisberg, 2006; Trenberth and Shea, 2006; Beven *et al*., 2008). Trenberth and Shea (2006) also noted that in 2005 atmospheric circulation was especially conducive for the development of tropical systems. But no study to date has comprehensively investigated the role D26 and U_h influenced U_{10} fluctuations during this very active season.

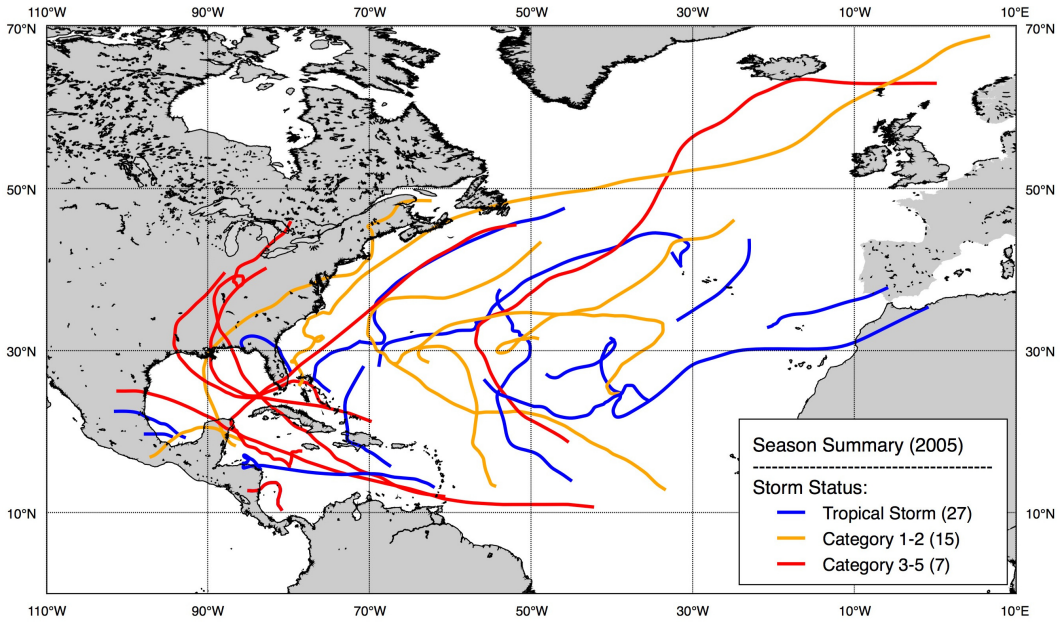

Figure 1.2: Season summary of tropical cyclone tracks with categories broken down into subgroups.

1.4 Significance of Proposed Research

This research is the first to comprehensively analyze the role of the three-dimensional oceanic thermal structure and U_h on the cyclogenesis and intensity fluctuations of tropical cyclones. An increased understanding of these two variables is of great importance to the scientific community. Specifically, investigating the role of U_h on intensity fluctuations of tropical systems could enhance the predictive capabilities of climatologists, meteorologists, and climate modelers. Given that some tropical systems have been known to undergo an unexpected, explosive intensification process and threaten coastal communities, the need for this increased understanding is vital in order to provide sufficient forecasts and lead times to citizens who live along the coast.

1.5 Organization of Thesis

Chapter 2 will provide a comprehensive literature review of past and present relevant research that pertains to this thesis. Then a review of data and methods implemented will follow in Chapter 3. Chapter 4 will review 23 storms in the 2005 North Atlantic basin hurricane season, including a history of their tracks and time series of the along-track D26, $U_{10,}$ and U_h. In addition, an in-depth analysis of the oceanic thermal structure during Hurricanes Dennis, Emily, Katrina, Rita, and Wilma will be completed on the daily time scale. A threshold analysis for minimum D26 for the genesis of tropical storms and hurricanes (category 1) will be performed. These thresholds will then be contoured and plotted for the 1st, 15th, and 30th of each month with genesis locations overlain. Chapter 4 also includes the results of the regression analysis and a discussion of the implications of the findings throughout the chapter. Finally, Chapter 5 will summarize the major contributions of this research and offer suggestions for future research to improve our understanding of one of nature's most impressive and ominous wonders.

CHAPTER 2: LITERATURE REVIEW

2.1 Sea Surface Temperatures and Tropical Cyclones

It has long been established that high sea surface temperatures (SSTs) are an essential prerequisite for tropical cyclogenesis and intensification (*i.e.,* Fisher, 1958; Perlroth, 1967; Perlroth, 1969; Gray, 1968). Palmén (1948) noted that tropical cyclones require SSTs of at least 26° – 27°C. Buyers (1974) supported Palmén (1948) by noting that SSTs must be at least 26°C. Dare and McBride (2011) found that between 1981 and 2008, 98.3% of tropical cyclones in all basins formed over SSTs that exceeded 25.5°C, while fewer than 2% of storms formed over SSTs below 25.5°C.

The importance of high SSTs was reiterated by Gray (1968), who noted that SST has a strong influence on the potential buoyancy of cumulus clouds, which acts to warm the middle to upper troposphere. This warming initiates the formation of a tropical disturbance and subsequent development of tropical storms and hurricanes (Gray, 1968). Ooyama (1969) found that high SSTs allow the transfer of a large amount of latent heat energy from the ocean to the tropical system via evaporation. Emanuel (1986) added additional support to this conclusion by noting that the intensification and maintenance of tropical systems rely exclusively on self-induced heat transfer from the ocean. Overall, these high SSTs are essential to the cyclogenesis and continued strengthening of tropical systems.

2.2 Three-Dimensional Oceanic Thermal Structure

While many studies (Emanuel, 1986; Emanuel, 2003; Dare and McBride, 2011; Elsner *et al*., 2013; Strazzo *et al*., 2013) have shown that tropical cyclone development requires high SSTs, others have noted the importance of the condition of the three-dimensional oceanic thermal structure before, during, and after the passage of a tropical cyclone. Perhaps one of the

first studies to investigate the role of the vertical oceanic temperature profile in the formation and intensification of tropical cyclones was performed by Perlroth (1969), who examined vertical temperature gradients from the sea surface down to 200 feet (~ 61 m) (ΔT) for 68 storms in the North Atlantic basin. The study showed that 92% of tropical storms reached hurricane status when ΔT was equal to or less than 7 F° (~ 3.8 C°) and that only 3% of tropical storms reached hurricane status when ΔT was 15 F° (~ 8.3 C°) or greater (Perlroth, 1969). In other words, the vast majority of tropical cyclones only strengthen to hurricane status when the temperature remains warmer than about 22°C for the topmost 200 feet (~ 61 m) of the sea. Leipper and Volgenau (1972) were some of the first researchers to attempt to quantify the amount of energy located within the water column. They coined the term "hurricane heat potential" (HHP), which is defined as the excess amount of heat (Q, with units of J m^{-2}) present in the water at 299 K (26°C) (Leipper and Volgenau, 1972). In order to calculate this quantity, the authors used the following equation:

$$Q = \rho\, C_p\, \Delta T\, \Delta Z,$$

where ρ equals the density of the water (1 gram cm^{-3}), C_p equals the specific heat at constant pressure (1005 J kg^{-1} K^{-1}), ΔT is the average temperature difference above 299 K (26°C) at sample depths, and ΔZ is the depth increment, taken at 5 m (Leipper and Volgenau, 1972). Calculating this quantity allows for an understanding of the oceanic heat content present that is capable of supporting a tropical cyclone. In a study on tropical cyclones in the western North Pacific basin, Holliday and Thompson (1979) found that systems formed in areas with high SSTs of at least 28°C to a depth of 30 m, with that depth necessary for rapid deepening of the tropical systems.

2.2.1 Applications of the Three-Dimensional Oceanic Thermal Structure

Given that temperatures throughout the upper ocean play an important role in tropical cyclone formation and further intensification, studies utilizing data from this level in the ocean have become increasingly important. Many recent studies have focused on the upper ocean's response to a moving tropical cyclone (*i.e.*, Price, 1981; Price *et al*., 1986; Sanford *et al*., 1987; Shay *et al*., 1992; Price *et al*., 1994; Falkovich *et al*., 1995; Jacob and Shay, 2003). While these studies provided information on how the ocean responds during and after the passage of a tropical system, specific information on the depth of the 26°C isotherm (D26) was not discussed in detail, nor did the studies emphasize the role of D26 on the storm formation and intensification.

Goni and Trinanes (2003) noted that D26 can extend down to hundreds of meters in the Loop Current and in oceanic mesoscale features such as warm-core eddies (WCEs). The authors calculated tropical cyclone heat potential (TCHP), which incorporates the amount of heat content from the sea surface down to the 26°C isotherm. Lin *et al*. (2008) discussed the importance of incorporating TCHP when studying tropical cyclone intensity changes because higher values of TCHP allow an abundance of energy for storm development. This abundance of energy can hinder negative feedback processes that would ultimately weaken the storm (storm induced cooling, entrainment mixing, and upwelling).

Results for Hurricanes Opal (1995), Mitch (1998), and Bret (1999), and Typhoon Imbudo (2003) showed that all storms experienced rapid intensification after passing over areas with high TCHP. Most storms were found to intensify after encountering WCEs (Goni and Trinanes, 2003). Hong *et al*. (2000) noted that the rapid intensification of Hurricane Opal (1995) occurred over a WCE, which provided the storm with abundant energy. Shay *et al*. (2000) expanded upon

this notion, and found that Hurricane Opal (1995) underwent a rapid intensification process, intensifying from 35 m s^{-1} to 60 m s^{-1} in a 14-hour period, after traveling directly over a WCE in the Gulf of Mexico. Specifically, it was found that D26 was 150 m in this WCE, as opposed to 50 m just outside the feature. Similarly, Jacob and Shay (2003) found that Hurricane Gilbert (1988) intensified over a WCE that shed from the Loop Current. Those authors found that D26 was 140 m in the WCE and 75 m outside. Lin *et al*. (2005) found that Supertyphoon Maemi (2003) in the western North Pacific basin traveled over a WCE whereupon its winds increased from 41 m s^{-1} to 77 m s^{-1} in a 36-hour period. It was found that in this WCE, D26 was in the 120 – 130 m range, compared with only 40 m just outside the eddy. Lin *et al*. (2008) found that typhoons in the western North Pacific basin that reach category 5 status (*i.e.*, winds $\geq$ 70 m s^{-1}) required D26 values of ~ 105 – 120 m in the absence of other supporting oceanic mesoscale features. The authors also found that if a typhoon traveled in an area where the average D26 values were "shallow" (D26 ~ 60 m), then encountering a WCE is essential to the intensification to a strong typhoon. Jaimes and Shay (2009) studied the influence of WCEs and cold core eddies (CCEs) on Hurricanes Katrina and Rita. They found that both storms experienced intensification and weakening after encountering WCEs and CCEs, where D26 was deep and shallow, respectively. Seo and Xie (2013) found that the intensity of Katrina (2005) was much more sensitive to D26 rather than SSTs.

In contrast, CCEs with a shallow D26 can provide a negative feedback to the storm. Walker *et al*. (2005) observed evidence of a rapid negative oceanic-atmospheric feedback to Hurricane Ivan (2004) from two large areas of cooling within CCEs where SSTs of 20 – 26°C were present. The implication is that D26 was likely shallow in these CCEs, thus maximizing

surface cooling from entrainment mixing and upwelling. The cooling provided immediate negative feedback to the storm, which caused it to decrease in intensity.

Given that the previous studies demonstrated that three-dimensional oceanic thermal structure was shown to have a large influence on the intensification of tropical systems, a more complete understanding is warranted to better predict these violent storms. Ali *et al*. (2010) revealed that incorporating upper oceanic heat content into models is more effective than only utilizing SSTs in the monitoring of intensity changes of tropical cyclones. Mainelli *et al*. (2008) found that by including oceanic heat content into the statistical hurricane intensity prediction model, it improved intensity forecasts by 5% for category 5 storms and up to 20% for all storms. They also indicated that the heat content of the ocean was more important to category 5 storms. This shows that the three-dimensional oceanic thermal structure plays a major role during the rapid intensification process. Lin *et al*. (2009) discussed the importance of incorporating TCHP when studying tropical cyclone intensity changes because higher values of TCHP allow an abundance of energy for storm development. This abundance of energy can lessen negative feedback processes that would ultimately weaken the storm (storm induced cooling). Wu *et al*. (2007) found that this negative feedback process is lessened in the presence of a deep thermocline, thus insulating the ocean from rapid sea surface cooling. Lin *et al*. (2013) provided an overview of the importance of including oceanic heat content in tropical cyclone prediction models.

2.3 Influence of Translation Speed

While the three-dimensional oceanic thermal structure plays a very important role in the cyclogenesis and intensification of tropical cyclones, of similar importance is its forward, or translation, speed (U_h). A tropical system's U_h can influence its intensity greatly, depending on

the state of the underlying oceanic thermal conditions. Price (1981) showed that upwelling causes a significant enhancement of the SST response (cooling) in a slow-moving hurricane (U_h ~ 4 m s^{-1}) and a negligible response in faster-moving hurricanes. Shay *et al*. (2000) found that during Hurricane Opal's (1995) motion through the Gulf of Mexico, its slow U_h at times caused a large vertical displacement of the isotherms. This was caused by a shallow thermocline and thus cool-nutrient rich waters were upwelled from below the surface. Shay *et al.* (2000) also found that faster-moving tropical systems (U_h ~ 5 – 10 m s^{-1}) have less time to cause vertical mixing, and thus cooling at the sea surface. Wu *et al*. (2007) found that U_h is important for tropical cyclones encountering WCEs because a slow U_h over these features can greatly increase upwelling and mixing. In contrast, a fast U_h over a WCE may slow upwelling and mixing due to limited time over the feature. For example, Shay and Uhlhorn's (2008) analysis of Hurricane Lili (2002) found that D26 displacements along-track were ~ 10 m, due to Lili's rapid U_h. There was insufficient time for the storm to cause turbulent mixing of the water column, and thus raise the thermocline. Uhlhorn and Shay (2012) also briefly mentioned Hurricane Lili's rapid U_h and its limited effect on the three-dimensional oceanic thermal structure due to its speed. The authors noted that Hurricane Lili's effects on the Loop Current specifically were minimal, a possible result of its fast U_h.

Lin *et al*. (2009) completed a 10-year study of typhoons in the Western North Pacific basin in order to understand the effects of U_h and D26 on category 5 storms (*i.e.*, winds $\geq$ 70 m s^{-1}). The authors found that if a shallow D26 layer is present (60 – 70 m), a U_h of 7 – 8 m s^{-1} is required for intensification to a category 5 storm. This fast U_h is required to limit displacement of the isotherm and also negative feedback to the system. However, if a deep warm layer exists (100 – 120 m), a slower U_h of 2 – 3 m s^{-1} can be present with intensification to category 5

possible. Lin *et al*. (2009) used the term "affordable minimum translation speed," which is the speed at which a storm needs to travel in order to reach category 5 status for a given D26. Mei *et al*. (2012) used 40-years of tropical cyclone track data in the western North Pacific basin to reveal that on average, category 5 hurricanes move 1 m s^{-1} faster than tropical storms. Those authors found that because faster-moving tropical cyclones are able to limit their negative feedback due to cooling of SSTs, they attain a higher intensity. Walker *et al*. (2014) demonstrated the importance of U_h for Eastern Pacific basin's Hurricane Kenneth (2005). The authors found that Hurricane Kenneth's slow U_h (< 1.5 m s^{-1}) caused a strong negative feedback to the storm by cutting off oceanic enthalpy flux. As a result, Hurricane Kenneth collapsed rapidly from a major hurricane with winds of 54 m s^{-1} to a tropical storm with winds of 28 m s^{-1}.

2.4 Summary

Overall, the existing literature demonstrates the importance of the three-dimensional oceanic thermal structure and U_h during the cyclogenesis and intensification of tropical systems. Studies indicate that the oceanic thermal structure can cause rapid intensification and can also cause weakening. U_h plays an important role by controlling the amount of time spent over the ocean and its thermal characteristics. Increasing the breadth of this literature can lead to a deeper scientific understanding and potentially increase forecasting accuracy and warning times for coastal residents. Past research has utilized D26 and U_h data, but to date, no study has comprehensively evaluated the relationship between these variables and wind speed. The present research will attempt to bridge this gap in our understanding of tropical cyclogenesis and intensification.

CHAPTER 3: DATA AND METHODS

3.1 Data

3.1.1 Hourly-Interpolated Hurricane Data

Data regarding tropical systems are typically obtained from the National Hurricane Center's (NHC) best-track data set (HURDAT), which includes 6-hourly measurements throughout the lifespan of a storm. However, these data are limited by their temporal resolution, as the storm's characteristics can vary greatly between the 6-hourly observations (see Appendix A). Therefore, a spline interpolation method using piecewise polynomials as described by Elsner and Jaggar (2012) was used to estimate hourly conditions for each North Atlantic tropical cyclone of 2005. With this increased temporal resolution, the possibility of missing positional and intensity fluctuations along-track decreases, but nevertheless, caution should be exercised in the interpretation of results because the "hourly data" between 6-hourly observations are estimated. The hourly-interpolated variables considered in this research are: latitude, longitude, wind speed (U_{10}; m s^{-1}), and translation speed (U_h; m s^{-1}).

3.1.2 Depth of the 26°C Isotherm Data

The gridded depth (m) of the 26°C isotherm (D26) for the North Atlantic basin was obtained from Dr. Gustavo Goni of the Physical Oceanography Division of the Atlantic Oceanographic and Meteorological Laboratory (AOML) in Miami, Florida. The D26 data were provided in a 0.25° x 0.25° grid cell spatial resolution with a daily temporal resolution. The daily fields were provided as .dat file types, which contain latitude, longitude, tropical cyclone heat potential (TCHP), and D26 for the 2005 North Atlantic basin hurricane season (data were provided from 1 June 2005 to 31 December 2005). The D26 was estimated using *in-situ* microwave sea surface temperature (SST) measurements and satellite altimetry measurements,

which measure the altitude of the sea surface. The methodology for producing the data has changed throughout the years, with three methodologies (Version 1.0, Version 2.0, and Version 2.1) used in the calculations. All three methodologies are explained below. However, Version 2.1 is the only version utilized to estimate D26 in this research.

3.1.2.1 D26 Version Calculation Methods

Version 1.0, the first methodology used to estimate D26, is based on a two-layer reduced gravity model (Goni *et al*., 1996; Figure 3.1).

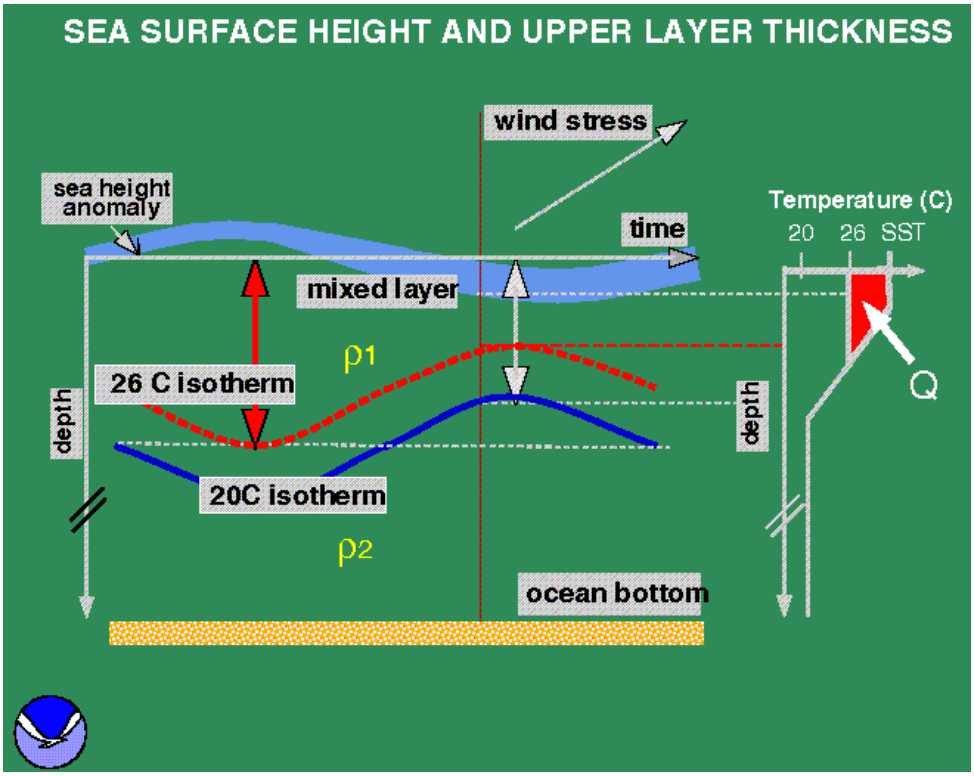

Figure 3.1: Schematic of the two-layer reduced gravity model used to calculate upper layer thickness (a variation from Goni *et al*., 1996).

This model allows for the calculation of the upper layer thickness (from the sea surface down to the 20°C isotherm). This model uses the 20°C isotherm simply because it was assumed to be located in the center of the thermocline. To estimate the temperature profiles at these locations,

three variables are used. The first is observed SST data obtained from the Tropical Rainfall Measurement Mission's (TRMM) microwave imager. Microwave SST can penetrate clouds, allowing a clear measurement of the SSTs below them (Wentz *et al*., 2000). The second variable is estimated sea surface height data obtained from altimeters that allow for the estimation of the depth of the 20°C isotherm. Finally, the method estimates the depth of the 26°C isotherm based on the climatological relationship between the 20°C and 26°C isotherm.

Version 2.0 uses a linear regression model based on the depths of the estimated 26°C and the 28°C isotherms. This method employs various techniques to estimate the depths such as slopes and intercepts in the regression model. This model is no longer used, and will not be discussed further in this research.

Version 2.1, the methodology used to calculate the data utilized in this research, incorporates various steps to estimate D26. First, *in-situ* temperature profiles are collected from eXpendable BathyThermograph and profiling-float observations. These temperature profiles are then grouped into 3°x 3° bins with a spatial resolution of 1°x 1°. Next, the depths of the 28°C and 26°C isotherm are estimated from each temperature profile, and the weekly sea surface height anomaly (SHA) gridded files obtained from AVISO (satellite altimetry data distribution website; http://www.aviso.altimetry.fr/en/home.html) are interpolated into the place and time of the temperature profiles. Within each of the 1°x 1° bins, the depths of the 28°C and 26°C isotherms are linearly regressed onto the SHA corresponding value. The method only uses linearly regressed values within a 1-sigma level. Finally, in each of the 1°x 1° bins the synthetic temperature profile is derived using the regression parameters. Version 2.1 was created to remove many outliers present in the derived data, mostly in the Gulf of Mexico region.

More detailed information on the methodologies used to estimate D26 can be found at: http://www.aoml.noaa.gov/phod/cyclone/data/method.html.

3.1.2.2 Data Masking

Given that the D26 data are calculated using sea surface height and ocean temperature data averaged in 1°x 1° bins, estimates in coastal areas tend to be less accurate than in the open ocean. Thus, the D26 values used in this research are confined to areas where the water depths exceed 200 m. To mask the original data set to exclude D26 estimates in areas with depths of less than 200 m, the following steps were taken:

1. A global relief data set (ETOPO1) was downloaded from the National Geophysical Data Center (NGDC; Amante and Eakins, 2009; http://www.ngdc.noaa.gov/mgg/global/global.html) website as a .netCDF file containing global relief and ocean bathymetry for the entire globe.
2. The .netCDF file downloaded in the previous step contained the global data set, so it was necessary to "cut out" the region of interest (North Atlantic, Caribbean Sea, and the Gulf of Mexico). This was done using the *grdcut* command (grid cut) in the Generic Mapping Tools (GMT) software. This command allows for the global data set to be subset to specified latitude/longitude bounds.
3. Once the data set was subset to include only the region of interest, the data then needed to be interpolated to match the resolution of the D26 data set (0.25° x 0.25°). This was done using the *grdsample* command (grid sample) in GMT. This command interpolated the global relief data set to match the resolution of the D26 data set.
4. Next, to mask D26 estimates in waters shallower than 200 m the subset global relief data set was set to a numerical python (numpy) array of 0s and 1s. This was done in

the Python programming language by assigning values less than or equal to 200 m to 0 and values greater than 200 m to 1.

5. The final step was to multiply the original D26 gridded values by the subset global relief dataset values with values less than or equal to 200 m set to 0 and values greater than 200 m set to 1. The result was that D26 values in ocean depths shallower than or equal to 200 m were set to 0 and in all other areas the value was left intact, since depths exceeding 200 m were set to 1, and multiplying by 1 left the original D26 value unaltered.

Once the above steps were taken, a masked D26 data set was available that excluded coastal regions, with the intention of providing a more accurate D26 data set.

3.2 Methods

3.2.1 Considerations

An important consideration when deciding how to analyze the D26 estimates was to determine which storms during the 2005 North Atlantic basin hurricane season to include. The optimal situation would have been to investigate all 28 storms that occurred during this record-breaking season. However, it was found that ~14% of the named storms during the season formed and maintained at least tropical storm status while D26 along their track was "masked" or 0 m throughout the entirety of the storm's lifespan, even over deep waters. For this reason, four late-season and (relatively) high-latitude storms (Vince, Delta, Epsilon, and Zeta) were excluded from this research. The nineteenth storm of the season, given the name "the 2005 Azores subtropical storm" was also excluded from this study because it formed in a high-latitude environment and it was categorized as subtropical in nature. Thus, D26 was assumed to have little to no effect on the genesis and eventual strengthening of these storms. This research

analyzed the remaining 23 named storms from the 2005 season. Another important consideration taken into account in this study was the issue of along-track storm status. Given that the NHC's measurements of tropical cyclone variables are on a 6-hour temporal resolution, the hourly-interpolated hurricane data used in this research indicated, at times, an upgrade in status (*e.g.*, from Category 1 to Category 2 on the Saffir-Simpson scale) before the official NHC's upgrade. Since the hourly data were interpolated, these discrepancies from the official NHC's storm status should be taken into account in the interpretation of the results.

3.2.2 Sampling Method

To begin analysis on the data used in this research, a sampling method was required. The hourly-interpolated hurricane data set includes precise latitudes and longitudes. The D26 data set was provided with a 0.25° x 0.25° grid cell resolution. To sample D26 data from the latitude and longitude given in the hourly-interpolated data set, the nearest neighbor (*i.e.*, corresponding latitude and longitude with the smallest difference) was chosen. To sample the data efficiently, a program in the Python programming language incorporated a total of four functions to accomplish the sampling. The first function returned the nearest neighbor for the provided value from the neighbor set. The second function returned the nearest position for the provided position. The third function returned the actual D26 data point from the nearest neighbor latitude and longitude. The fourth function returned the D26 estimate given a specified latitude and longitude (from the hourly-interpolated .csv files), the D26 masked data set, and a meshed grid. The program sampled from the masked D26 data set, so all D26 values were considered valid throughout the entire sampling period. This returned .csv file contained the hourly-interpolated latitudes and longitudes, U_{10} (m s^{-1}), U_h (m s^{-1}), and daily D26 (m) values.

3.2.3 Along-Track Storm Analysis

To visualize how D26, U_{10}, and U_h vary along-track of the 23 named storms in this study, graphs were created with each set of the three variables plotted together at the point in time in which the storm became a tropical depression (*i.e.*, $U_{10} \leq 17$ m s^{-1}). To aid in the analysis, the storm's strength category (*e.g.*, tropical storm, category 1 hurricane, etc.) was added in the foreground as lightly shaded bars corresponding to storm strength. These graphs were also used to reveal correlation of the variables and to investigate any lags present in the data.

3.2.4 Analysis of Major Storms

Along with plotting D26, U_{10}, and U_h along-track, a visualization of five Saffir-Simpson category 3 or stronger storms (*i.e.*, $U_{10} \geq 50$ m s^{-1}; Dennis, Emily, Katrina, Rita, and Wilma) was completed to visualize D26 values in and around the storm, using the Python programming language with the track overlain. Storm status (*e.g.*, tropical depression, tropical storm, category 1, etc.) was indicated using color-coded dots. Although Hurricane Maria, the thirteenth named storm of the season, attained major status (*i.e.*, $U_{10} \geq 50$ m s^{-1}), it was excluded from the major storm visualization method used in this section simply because it did not affect any landmasses. Also, Hurricane Beta, the twenty-fourth named storm, attained its major status while located in coastal waters. Since data was masked in ocean depths ≤ 200 m, Beta was excluded from this major storm analysis. To ensure that these figures incorporated an appropriate area around the storm for visualization purposes, 8° x 8° boxes (see Appendix B) were drawn around the centermost position on that day. The box was then cut out and zoomed in for a clear view of the ocean thermal structure during the current day. These figures were produced each day during the storm's lifetime with the current day's D26 data plotted. This visualization method also allowed for the detection of ocean mesoscale features, such as warm-core eddies (WCEs) and cold-core

eddies (CCEs) that may have influenced the storm's intensity fluctuations. Although daily figures were produced for each storm during its lifetime, only ones that were considered pertinent to the discussion were included in the research.

3.2.5 Determining Thresholds

A search was completed to identify the minimum D26 in which a tropical storm formed during the season. The same search was completed for the point at which a tropical storm was upgraded to a hurricane (*i.e.*, category 1; $U_{10} \geq 33$ m s^{-1}). Once the minimum D26 for the two thresholds was found, it was then contoured for the 1st, 15th, and 30th of each month during the season (June – November). This analysis was completed to show the temporal and spatial extent of the thresholds during different times of the season, regardless of whether tropical cyclones were present on that day. The genesis location for tropical storms (*i.e.*, $U_{10} \geq 18$ m s^{-1}) and hurricanes (*i.e.*, category 1; $U_{10} \geq 33$ m s^{-1}) that formed in each month was plotted as a reference.

3.2.6 Regression Analysis

A statistical analysis of the data used in this research was completed using regression models. A total of eight models (labeled A-H) were run on various subsets of the data. Given that in regression analysis, the residuals of the model must assume normality, the QQ-plots of the residuals were examined for each model. Williams *et al*. (2013) noted that given a large sample size, the assumption of normality-distributed residuals is of less importance according to the central limit theorem. Each model used in this research included over 30 data points. If the QQ-plots of the residuals were found to deviate from normality only slightly, the model was still considered useful. Other regression assumptions such as multicollinearity and homoscedasticity of the errors were checked as well. The results were interpreted with extreme caution when any one of the assumptions were violated. The R programming language was used to run the

statistics in this research. Table 3.1 shows the regression models used and the variables they included.

Table 3.1: Summary of regression models.

Name:	Type:	Independent Variable(s):	Dependent Variable:
A – all named storms in 2005	Simple	D26	U_{10}
B – all named storms in 2005	Multiple	D26, U_h	U_{10}
C – Major hurricanes	Multiple	D26, U_h	U_{10}
D – Dennis	Multiple	D26, U_h	U_{10}
E – Emily	Multiple	D26, U_h	U_{10}
F – Katrina	Multiple	D26, U_h	U_{10}
G – Rita	Multiple	D26, U_h	U_{10}
H –Wilma	Multiple	D26, U_h	U_{10}

"Regression A – all data" incorporates D26 and U_{10} data from all named storms sampled from the time they became named (*i.e.*, $U_{10} \geq 18$ m s^{-1}) throughout the storms' entire lifespan, except when they moved into waters shallower than 200 m in depth. This model was run to determine whether any linear relationship exists between D26 and along-track U_{10}. "Regression B – all data," a multiple regression, contains the same variables as Regression A – all data, but with U_h included in the model. It has been shown that U_h plays an important role in the intensification of tropical systems (Lin *et al*., 2009; Mei *et al*., 2012; Walker *et al*., 2014). Next, "Regression C – Majors" is a multiple regression that uses D26 and U_h as the independent variables and U_{10} as the dependent variable. This model includes only the 2005 storms that reached major status (*i.e.*, $U_{10} \geq 50$ m s^{-1}; Dennis, Emily, Katrina, Rita, and Wilma). Hurricane's Maria and Beta are excluded from "Regression C – Majors" because they were only at major status for a brief period of time (< 10 hours), thus data are insufficient to produce meaningful results for those storms. Regression models D-H are run as separate multiple regressions on the

major storms during the season. U_{10}, U_h, and D26 data are subset to include only the period when the storm reached major status, with $U_{10} \geq 50$ m s^{-1}. All eight of these regression models attempt to explain the variation in intensity fluctuations in along-track U_{10} during the storm.

CHAPTER 4: RESULTS AND DISCUSSION

4.1 Along-Track Storm Analysis

Each storm in the following subsections was given a brief synoptic history and an analysis of along-track wind speed (U_{10}), translation speed (U_h), and the depth of the 26°C isotherm (D26). In general, a slow U_h provides more time for an overlying storm to acquire the characteristics of the water; if the pool is warm and deep, abundant ocean-to-atmosphere energy transfer can occur in such conditions. If the warm pool is shallow and cooler, the storm is more likely to weaken as enthalpy fluxes are reduced (Emanuel, 1986; 2003).

Storm track figures and time series graphs based on the hourly-interpolated data were generated for each storm. The time series graphs include hourly U_{10}, U_h, and daily D26 values along-track with intensity category in the foreground. Abbreviations for intensity category are as follows: tropical depression (TD), tropical storm (TS), category 1 (H1), category 2 (H2), category 3 (H3), category 4 (H4), category 5 (H5), extratropical cyclone (EX), and low-pressure (LO).

Although specific data about each storm was obtained from HURDAT and the D26 data set, general historical information about the storms in Sections 4.1.1 through 4.1.23 was obtained from Beven *et al.* (2008)'s *Annual Summary of the Atlantic Hurricane Season of 2005*. Beven *et al.* (2008) also includes comments from researchers affiliated with the Tropical Prediction Center, the National Oceanic and Atmospheric Administration, the National Weather Service, and the National Hurricane Center in Miami, Florida. Hurricanes Dennis, Emily, Katrina, Rita, and Wilma were analyzed on the daily timescale to further investigate the influence of D26, U_{10}, and U_h on the cyclogenesis and along-track intensity fluctuations. In addition, the effects of oceanic mesoscale features such as warm-core eddies (WCEs) and cold-core eddies (CCEs) were analyzed. Daily D26 panels were provided for each storm as part of this daily analysis. These

indicate the depth of the pool of waters warm enough to sustain hurricane growth (*i.e.*, 26°C or warmer).

4.1.1 Tropical Storm Arlene

The first named storm of the season formed from a tropical wave that interacted with the intertropical convergence zone on 8 June 2005 (Figure 4.1).

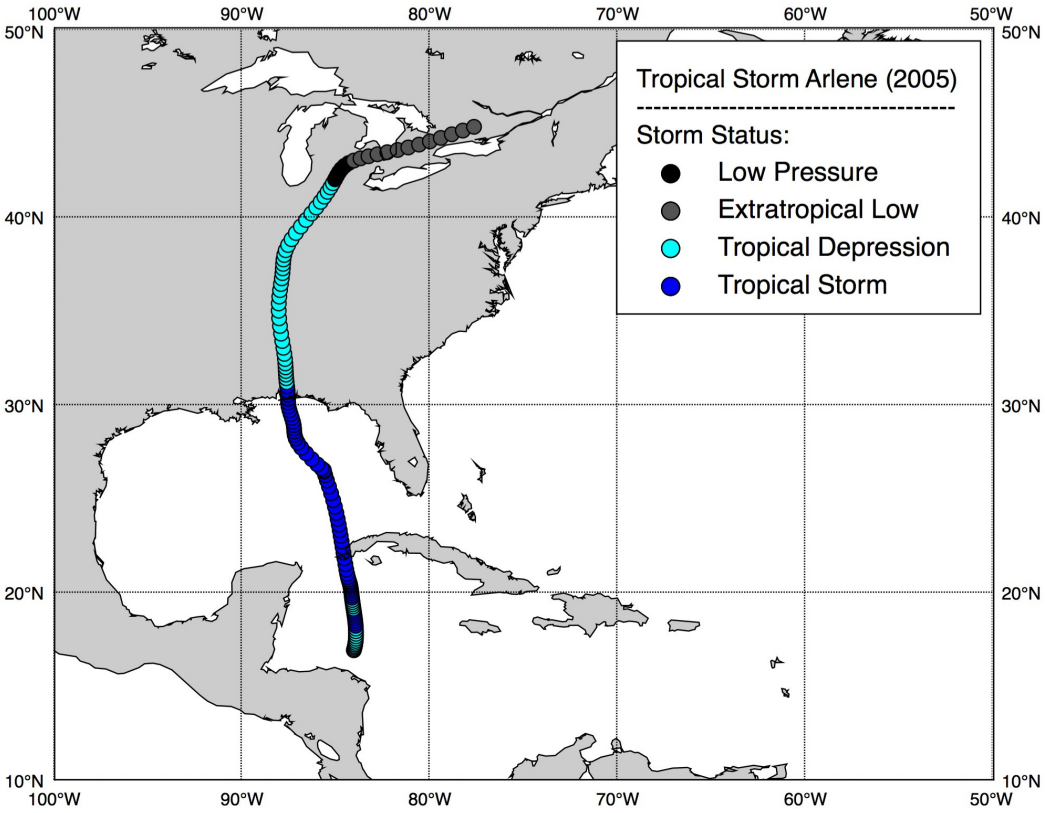

Figure 4.1: Tropical Storm Arlene's (8 – 14 June 2005) track.

The storm formed just to the northeast of Honduras and moved northward toward the western tip of Cuba, making a brief landfall near Cabo Corrientes on 10 June with winds of approximately 23 m s^{-1}. Yoo *et al*. (2015) found that strong westerly and easterly winds enhanced low-level vorticity, thus allowing Arlene to form on 8 June and continue to strengthen to a tropical storm on 9 June while located in the Caribbean Sea. The storm continued to move slowly northward

while maintaining tropical storm status and reaching a peak intensity of approximately 30 m s^{-1} on 11 June while located over the central Gulf of Mexico. Arlene went on to make landfall in the Florida panhandle on 11 June as a tropical storm with winds of 25 m s^{-1}. After landfall, Arlene moved north and then northeastward over the central United States and became an extratropical storm on 13 June.

Tropical Storm Arlene's along-track analysis (Figure 4.2) revealed that the storm passed over large D26 values throughout most of its track.

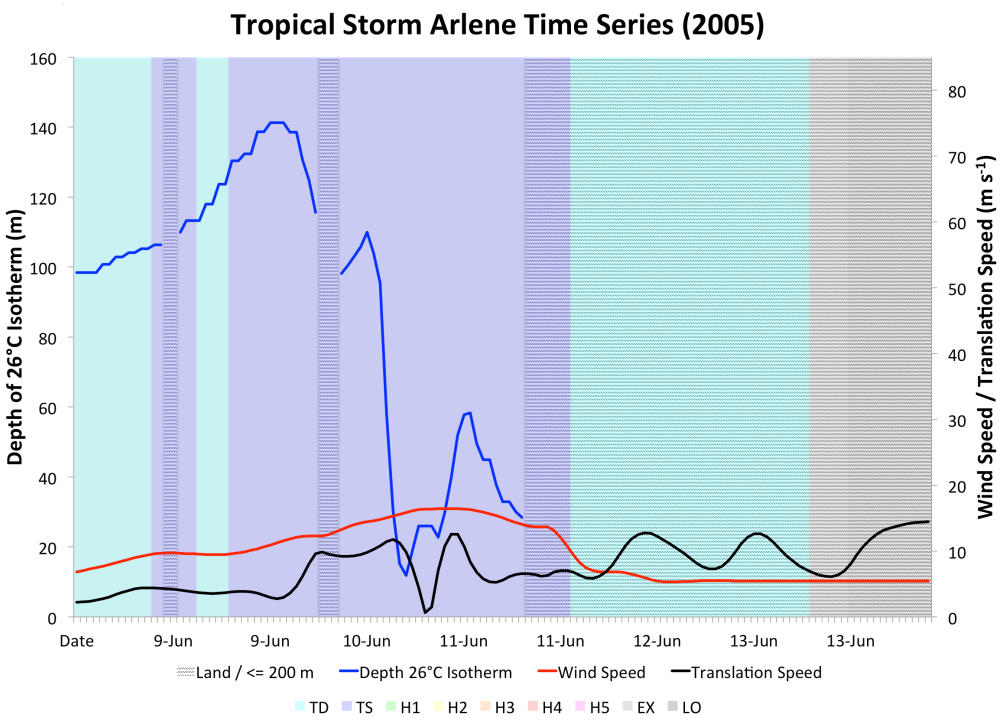

Figure 4.2: Tropical Storm Arlene's time series of D26, U_{10}, U_h, and intensity category.

The deepest D26 value that the storm encountered was 141.3 m, which occurred on 10 June. During that time period, Arlene was located in the western Caribbean Sea. Although Arlene had an abundant amount of oceanic heat content to supply energy throughout its track (as apparent with an average D26 of 88.2 m), it failed to strengthen past tropical storm status. A look at U_h indicates that the storm had an average along-track speed of 7.6 m s^{-1}. As the storm passed over

the thickest layer of warm near-surface water (*i.e.*, largest D26 value) in the western Caribbean Sea (141.3 m), its U_h was 2.9 m s^{-1}. Lin *et al.* (2009) noted that slower-moving tropical systems (U_h ~ 2 – 3 m s^{-1}) require greater D26 values (D26 ~ 115 – 140 m) for intensification to occur. Despite the fact that both D26 and U_h fell into the categories determined by Lin *et al.* (2009) as sufficient for strengthening, the storm did not attain hurricane status. One possible factor that negatively influenced Arlene, thus limited its intensity, was dry air. Beven *et al.* (2008) found that Arlene experienced dry air entrainment as it moved northward into the Gulf of Mexico, possibly limiting its peak intensity to only 30 m s^{-1}.

4.1.2 Tropical Storm Bret

Tropical Depression # 2 formed on 28 June 2005 in the Bay of Campeche from the interaction of a tropical wave and a surface low-pressure system (Figure 4.3).

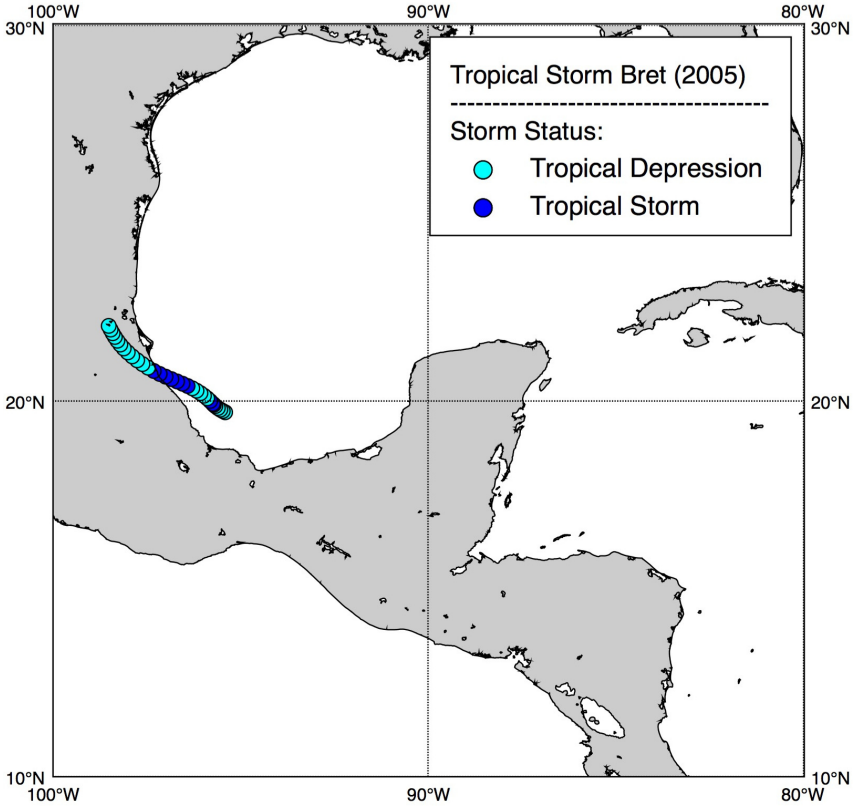

Figure 4.3: Tropical Storm Bret's (28 – 30 June 2005) track.

The system became a tropical storm on 29 June and achieved the name Bret. Bret moved northwestward as a ridge to its north provided steering. Bret made landfall in Mexico near the city of Tuxpan on 29 June with winds of approximately 18 m s^{-1}. Analysis of along-track data for Tropical Storm Bret revealed that the storm encountered relatively small D26 values, with an average of 37.7 m. The maximum D26 value of 40.7 m was present as the storm neared landfall (Figure 4.4).

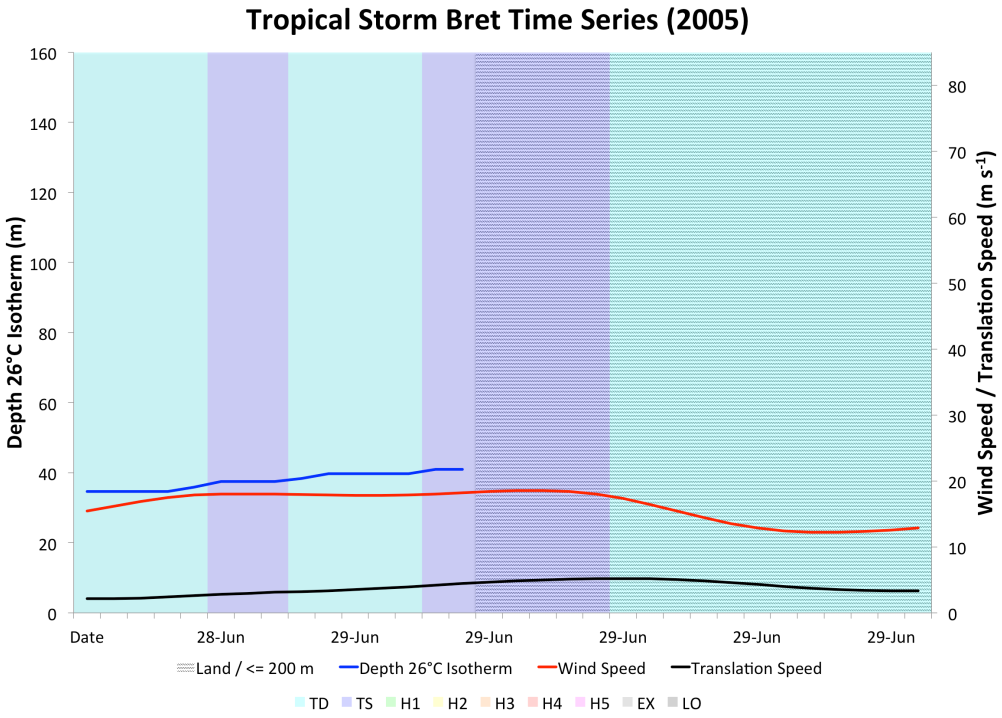

Figure 4.4: Tropical Storm Bret's time series of D26, U_{10}, U_h, and intensity category.

Average U_h was found to be 3.8 m s^{-1}. This speed, coupled with the low D26 values, could have contributed significantly to limiting Bret's strength to minimal tropical storm status (18 m s^{-1}).

4.1.3 Hurricane Cindy

The season's first hurricane can be traced back to a tropical wave that exited the coast of Africa on 24 June 2005. This Cape Verde wave moved slowly westward, with little organization.

However, on 4 July, the wave had attained enough convection to be labeled tropical depression # 3 in the Caribbean Sea. The storm continued to move westward then northwestward, crossing the Yucatán peninsula later on 4 July. Yoo *et al*. (2014) credited Cindy's genesis on 3 July to favorable upper-level winds. The storm attained tropical storm status on 5 July while located in the central Gulf of Mexico. On 6 July, Cindy attained category 1 hurricane status, with winds of 33.5 m s^{-1} just south of the Louisiana coast. Cindy made landfall on 6 July just to the southwest of Grand Isle, Louisiana. The storm then moved northeastward toward the Mississippi coast, where it made a second landfall as a tropical storm (Figure 4.5).

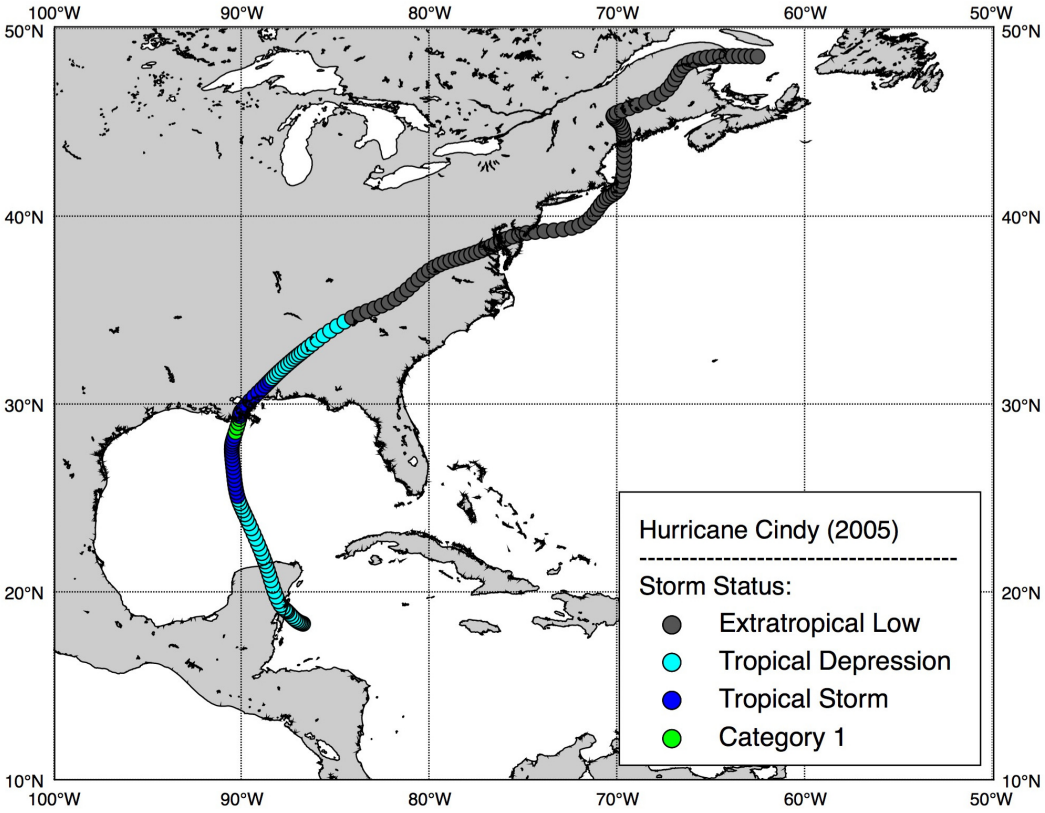

Figure 4.5: Hurricane Cindy's (3 – 11 July 2005) track.

Hurricane Cindy's highest attained U_{10} was 34.2 m s^{-1} (minimal category 1), which occurred on 6 July as the storm neared the Louisiana coast. The average along-track D26 of 72.7 m indicated that Cindy had a modest amount of oceanic heat content at its disposal (Figure 4.6).

The average U_h was 7.5 m s^{-1}. This speed, coupled with the average D26 of 72.4 m, led to the storm's eventual strengthening to a minimal category 1 hurricane. Beven *et al.* (2008) mentioned that the storm did encounter moderate southerly wind shear as it moved through the Gulf of Mexico. However, despite this southerly wind shear, which would have disrupted continued vertical development, Cindy continued to strengthen. This strengthening may be a result of the moderate D26 values along-track coupled with the storm's average translation speed of 7.5 m s^{-1}, the latter of which would have provided sufficient time for ample evaporation, condensation, and subsequent latent heat release to fuel the storm.

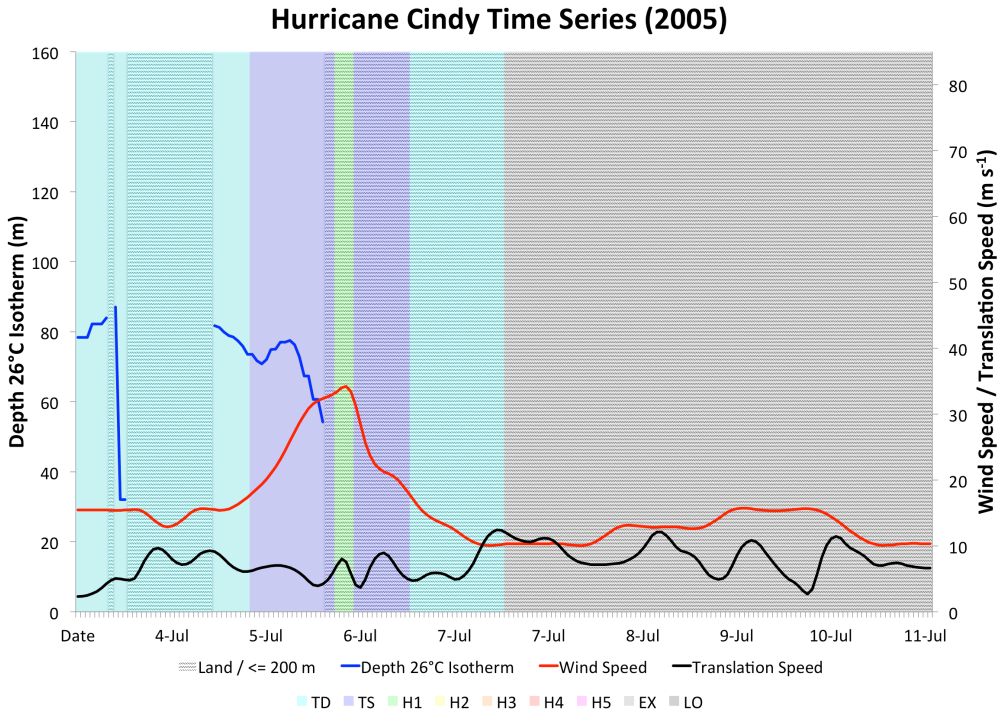

Figure 4.6: Hurricane Cindy's time series of D26, U_{10}, U_h, and intensity category.

4.1.4 Hurricane Dennis

The first major hurricane of the 2005 North Atlantic basin hurricane season formed from a tropical wave that moved off the coast of Africa on 29 June 2005. This Cape Verde wave was composed of two low-level centers, each with its own swirl of clouds. On 4 July, conditions were

favorable enough to allow for the formation of a tropical depression near the southern Windward Islands (Figure 4.7). The depression continued to organize and became a tropical storm on 5 July. As Dennis moved northwestward, it intensified into a category 1 hurricane near Hispaniola late on 6 July. Hurricane Dennis then experienced a rapid intensification process in which a drop of 31 mb occurred in a 24-hour period. Hurricane Dennis attained category 4 status as it made landfall in southeastern Cuba on 8 July. The interaction with Cuba caused Dennis to weaken substantially to a category 1. Once Dennis moved over the Gulf of Mexico, it again experienced a rapid intensification wherein pressure fell 37 mb in a 24-hour period beginning on 9 July. The storm attained winds of approximately 64 m s^{-1} (category 4) during this rapid intensification process. The storm slowly weakened thereafter to a category 3 before making landfall near Santa Rosa, Island in Florida.

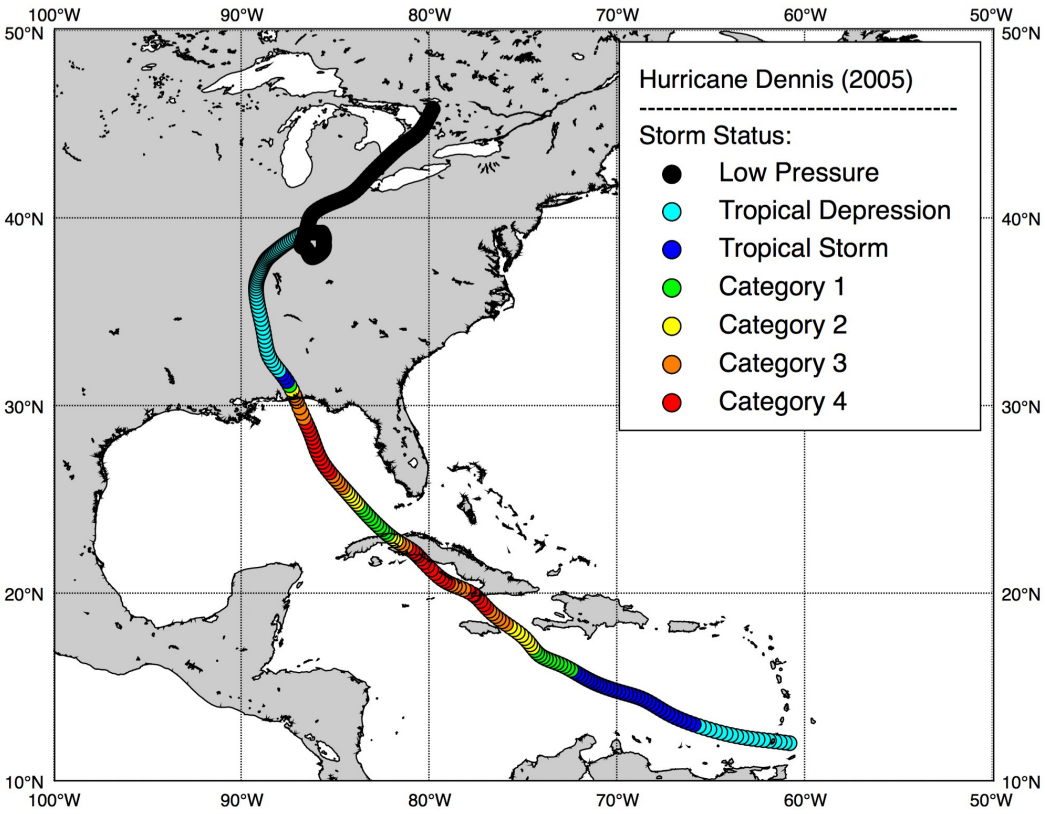

Figure 4.7: Hurricane Dennis' (4 – 18 July 2005) track.

The analysis of along-track conditions during Hurricane Dennis revealed that the storm had an average D26 of 82.5 m and an average U_h of 5.3 m s^{-1}. The average D26 of 82.5 m suggests that Dennis had a large amount of oceanic heat content during its lifetime, and at times it experienced D26 values over 120 m (Figure 4.8).

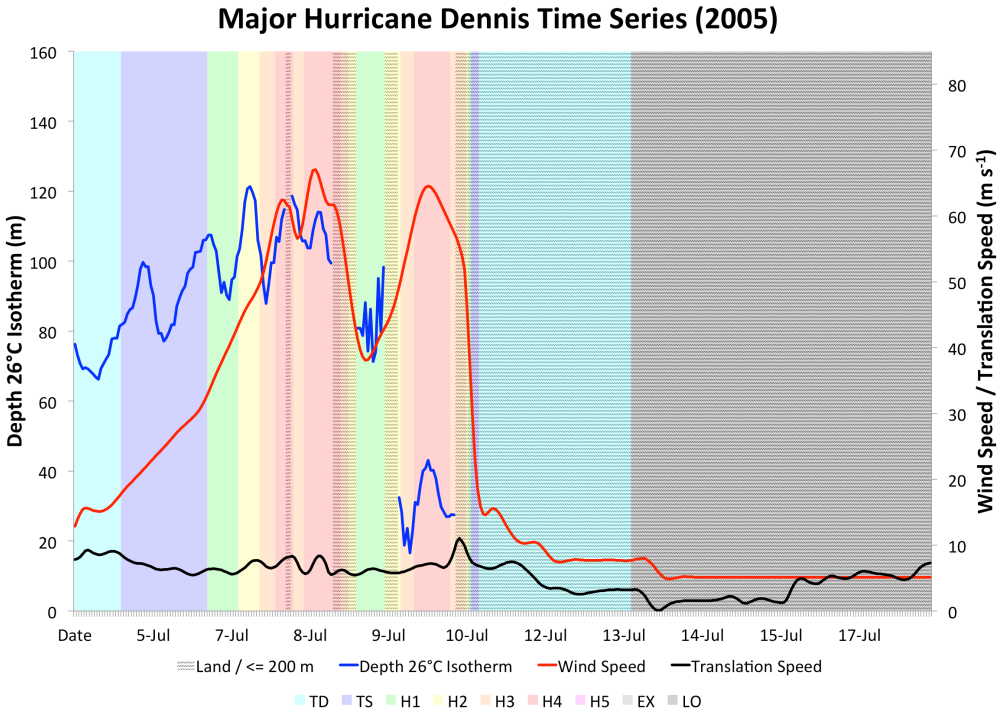

Figure 4.8: Hurricane Dennis' time series of D26, U_{10}, U_h, and intensity category.

A more in-depth analysis of along-track variables on the daily timescale reveals some interesting patterns (Figure 4.9). It appears that Hurricane Dennis passed very near both WCEs and CCEs throughout its track. On 5 July Dennis encountered its first possible WCE as the storm moved through the Caribbean Sea (Figure 4.9a). Prior to encountering the weak WCE, U_h was approximately 8 – 9 m s^{-1} and D26 values were in the 60 – 80 range with U_{10} just below tropical storm strength at ~ 15 – 17 m s^{-1}. As Dennis approached the WCE, U_h decreased to the 6 – 7 m s^{-1} range with D26 values increasing to the high 80s and 90s. Wind speed also increased to tropical storm strength (U_{10} > 18 m s^{-1}) with a peak of 22.7 m s^{-1} just outside the possible WCE. The

results indicate that Dennis may have strengthened to tropical storm status as it encountered higher D26 values along with a slower U_h, as the storm decelerated over the WCE. On 6 July, as Dennis tracked south of Cuba, it again seems to have been influenced by the ocean thermal structure along with U_h. Dennis traveled over deep D26 values throughout most of the day, with a maximum D26 of 107.4 m. The storm intensified to a category 1 hurricane with winds of 33.2 m s^{-1}, which occurred as the storm passed over the maximum of 107.4 m. On 7 July, Dennis traversed an area with abundant oceanic heat content. The storm intensified to category 2 status with U_{10} of 43.9 m s^{-1}, a D26 value of 103.5 m, and U_h of 6.0 m s^{-1}. It appears that Dennis passed over a possible weak CCE (Figure 4.9b) early on 7 July, but this CCE does not appear to have weakened the storm.

Hurricane Dennis underwent a rapid intensification process starting on 8 July, as it moved south of Cuba. The storm traveled over deep D26 values throughout that entire day, with an average D26 of 98.8 m. A translation speed of 7.0 m s^{-1} coupled with these large D26 values apparently allowed the rapid intensification and sharp pressure drop of 31 mb. Another rapid intensification occurred beginning on 9 July, when a 37 mb drop occurred in just 24 hours. Dennis appears to have traveled over a WCE and CCE during this time period (Figure 4.9c). D26 values in and around the WCE averaged 82.5 m. U_h varied from 10 – 12 m s^{-1}. The results indicate that the second rapid intensification could have taken place as a result of large D26 values along with favorable atmospheric conditions. The CCE that Dennis encountered was located to the southwest of the Florida shelf. There, D26 values averaged 25.4 m, with a U_h of approximately 11 m s^{-1}. However, Dennis continued to intensify into a category 3 with U_{10} of 54.7 m s^{-1}. This continued strengthening despite the proximity of a CCE and small D26 values may be explained by the relatively fast translation velocity to the northwest at 11 m s^{-1}. On 10

July, Dennis continued to travel over the same CCE previously mentioned on 9 July (Figure 4.9d). Once again, no signs of weakening were present, as the storm intensified to category 4 strength with winds of 60 m s^{-1}. Dennis steadily increased in intensity despite D26 values in the 15 – 40 m range with an average D26 on 10 July of 32.2 m. U_h was found to average 7.7 m s^{-1} throughout the day, indicating that Dennis progressed at an appreciable speed. This speed may have allowed Dennis to strengthen despite the low D26 values associated with a possible CCE.

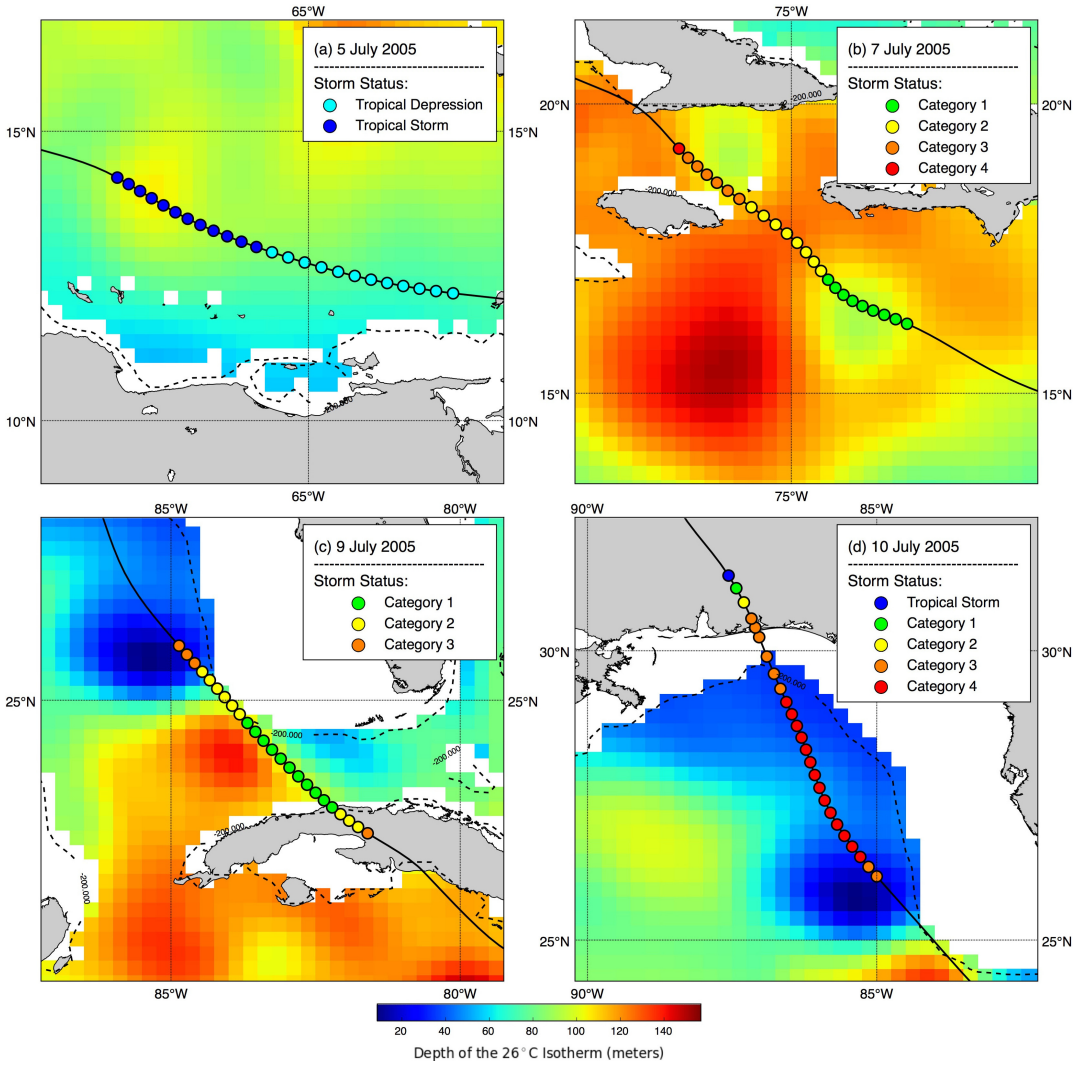

Figure 4.9: Hurricane Dennis' panel showing D26 with track overlain for each day. Areas where ocean depth is $\leq$ 200 m are masked in white.

The daily analysis of Dennis reveals that the storm underwent strengthening despite small D26 values as it passed near and over potential CCEs. In addition, strengthening occurred as Dennis tracked over areas where D26 exceeded 120 m. U_h was found to play an important role in the intensity fluctuations as a faster U_h indicates less time spent over small D26 values and thus continued strengthening.

4.1.5 Hurricane Emily

The first category 5 storm of the season formed from a tropical wave that exited the coast of Africa on 6 July 2005. On 11 July, the wave strengthened to tropical depression status as it moved westward over the Atlantic under a ridge. The depression was slow to develop initially because of the presence of moderate shear and dry air. However, on 12 July, the tropical depression became a tropical storm with winds of 18 m s^{-1} (Figure 4.10).

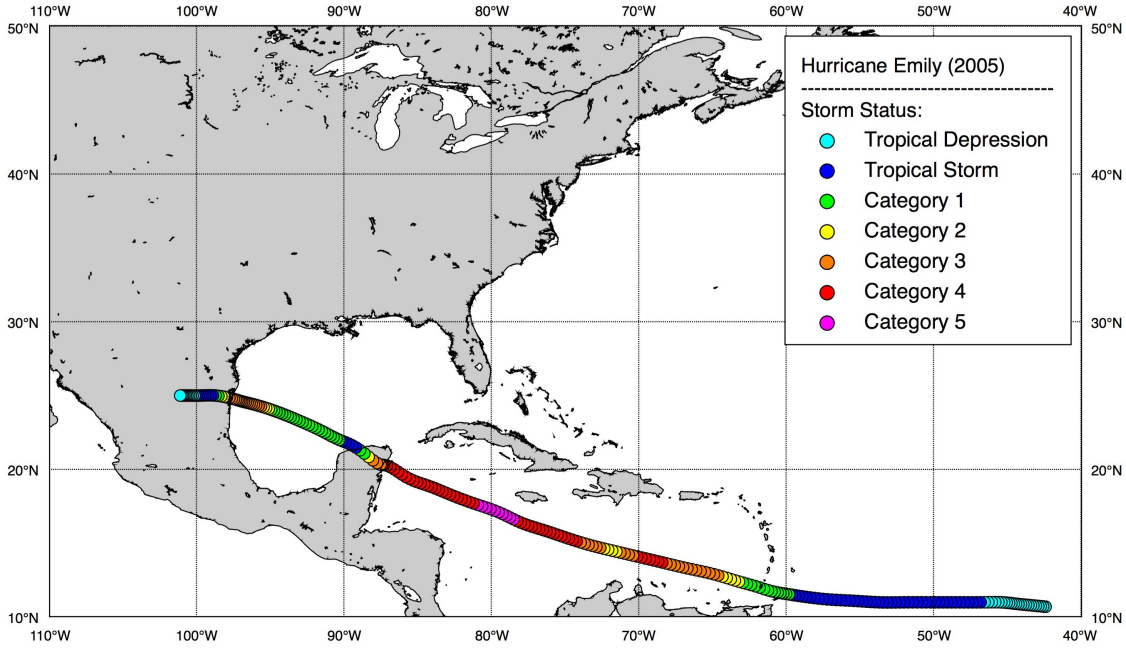

Figure 4.10: Hurricane Emily's (11 – 21 July 2005) track.

Emily continued to move westward and became a category 1 hurricane late on 13 July with winds of 33 m s^{-1}. Once Emily entered the Caribbean Sea, it further strengthened steadily to a

category 4 hurricane on 15 July with winds of 59.2 m s^{-1}. Emily then moved west-northwestward under a strong ridge located to the north. Later on 15 July, the storm briefly weakened to a category 2 with winds of approximately 49 m s^{-1}. By late on 16 July, Emily grew to category 5 strength for a few hours, with winds of 70.5 m s^{-1}, before weakening back down to category 4 strength later that same day. Emily made landfall on the island of Cozumel, Mexico, on 18 July as a category 4 storm with winds exceeding 58 m s^{-1}. The storm then made a second landfall in the Yucatán Peninsula again as a category 4. Emily entered the Gulf of Mexico where strengthening was initially slow. However, on 18 July, Emily underwent a rapid intensification, wherein pressure dropped approximately 32 mb and the storm intensified from a category 1 to category 3 hurricane in this 24-hour period. Emily made a third landfall near San Fernando, Mexico, on 20 July as a category 3 storm.

Hurricane Emily's along-track analysis (Figure 4.11) revealed favorable conditions.

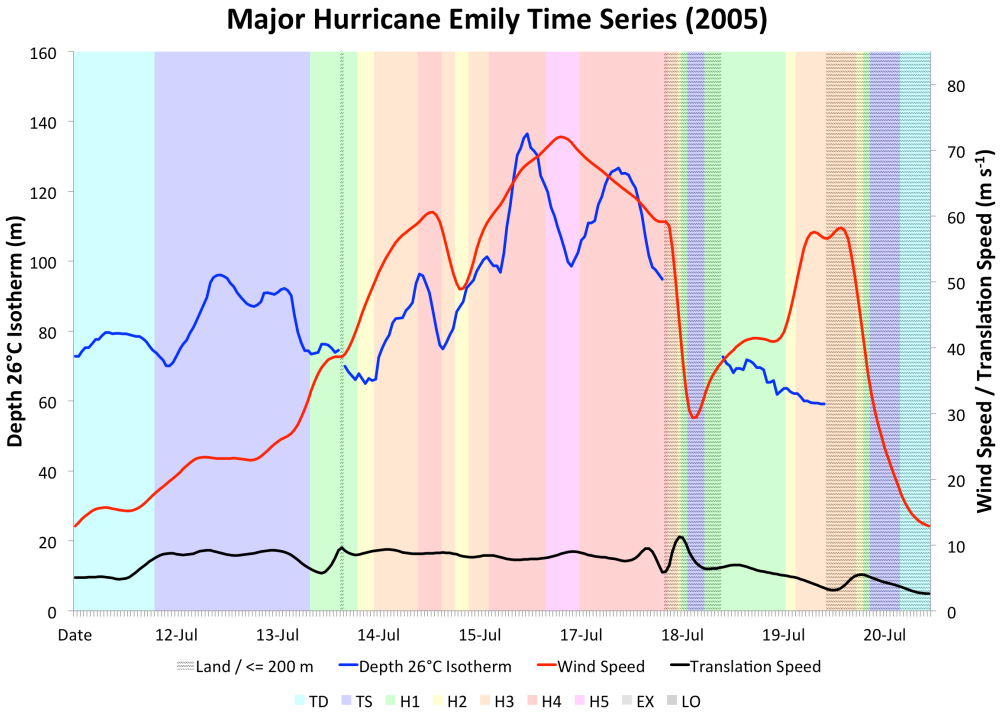

Figure 4.11: Hurricane Emily's time series of D26, U_{10}, U_h, and intensity category.

Emily had an average D26 of 87.5 m and an average U_h of 7.2 m s^{-1}. Hurricane Emily experienced a very deep layer of warm surface waters (*i.e.*, large D26 values) at times, with the maximum along-track value being 136.4 m on 16 July. The minimum along-track D26 value was 59.1 m, when the storm was located in the Bay of Campeche on 20 July. These results showed that Emily did not experience any substantially low D26 values, with a minimum of 59.1 m.

The along-track analysis of Hurricane Emily indicated that, like Hurricane Dennis, the storm had abundant oceanic heat content throughout most of its track. Emily also appears to have traveled either directly over or very near several WCEs and CCEs. The first possible WCE that Emily appears to have encountered was on 15 July as the storm moved westward in the Caribbean Sea. Emily tracked just to the south of this feature (Figure 4.12a) with an intensity increase to a category 4 with winds of 59.2 m s^{-1}. Emily was previously a category 3 storm prior to encountering the WCE. D26 values near the eddy were in the 90 – 95 m range with U_h approximately 8 m s^{-1}. Given the high D26 values and moderate U_h, it appears likely that this feature caused Emily to increase in intensity from a category 3 to a category 4. Later on 15 July, Emily moved out of this WCE and into shallower warm water layers, with D26 in the 70 – 85 m range and U_{10} decreasing to a minimum of 48.2 m s^{-1}, equivalent to a category 2 storm. The drop in D26 values after Emily exited the WCE may be partly responsible for this drop in strength from a category 4 to a category 2 within a 24-hour period.

On 16 July, Emily appeared to have directly encountered a large WCE (Figure 4.12b). Shortly afterwards, intensity increased to category 5 status, with winds of over 70 m s^{-1}. As Emily tracked over this WCE, it was at category 4 status for most of the time period. However, as Emily neared the western edge of the eddy, it increased to a category 5 with winds of 70.5 m s^{-1}. D26 values in the WCE averaged well over 100 m, with a maximum of 136.4 m. U_h

throughout most of 16 July was 7 m s^{-1}, with a slight increase to 8 m s^{-1} toward the end of the day. Although Emily spent only a few hours over this WCE, along-track D26 averaged 115.8 m. Emily's encounter with this large WCE, coupled with the U_h of 7 m s^{-1}, likely had a significant role in the increase to category 5 status.

Emily encountered a second WCE on 17 July as the storm moved northwestward toward the Yucatán (Figure 4.12c). Early on 17 July, Emily remained at category 5 status. However, after the storm encountered slightly smaller D26 values in the upper 90s, the storm decreased to a high-end category 4 with U_{10} of 69.4 m s^{-1}. However, later on 17 July, Emily once again tracked over an apparent WCE, where D26 values exceeded 120 m, with a peak of 126.6 m. U_h again averaged approximately 8 m s^{-1} with a decrease to 7 m s^{-1} later on 17 July. An average D26 value of 114.7 m indicated that this maintenance of strength was likely due in part to the abundant oceanic heat content that the storm encountered along with favorable atmospheric conditions.

As Emily made landfall on the Yucatán peninsula, it weakened to a category 1 due to the interaction with land. As it emerged back into the Gulf of Mexico on 19 July, it regained intensity to a category 3 storm with U_{10} of 50.6 m s^{-1}. A look at D26 indicates that Emily avoided substantial oceanic thermal features, as D26 values averaged 66.5 m throughout 19 July (Figure 4.12d). U_h also slowed to an average of 6 m s^{-1}. U_h and D26 seem to have played little role in the strengthening due to their marginal nature, although some contribution cannot be dismissed.

The daily analysis of Emily reveals that the storm passed directly over WCEs and CCEs. These features explain a portion of Emily's intensity fluctuations. U_h also played a role in the intensity as well by either increasing or decreasing the time spent over these features. Emily was found to intensify while located in the southwestern Gulf of Mexico despite modest D26 values

and a slowed U_h, indicating that atmospheric conditions were likely a cause for this increase in intensity.

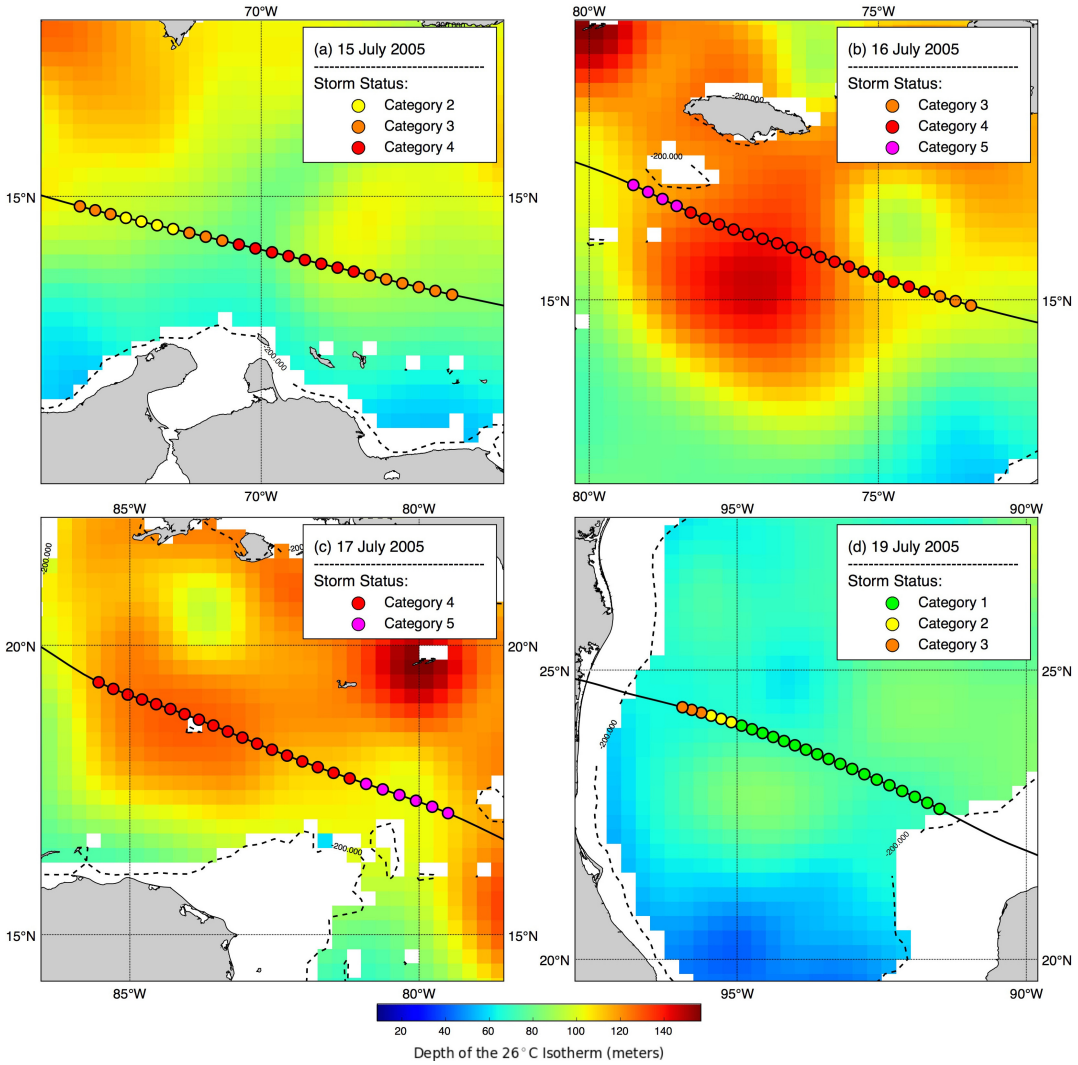

Figure 4.12: Hurricane Emily's panel showing D26 with track overlain for each day. Areas where ocean depth is $\leq$ 200 m are masked in white.

4.1.6 Tropical Storm Franklin

Tropical Storm Franklin formed from a tropical wave that exited the coast of Africa on 10 July 2005. This wave eventually approached the Lesser Antilles on 18 July. However, it lacked deep convection and was being impacted by strong vertical wind shear. Once shear relaxed and convection increased, the wave became a tropical depression on 21 July. The

depression intensified to Tropical Storm Franklin late on 21 July with winds of 18.6 m s^{-1} (Figure 4.13). The storm moved northwestward with most of its heavy convection on the eastern side. Strengthening was again slow to occur as strong shear returned. Once this shear abated, the storm reached its peak intensity of 31.6 m s^{-1} on 23 July. Shear again increased, causing the storm to weaken to a depression briefly on 26 July. Once shear decreased, the storm strengthened back to tropical storm status while moving northeastward. Franklin eventually became an extratropical low on 30 July.

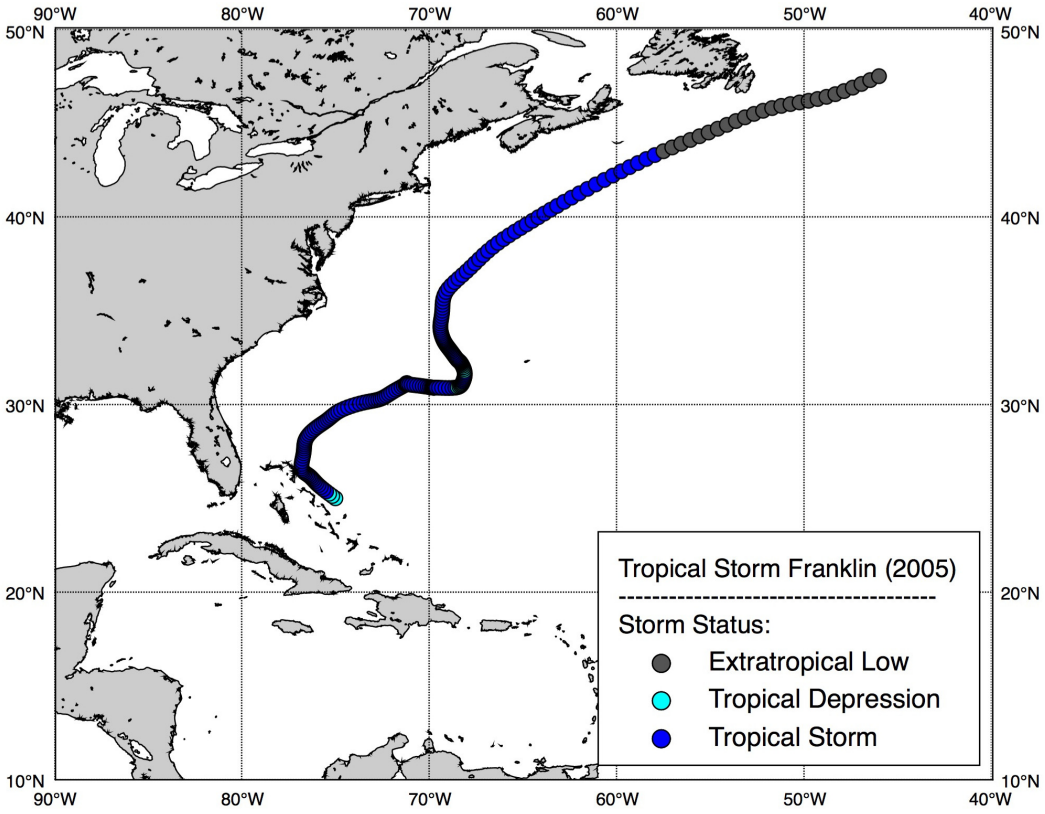

Figure 4.13: Tropical Storm Franklin's (21 – 31 July 2005) track.

Tropical Storm Franklin's along-track data analysis shows that the storm experienced small D26 values throughout its entire track (Figure 4.14). With an average D26 of only 36.3 m, it was apparent that the storm averted abundant oceanic heat content during its entire lifespan. Coupled with the small along-track D26 values, the storm's U_h was very low (average of 5.3 m s^{-1})

throughout most of its lifespan, with an acceleration in speed as the storm moved into higher latitudes. As Franklin traveled over these low D26 values, its U_h was typically below 5 m s^{-1}, and at times, below 2 m s^{-1}. Beven *et al.* (2008)'s report indicates that shear played an important role in stifling the intensity of the storm, but these results indicate that very small D26 values along with a slow U_h may have also significantly contributed to Franklin's minimal intensity.

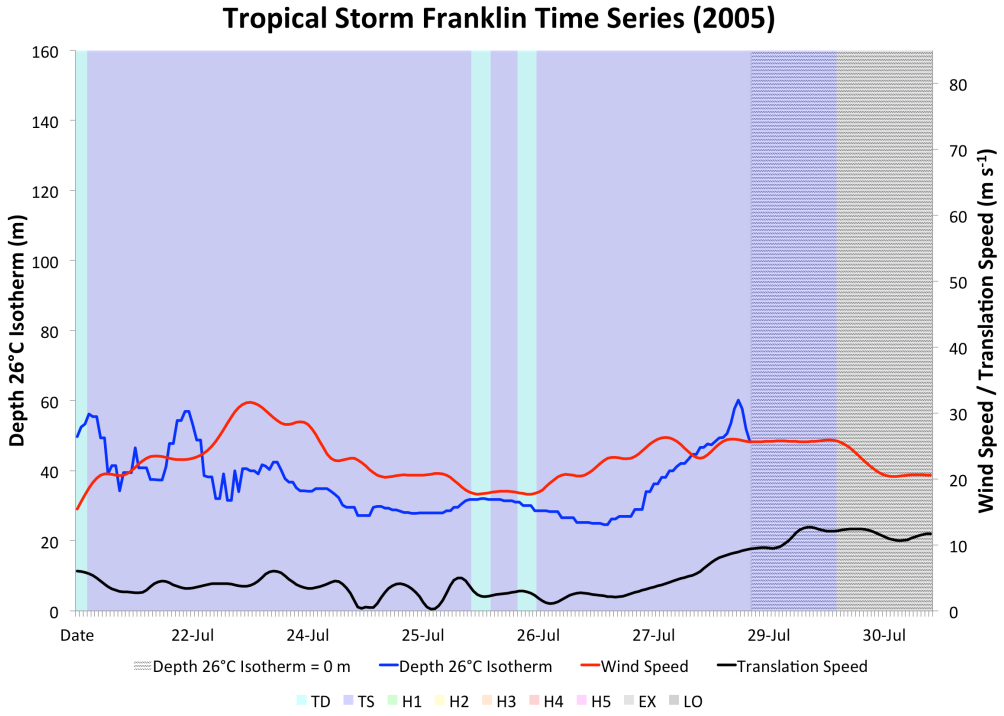

Figure 4.14: Tropical Storm Franklin's time series of D26, U_{10}, U_h, and intensity category.

4.1.7 Tropical Storm Gert

Tropical Storm Gert formed from the same tropical wave that bred Tropical Storm Franklin, which initially moved off the African coast on 10 July 2005. The southern portion of the wave continued to move westward into the Caribbean Sea, without any development. The wave moved over the Yucatán peninsula and emerged into the Bay of Campeche on 23 July (Figure 4.15). The system became a tropical depression on 23 July and a tropical storm on 24

July. Gert's peak intensity was 20.6 m s^{-1} late on 24 July. The storm's intensity fluctuated from tropical storm back to depression, then back to a tropical storm, during the day on 24 July.

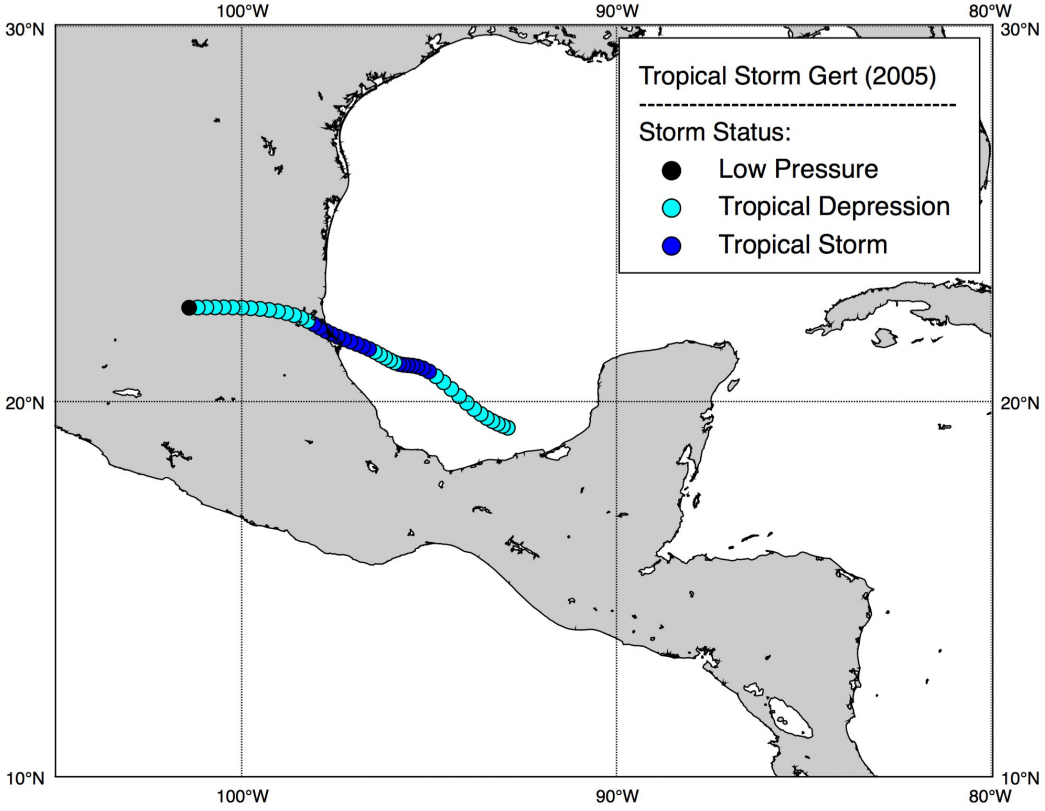

Figure 4.15: Tropical Storm Gert's (23 – 25 July 2005) track.

The storm made landfall near Cabo Rojo, Mexico, on 25 July. Gert weakened rapidly to a low-pressure system as it encountered the rugged terrain in Mexico.

Tropical Storm Gert's analysis revealed that the storm experienced similar conditions as Tropical Storm Franklin did. The warm pool was extremely shallow; D26 values were very small throughout the track (Figure 4.16), with an average of 46.9 m. U_h was also low, with an average of 5.7 m s^{-1}. U_h dropped to approximately 3 m s^{-1} at times while the storm was situated over D26 values in the low 50s. It appears that Tropical Storm Gert did not experience highly favorable oceanic conditions during its time as a storm. This finding along with a slow U_h led to the storm

only attaining tropical storm status. Atmospheric conditions could have also played an important role in limiting the intensity of this storm.

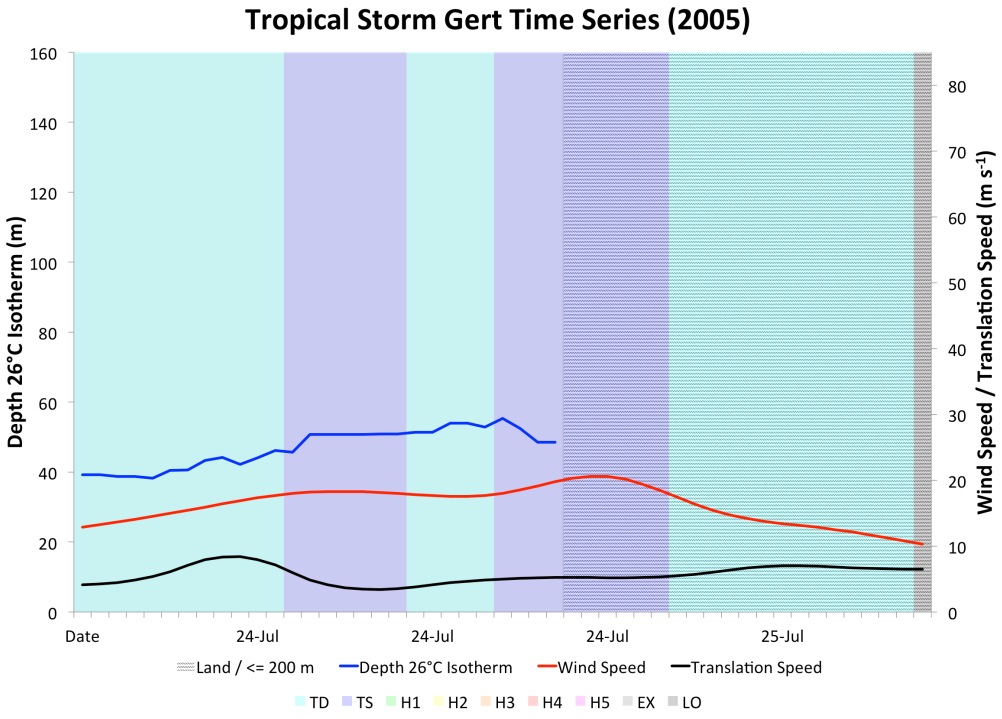

Figure 4.16: Tropical Storm Gert's time series of D26, U_{10}, U_h, and intensity category.

4.1.8 Tropical Storm Harvey

Tropical Storm Harvey formed from a tropical wave that entered the Atlantic Ocean from the African coast on 22 July 2005. This wave moved westward with little to no development. As the wave moved north of Puerto Rico, it gave rise to a tropical depression on 2 August. Despite being poorly organized due to strong southerly wind shear, the depression became Tropical Storm Harvey on 3 August (Figure 4.17). Harvey moved mostly eastward, then northeastward while it accelerated. The storm continued to strengthen and reached a peak intensity of 28.5 m s^{-1} on 4 August. The storm then weakened due to strong shear, which caused winds to weaken slightly. The storm became extratropical on 9 August and degenerated into a low-pressure system on 12 August.

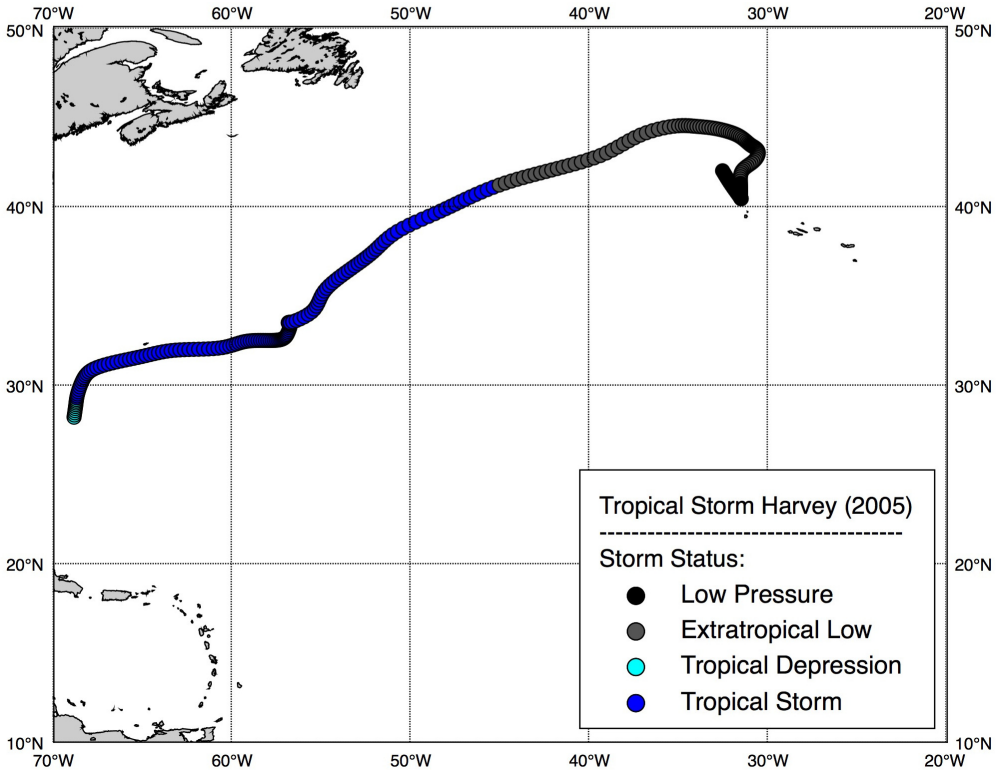

Figure 4.17: Tropical Storm Harvey's (2 – 14 August 2005) track.

Analysis of Tropical Storm Harvey suggests that the storm had a limited amount of oceanic heat content available during its entire track. This was no surprise given Harvey's track northeastward in the Atlantic Ocean, where ocean temperatures cool significantly with increasing latitude and thus has a thinning warm surface water pool (*i.e.*, decreasing D26 values; Figure 4.18). The average D26 value was 31.2 m, and as Harvey increased in latitude, D26 values decreased to 0 m. This indicates that even the sea surface temperatures were below 26°C. Harvey's limited intensity as only a modest tropical storm was likely a result of these small D26 values and the storm's northward migration. U_h averaged 4.8 m s^{-1} along-track, while U_h decreased to less than 1 m s^{-1} at times. It is likely that these small D26 values, coupled with a slow U_h, limited the intensity of Harvey. Atmospheric conditions also played a role in limiting

intensity, as Beven *et al.* (2008) noted the storm was impacted multiple times with strong vertical shear.

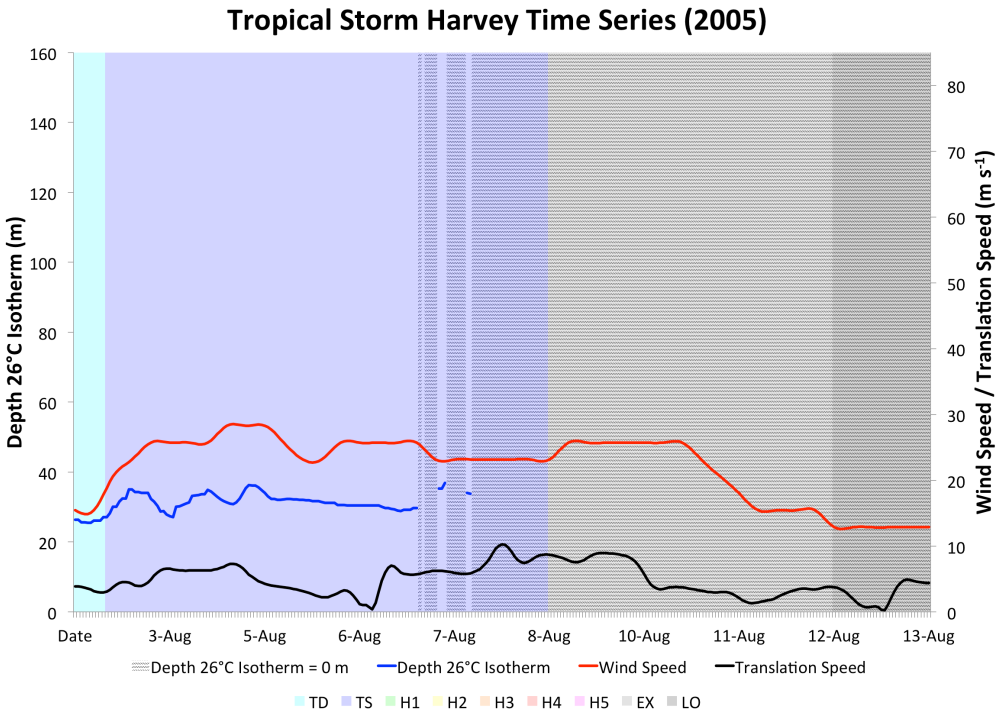

Figure 4.18: Tropical Storm Harvey's time series of D26, U_{10}, U_h, and intensity category.

4.1.9 Hurricane Irene

Hurricane Irene (Figure 4.19) formed from a strong tropical wave that originated over the African continent. This well-organized wave entered the Atlantic Ocean on 1 August 2005. However, cooler waters apparently caused the wave to weaken substantially as it moved near the Cape Verde Islands. The wave continued westward and began to encounter warmer waters, where convection increased enough for it to be labeled a tropical depression on 4 August. Conditions favorable for development continued, and on 7 August the depression became Tropical Storm Irene. This status was short-lived, as the storm encountered cooler waters and dry, stable air. This caused the storm to downgrade back to a tropical depression later on 7 August. Once shear decreased, Irene again regained tropical storm status on 11 August. The

storm moved into an area with weak vertical wind shear and a statically unstable environment. Irene became a hurricane late on 14 August. On 15 August, Irene attained category 2 status, with winds of 43.1 m s^{-1}. Shortly after this continued strengthening, Irene experienced increased southwesterly wind shear, causing the storm to weaken to a tropical storm on 17 August. Irene was then absorbed by an extratropical low on 18 August.

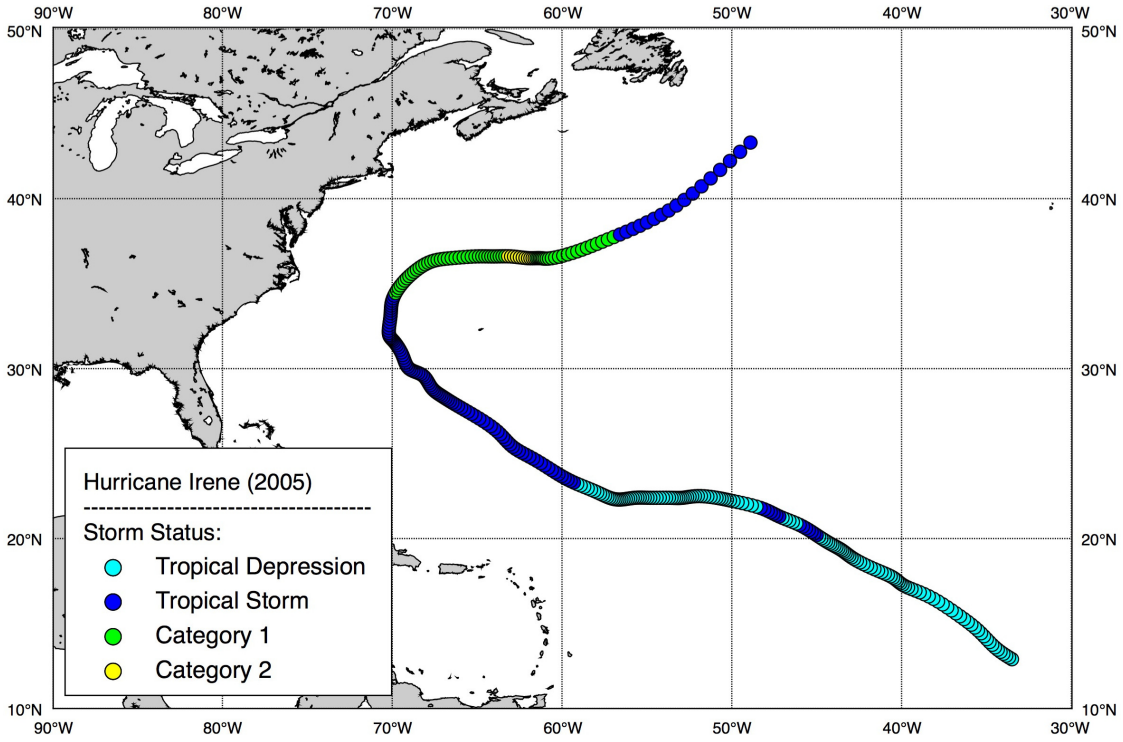

Figure 4.19: Hurricane Irene's (4 – 18 August 2005) track.

Hurricane Irene experienced unfavorable atmospheric conditions (strong vertical wind shear) frequently throughout its track. Along with these unfavorable atmospheric conditions at times, oceanic conditions were also not ideal for rapid intensification as evidenced by an average D26 of 46.4 m (Figure 4.20). Early in Irene's track, it did experience D26 values in the mid-70s. The maximum D26 value of 74.5 m occurred on 6 August with a U_h of 4.4 m s^{-1}. The storm continued to travel over thick warm-water layers, with D26 values in the 60 – 70 m range throughout the rest of 6 August and U_h in the 3 – 4 m s^{-1} range.

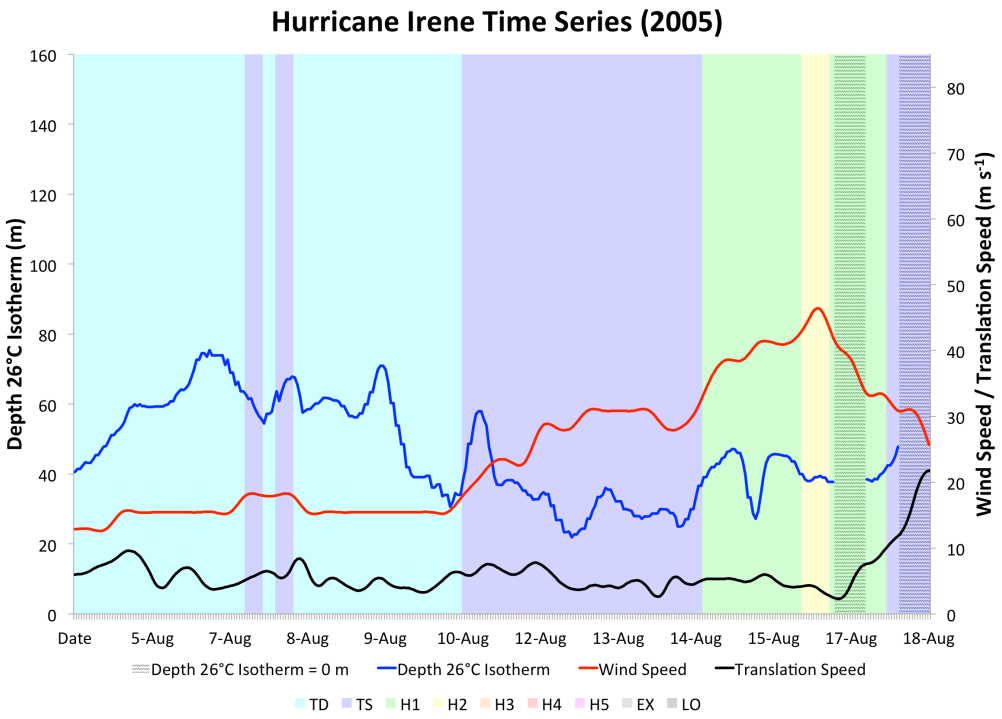

Figure 4.20: Hurricane Irene's time series of D26, U_{10}, U_h, and intensity category.

Shortly after the storm experienced these conditions, it became a tropical storm on 7 August. These large D26 values in the 60s and 70s along with a slow U_h may explain the intensification to tropical storm status on 7 August. However, as Irene continued to move along its track, D26 values steadily decreased. On 14 August Irene became a category 1 hurricane with U_{10} of 33.4 m s^{-1}. During this time period, Irene was over a thin layer of warm water (*i.e.*, D26 values in the mid-30s). The storm's U_h was also approximately 4 – 5 m s^{-1}. Given these small D26 values and slow U_h, it was apparent that oceanic and U_h conditions were not ideal for intensification to a category 1. By contrast, atmospheric conditions during the time of intensification were noted by Beven *et al.* (2008) to be favorable with low vertical wind shear and a convectively unstable environment present. Thus, it is likely that atmospheric rather than oceanic conditions were largely responsible for this intensification. On 16 August, Irene strengthened to a category 2 storm with U_{10} of 43.1 m s^{-1}. Again, D26 values were relatively small (upper 30s). Atmospheric

conditions were once again likely to be largely responsible for Irene's intensification to category 2 status, particularly because of small D26 values and a U_h of approximately 4 m s^{-1}. As Irene moved northeastward, D26 values decreased to 0 m, as expected. The storm weakened and was absorbed by an extratropical system.

4.1.10 Tropical Storm Jose

Tropical Storm Jose (Figure 4.21) formed from a tropical wave that moved off the African coast of 8 August 2005.

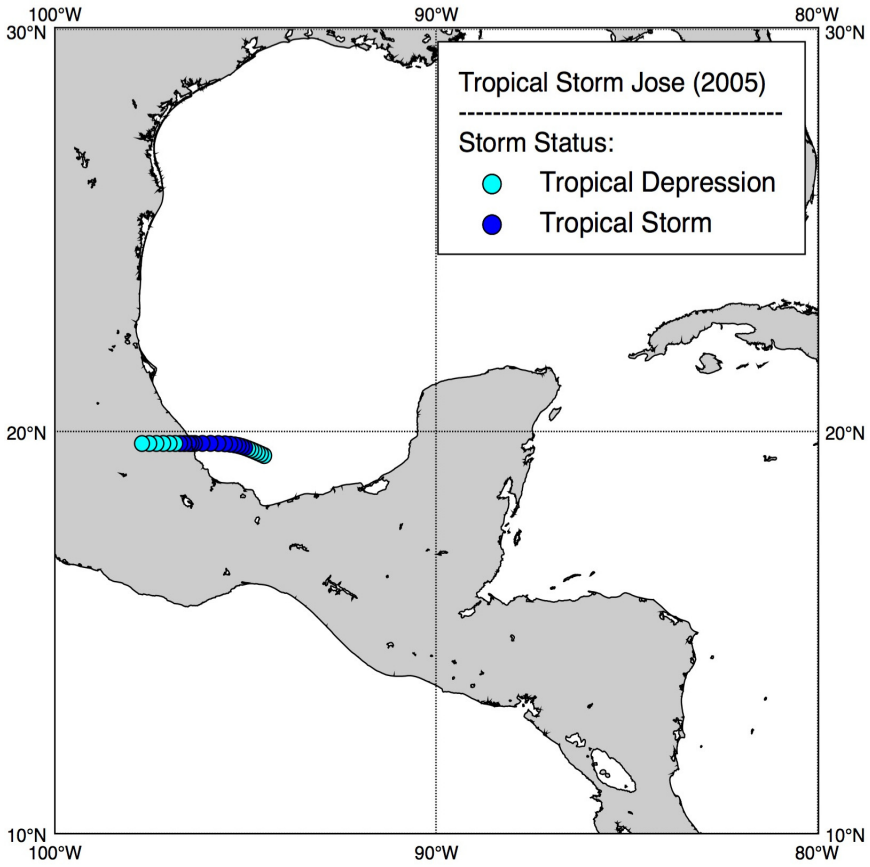

Figure 4.21: Tropical Storm Jose's (22 – 23 August 2005) track.

This wave moved into the Caribbean Sea with no further development. However, once the convection entered the Bay of Campeche on 21 August, convection developed slowly.

On 22 August, the system began to organize rapidly and a tropical depression formed in the Bay of Campeche. The system continued to organize while convection increased. Later on 22 August, the depression became Tropical Storm Jose with U_{10} of 18 m s^{-1}. Jose's maximum U_{10} reached 26.3 m s^{-1} on 23 August just before landfall 30 miles north of Veracruz, Mexico.

Tropical Storm Jose's along-track data suggests that this system experienced unfavorable oceanic conditions. The warm layer was thin (Figure 4.22) with a mean D26 of 35.3 m. Jose's U_h averaged only 4 m s^{-1}.

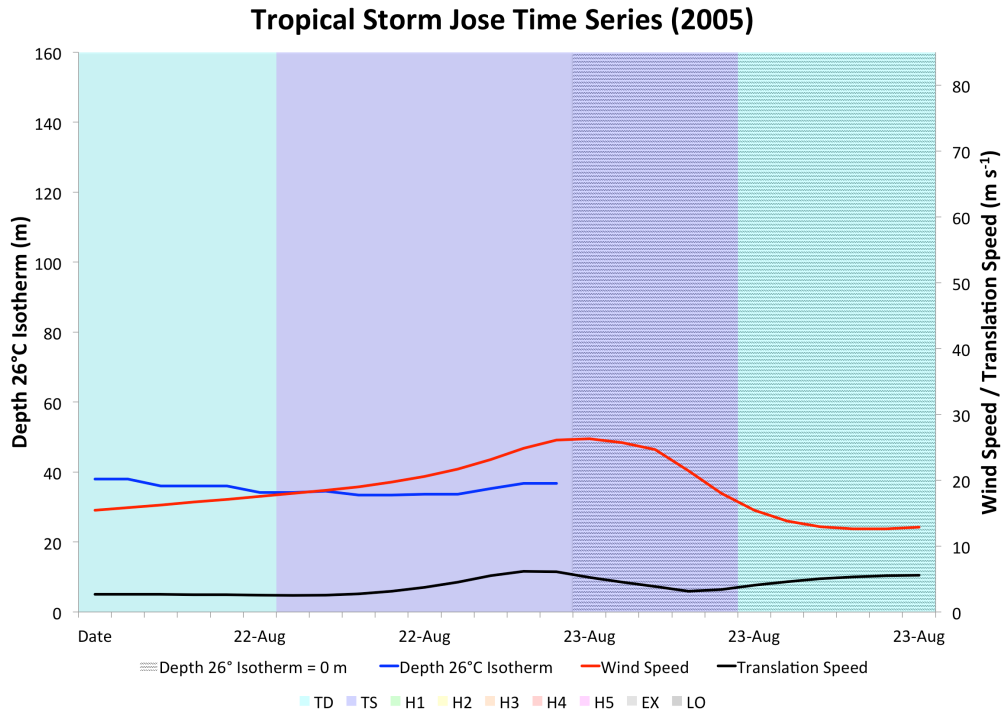

Figure 4.22: Tropical Storm Jose's time series of D26, U_{10}, U_h, and intensity category.

This U_h, along with small D26 values, likely limited intensity despite favorable atmospheric conditions, as Beven *et al.* (2008) noted Jose's ominous strong upper-tropospheric divergence due to anticyclonic flow. This strong upper-level divergence likely explained Jose's intensification to a tropical storm despite unfavorable oceanic conditions.

4.1.11 Hurricane Katrina

Hurricane Katrina, the deadliest and one of the most powerful hurricanes of the 2005 North Atlantic basin hurricane season (Figure 4.23), formed from complex interaction of three atmospheric systems.

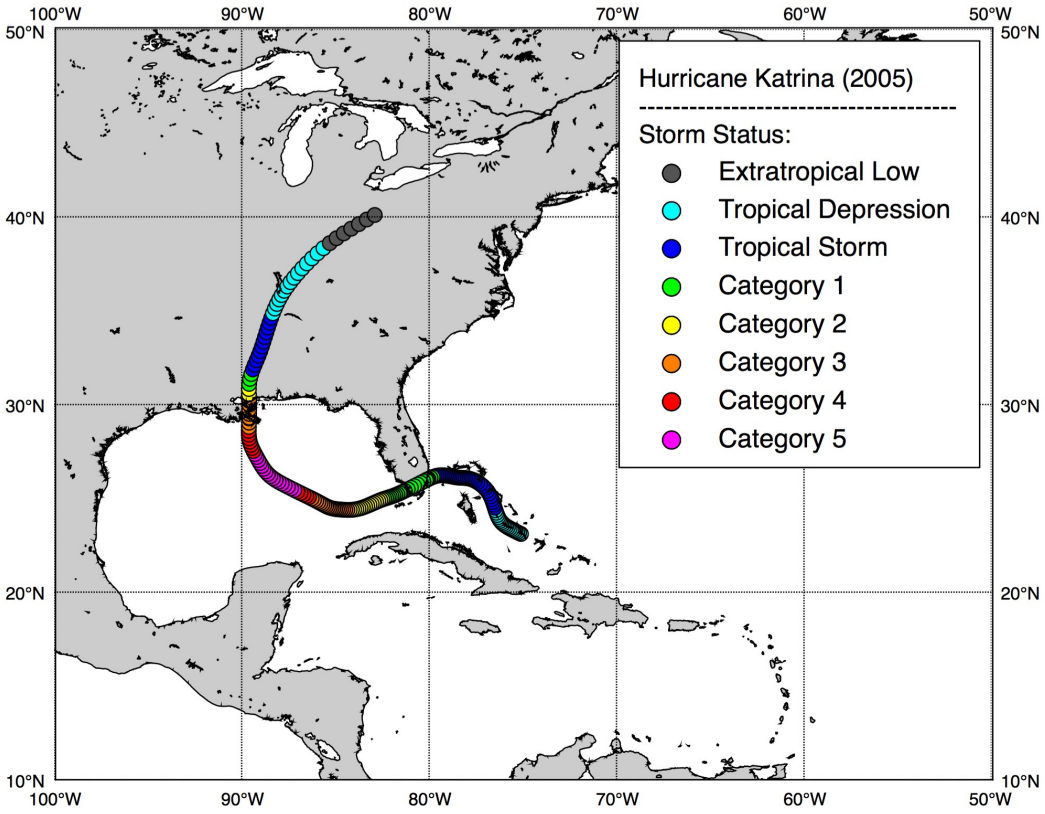

Figure 4.23: Hurricane Katrina's (23 – 31 August 2005) track.

These included a tropical wave, the remnants of tropical depression #10, and an upper-tropospheric trough (Beven *et al*., 2008). As tropical depression #10 dissipated, its mid-tropospheric circulation remained. This circulation merged with a tropical wave that moved off the coast of Africa on 11 August 2005. This merge took place near the Leeward Islands, and on 23 August, a tropical depression formed. Conditions became increasingly favorable and Tropical Storm Katrina formed near the Bahamas on 24 August with winds of 18 m s^{-1}. Initially after reaching named status Katrina moved northwestward, but a strong ridge over the eastern United

States and Gulf of Mexico steered the storm westward toward Florida. Katrina slowly intensified and became a category 1 hurricane on 25 August just before landfall near Miami, Florida. Moving over the Gulf of Mexico, the storm experienced two rapid intensification processes, both of which took place during the time period 26 – 28 August (Beven *el al*. 2008). On 28 August, during the second rapid intensification, Katrina became a category 5 storm with U_{10} of 70.4 m s^{-1}. A peak U_{10} of 77.4 m s^{-1} occurred on 28 August. Katrina continued its movement through the Gulf of Mexico, moving generally northwestward to north-northwestward. As Katrina neared the Louisiana coast, it weakened to a category 3 storm with U_{10} of 58.7 m s^{-1}. Katrina made its second landfall in Buras, Louisiana, on 29 August and its third and final landfall near the mouth of the Pearl River located on the border of Louisiana and Mississippi.

Analysis of D26 and U_h associated with Katrina reveals why it attained category 5 status and was one of the most powerful storms of the season. D26 averaged 68.8 m along-track and reached the upper 80s at times, with a maximum of 88.6 m, and relatively deep warm water pool throughout most of its track (Figure 4.24). The storm also had a slow mean U_h of 5.3 m s^{-1}, with speeds of only 2 m s^{-1} at times. This slow speed, coupled with a deep along-track warm water pool, likely influenced Katrina's rapid intensification processes. Walker *et al*. (2006) found that Katrina's rapid intensification while in the Gulf of Mexico was attributed to very high sea surface temperatures (SSTs) (*i.e*., > 30°C) between 15° N and 25° N. These highly favorable SSTs coupled with the deep along-track warm water pool and slow U_h all appeared to have combined to allow Katrina to reach its peak intensity of 77.4 m s^{-1} on 28 August. In addition, Walker *et al.* (2006) noted the importance of the Loop Current in Hurricane Katrina's rapid intensification, as there was an abundance of oceanic heat content available as the storm traveled directly over this current.

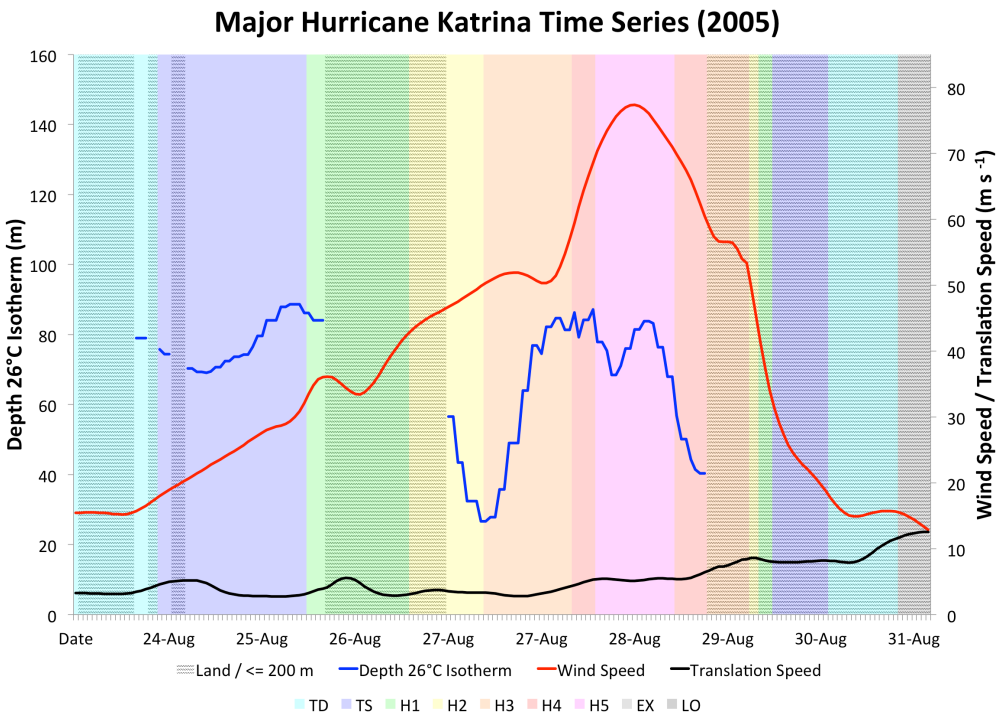

Figure 4.24: Hurricane Katrina's time series of D26, U_{10}, U_h, and intensity category.

Daily analysis of Katrina's oceanic conditions along with U_h along-track suggests that the storm encountered both WCEs and CCEs. Katrina also passed directly over the Loop Current. The storm traveled over a deep warm water pool as evidenced by large D26 values. However, it also traversed waters with much smaller D26 values; both the deep and shallow warm water pools appear to have influenced the eventual strength of the storm. On 25 August, just before Katrina's first landfall near Miami, Florida, the storm strengthened to category 1 with U_{10} of 33.5 m s^{-1}. D26 values on this day averaged 80.7 m, and increased to the mid- and upper 80s as Katrina neared the coast of Florida. During that time, U_h was in the 2 – 3 m s^{-1} range. It appears that these favorable conditions assisted in Katrina's intensification into a category 1 hurricane just before landfall in Florida (Figure 4.25a). As Katrina entered the southeastern Gulf of Mexico on 26 August, it slowly strengthened. On 27 August, Katrina passed directly over a CCE (Figure 4.25b), and D26 values decreased to the lower-30s to mid-20s in this CCE, with a minimum of

26.7 m. U_h was approximately 3 m s^{-1} as Katrina moved over this CCE, with an average of 3.2 m s^{-1} during the 27 August. These conditions would presumably have weakened Katrina as it passed over this CCE. However, the storm did not weaken, but instead strengthened to a category 3 status with U_{10} of 50.3 m s^{-1}. Given the small D26 values and slow U_h during this period, it appears that atmospheric conditions must have been highly favorable for development during this time period to compensate for the unfavorable warm pool thickness and translational speed. Beven *et al.* (2008) noted that wind shear was minimal in the Gulf of Mexico during this time due to the presence of a large upper-tropospheric anticyclone. This anticyclone allowed for efficient upper-level outflow, assisting in Katrina's strengthening despite being situated over a CCE.

On 28 August, Katrina experienced a rapid intensification process whereby it strengthened to a category 5 storm with a mean U_{10} of 70.4 m s^{-1}. A maximum U_{10} of 77.4 m s^{-1} also occurred on this day. Katrina passed over the Loop Current and a WCE (Figure 4.25c), a possible cause for this rapid intensification to a category 5 storm. Walker *et al*. (2006) and Jaimes and Shay (2009) also noted the influence of the Loop Current on Katrina's rapid intensification. D26 averaged 79.6 m and U_h was 5 m s^{-1} during this period. As Katrina passed over the Loop Current, D26 values were in the mid-80s, while U_h was a slow 3 – 4 m s^{-1}. This slow speed along with a deep warm pool likely worked together to cause Katrina to strengthen from a category 3 to a category 5. The WCE that Katrina encountered later on 28 August contained D26 values in the mid-80s. Katrina's U_{10} continued to increase, reaching a maximum of 77.4 m s^{-1} while the storm was located directly over this WCE. U_h was also a modest 5 m s^{-1}, which indicated that the storm spent a moderate amount of time over this feature. On 29 August, the day in which Katrina made its last two landfalls in Louisiana and it weakened from

a category 5 to a category 3. Beven *et al.* (2008) attributed this weakening to dry air, cooler SSTs, and increased wind shear. Katrina experienced low D26 values prior to landfall (Figure 4.25d).

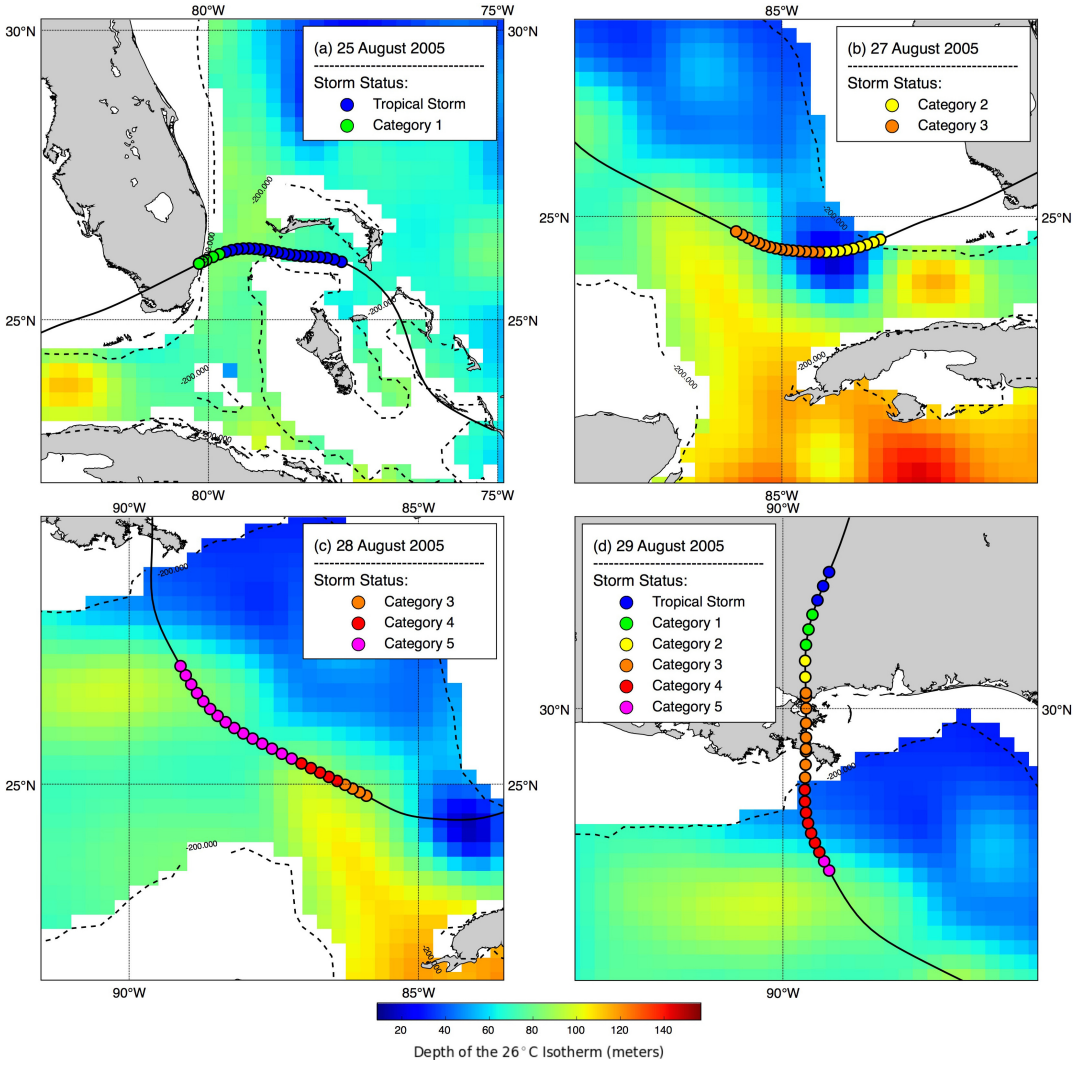

Figure 4.25: Hurricane Katrina's panel showing D26 with track overlain for each day. Areas where ocean depth is ≤ 200 m are masked in white.

Values rapidly decreased from the upper 60s to a minimum of 40.3 m prior to landfall. U_{10} weakened from 72 m s^{-1} to 60.5 m s^{-1} during the first 9 hours of 29 August (only 9 hours of usable D26 data were available on 29 August due to the storm's proximity to the coast). U_h was not particularly slow, at 5 – 6 m s^{-1} during this same time. These results indicate that Katrina's

weakening prior to landfall may have been partially caused by a sudden decrease in D26 from 67.9 m to 40.3 m in a 9-hour period, along with dry air intrusion and increased shear.

Katrina's daily along-track analysis reveals that the storm passed over a small CCE, the Loop Current, along the northern margin of a WCE, and experienced shifts in D26 values near coastal areas that contributed to its intensity fluctuations. The slow U_h was also likely to contribute to the storm's intensity by allowing abundant time over the Loop Current and WCE. Katrina's intensification to a category 1 prior to its first landfall in Florida was found to be influenced by high D26 values and a slow U_h. Katrina's weakened state as it approached landfall in Louisiana was also found to be the result of an abrupt change in D26 values. These findings combined to help explain Katrina's intensity.

4.1.12 Tropical Storm Lee

Tropical Storm Lee formed from a strong tropical wave that entered the Atlantic Ocean on 24 August 2005 from Africa (Figure 4.26).

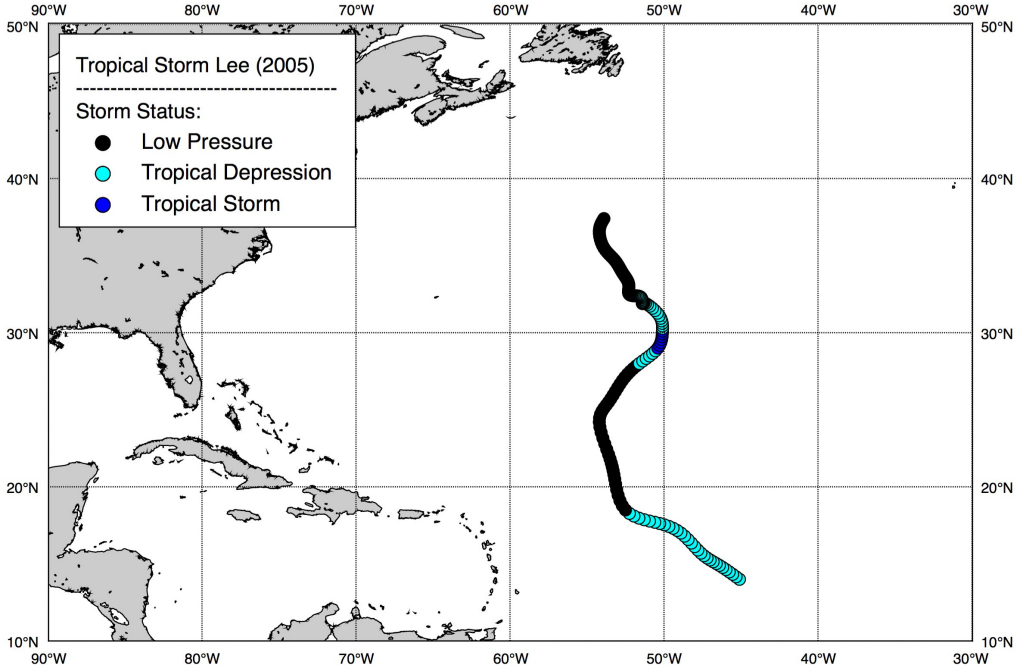

Figure 4.26: Tropical Storm Lee's (28 – 3 September 2005) track.

The wave became better organized with increased shower activity, and on 28 August the system became a tropical depression with U_{10} of 12.9 m s^{-1}. The system then experienced strong northeasterly wind shear, which led the storm to degenerate back to a broad area of low-pressure early on 29 August. The system moved northwestward and then northeastward in the open Atlantic Ocean. As the system moved northward, convection increased enough for the storm to intensify back to a depression on 31 August. Just a few hours after the storm intensified to a depression, it became Tropical Storm Lee with U_{10} of 18 m s^{-1}. Lee was only at tropical storm status for approximately seven hours, as it degenerated back to a depression late on 31 August. The storm moved erratically for the rest of its lifetime, switching between northwestward and northeastward around a non-tropical area of low-pressure (Figure 4.26). Lee became a large, disorganized area of low-pressure on 2 September while moving off to the northeast.

Tropical Storm Lee initially had a large amount of oceanic heat content to tap, but D26 values slowly decreased as the storm moved northward (Figure 4.27). Early in Lee's lifetime as a tropical system, it was traveling over D26 values in the high 60s and low 70s. Around the time period when the depression degenerated back to an area of low-pressure on 29 August, D26 values were in the mid- to upper-80 m range. U_h was approximately 10 m s^{-1}, a high rate of speed. Given the large D26 values near the time when the depression weakened to a broad area of low-pressure, it appears that oceanic factors were not a large contributor to the degeneration. Beven *et al.* (2008) noted that excessive northeasterly wind shear caused the demise of Lee, and these results appear to support that finding as oceanic conditions were favorable with D26 values in the 80s. On 31 August, when Lee became a depression once again, D26 values were in the low 40s and upper 30s. U_h slowed to the 6 – 7 m s^{-1} range. Later on the 31 August, Lee became a tropical storm under D26 values in the low 30s and with a U_h of approximately 5 – 6 m s^{-1}. The

low D26 values and modest U_h suggest that Lee must have experienced favorable atmospheric conditions such as weak vertical wind shear and a moist environment. The results from Tropical Storm Lee suggest that oceanic factors did not play an important role in the intensity fluctuations. Atmospheric factors seemed to be responsible as Lee weakened over deep warm pools (*i.e.*, areas of large D26 values) and strengthened over areas of shallow warm pools (*i.e.*, low D26 values).

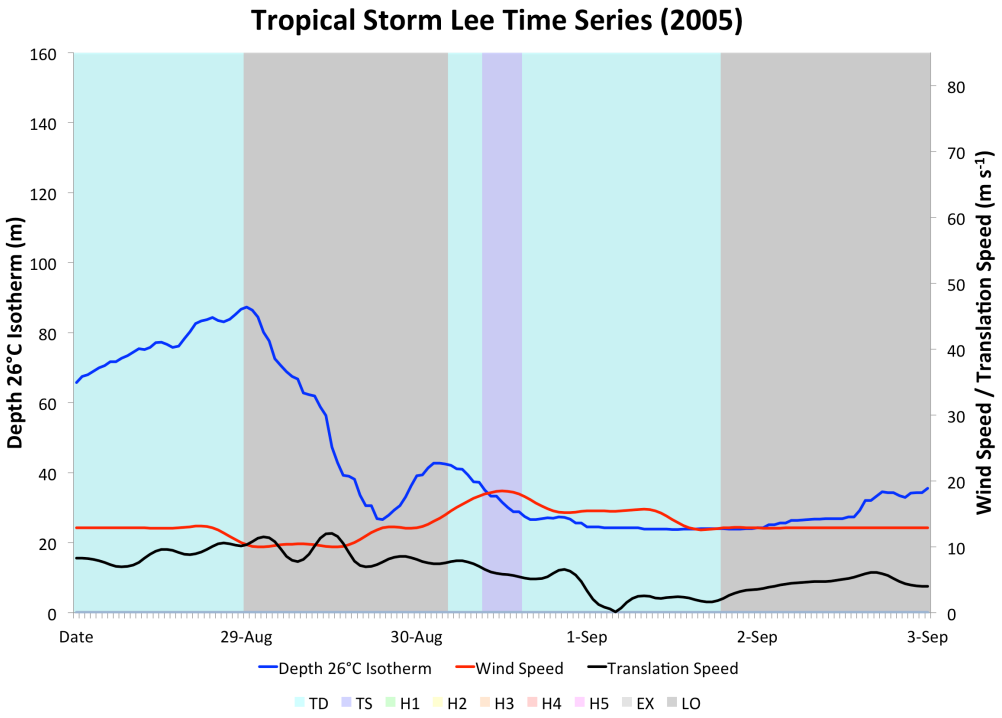

Figure 4.27: Tropical Storm Lee's time series of D26, U_{10}, U_h, and intensity category.

4.1.13 Hurricane Maria

Hurricane Maria was a long-lived tropical cyclone that originated from a tropical wave off the coast of Africa on 27 August. A portion of the wave moved westward and slowly intensified. Strong shear from the southwest caused slow development. However, on 1 September 2005, the convection persisted enough to designate the system as a depression. The depression moved northwestward around a subtropical high-pressure system and became a

tropical storm on 2 September and a hurricane on 4 September (Figure 4.28). Maria continued to strengthen slowly, and on 5 September became a major storm with U_{10} of 50.4 m s^{-1} (category 3). This major status was only to last for approximately five hours. Maria then slowly weakened as it moved off to the northeast – to a tropical storm on 8 September and an extratropical system on 10 September. Note in Figure 4.29 that category 2 and 3 status points are not seen on the track due to their brief nature (Figure 4.28).

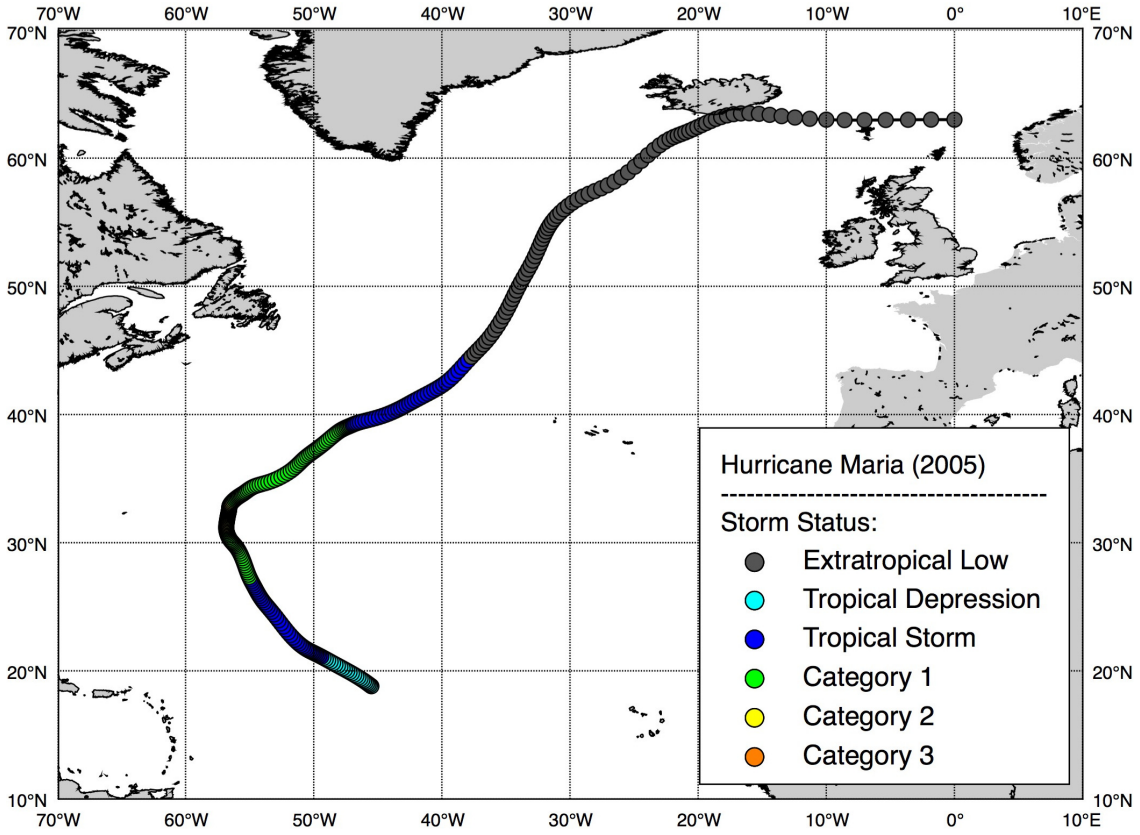

Figure 4.28: Hurricane Maria's (1 – 14 September 2005) track.

Like Tropical Storm Lee, oceanic conditions were not ideal for Maria (Figure 4.29). With an average D26 of 45.8 m, the oceanic heat content available to the storm was limited, especially as the storm gained latitude. As expected, D26 values were greatest near the genesis location and decreased sharply as the storm moved to the north. The largest D26 value of 72.7 m occurred just

before the storm intensified into a tropical storm on 2 September. From that time forward, D26 values decreased from the upper 60s to the lower 30s. As Maria strengthened to category 1 status, D26 values were in the mid-30s. Values decreased to the lower 30s as the storm reached category 2 and eventually category 3 status. U_h was in the 3 – 4 m s^{-1} range when Maria was a category 1 and decreased to approximately 2 m s^{-1} as the storm intensified to a category 2 with U_{10} of 43.1 m s^{-1} on 5 September. Once Maria attained category 3 status late on 5 September, D26 was 31.2 m with a U_h of 2.5 m s^{-1}. This small D26 value coupled with a slow U_h may partially explain why Maria was only at category 3 status for approximately five hours. A favorable atmospheric environment during this time could explain the strengthening that occurred despite low D26 values. D26 values eventually reached 0 m throughout the rest of the track as Maria gained latitude.

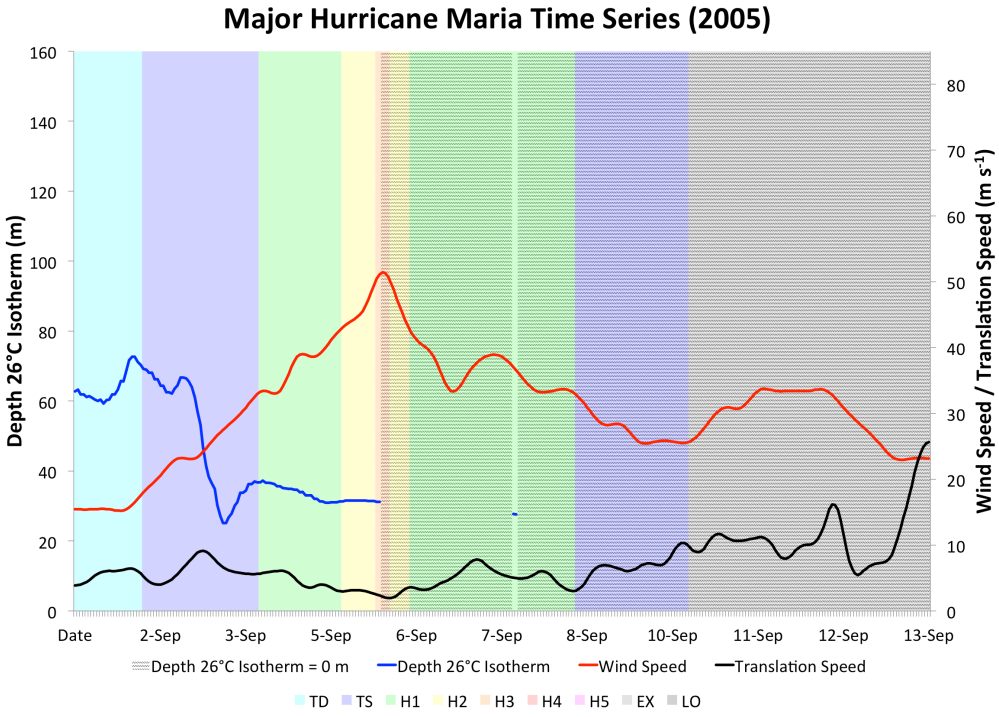

Figure 4.29: Hurricane Maria's time series of D26, U_{10}, U_h, and intensity category.

4.1.14 Hurricane Nate

Hurricane Nate formed from the interaction of a tropical wave and an upper-tropospheric low (Figure 4.30). These two features eventually led to the formation of a tropical depression on 5 September 2005. The depression moved toward the northeast and became Tropical Storm Nate early on 6 September just six hours after its designation as a tropical depression. Strengthening continued and on 7 September Nate became a category 1 hurricane with U_{10} of 33 m s^{-1}. The storm increased in intensity and on 9 September, Nate reached its peak with U_{10} of 41.2 m s^{-1} despite increased vertical wind shear ahead of a short wave trough. As Nate's U_h increased, so did vertical wind shear and mid-level dry air advection. Nate eventually weakened to a tropical storm on 9 September while moving to the northeast. Nate soon transitioned into an extratropical low on 10 September west of the Azores Islands.

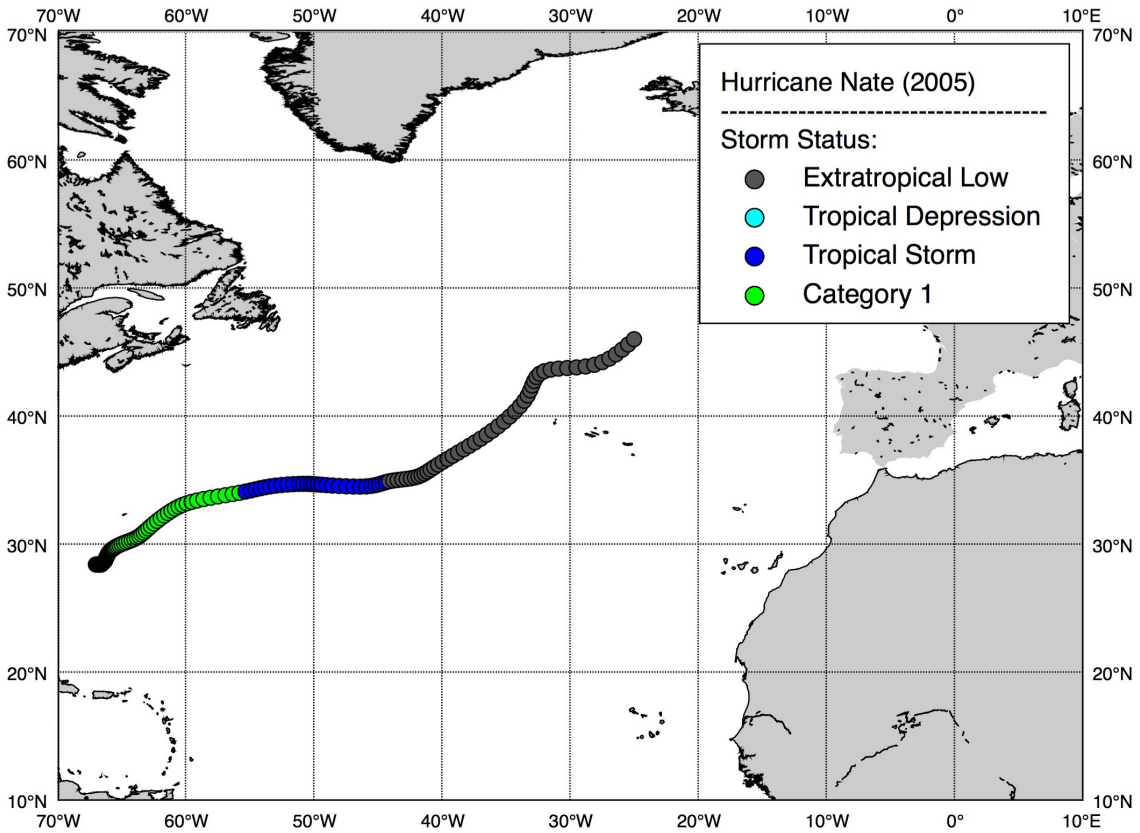

Figure 4.30: Hurricane Nate's (5 – 12 September 2005) track.

Hurricane Nate experienced highly unfavorable oceanic conditions and U_h during its lifetime (Figure 4.31). During Nate's genesis as a tropical depression, D26 values were in the low 20s, with a genesis D26 value of 21.6 m. D26 values remained in 20 – 25 m range throughout all of 6 – 7 September. As Nate strengthened to a tropical storm, D26 values had only increased to the mid-20s, with a D26 value of 23.5 m at tropical storm designation. Along with very low D26 values, U_h was also very low.

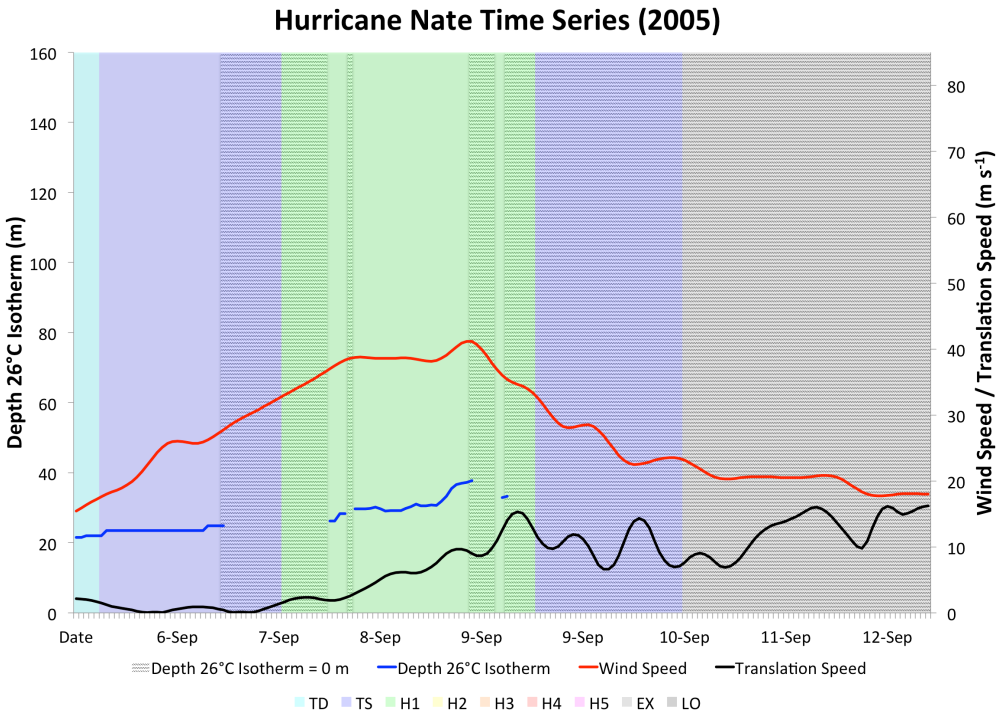

Figure 4.31: Hurricane Nate's time series of D26, U_{10}, U_h, and intensity category.

Throughout 6 – 7 September, Nate's U_h was in the 0 – 2 m s^{-1} range. Thus, strengthening occurred despite a track over a very shallow warm pool. U_h decreased to 0 m s^{-1} at times on both 6 and 7 September. On 7 September as Nate became a category 1 storm, D26 values were at 0 m, which indicated that SSTs were below 26°C. In addition, Nate's U_h at category 1 genesis was 1.6 m s^{-1}. As Nate moved to the northeast it encountered slightly higher D26 values -- in the mid- to upper-20s and 30s. The storm's weakening as it traveled northward was attributed by Beven *et*

al. (2008) to be a result of excessive vertical wind shear and dry air. It is possible that this weakening was caused by the small D26 values as Nate gained latitude along with Beven *et al.* (2008)'s finding of unfavorable atmospheric conditions. These results also indicate that early in Nate's lifetime, atmospheric conditions must have been highly favorable given D26 values in the low 20s and U_h below 3 m s^{-1}. Oceanic conditions throughout most of Nate's track indicated a shallow D26 layer and a slow U_h.

4.1.15 Hurricane Ophelia

Hurricane Ophelia was a unique storm that took an erratic path just off the east coast of the United States (Figure 4.32). Ophelia formed from the remnants of a frontal system that moved off Florida's east coast on 1 September 2005. This frontal system created a trough of low-pressure. Convection slowly organized and on 6 September a tropical depression formed between Andros Island and Grand Bahaman Island.

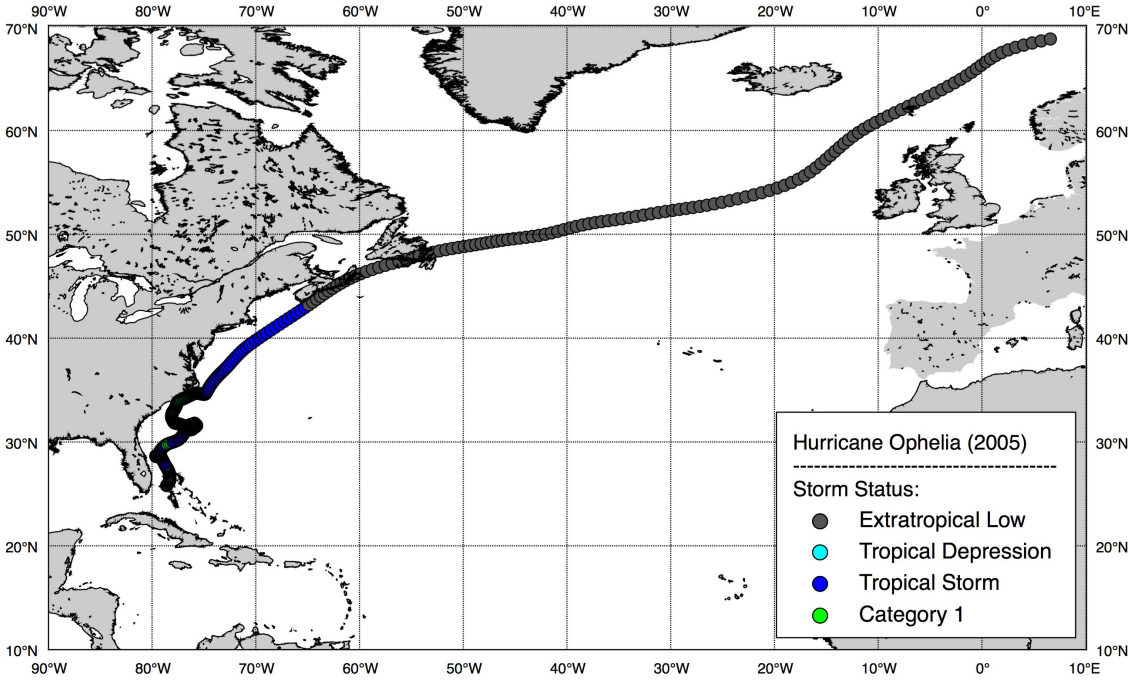

Figure 4.32: Hurricane Ophelia's (6 – 23 September 2005) track.

The depression moved slowly to the north and on 7 September became Tropical Storm Ophelia. Ophelia then moved northwestward just off the coast of Florida and began a counterclockwise loop on 8 September. This loop took place as a result of very weak steering currents. Ophelia became a hurricane late on 8 September very briefly during this loop, with category 1 status only maintained for approximately three hours. Ophelia then weakened back to a tropical storm and moved to the east northeastward. Late on 9 September, Ophelia again became a category 1 storm. This second category 1 status was also very brief, again with a duration of approximately three hours on 9 September. Ophelia weakened back to a tropical storm late on 9 September. The storm became a category 1 hurricane for the third time on 10 September, with a maximum U_{10} of 38.6 m s^{-1}. This third hurricane status lasted the longest, over 30 hours. On 11 September, Ophelia began a second loop, this time clockwise. This loop continued into 12 September, and near the end of the loop cycle, Ophelia weakened back to a tropical storm. Beven *et al.* (2008) noted this weakening could have been the result of Ophelia moving back over its own cool wake. Ophelia exited this loop and became a hurricane for the fourth time on 14 September while located just off the coast of North Carolina, but the storm never officially made landfall. Ophelia then moved northeastward, while increased vertical wind shear caused slow weakening. On 18 September, Ophelia became an extratropical cyclone while it raced off to the northeast in the North Atlantic.

Hurricane Ophelia's analysis of along-track data reveals that the storm began with an appreciable amount of oceanic heat content, with D26 values in the 80s (Figure 4.33). As the storm moved northward, values decreased slightly to the upper-60s and 70s. As expected, values decreased as Ophelia gained latitude. U_h was very slow during most of Ophelia's track, with an average of 6 m s^{-1}. However, at numerous times during the track U_h dropped below 1 m s^{-1},

which indicates that Ophelia's extended time over small D26 values could explain why its intensity fluctuated so rapidly. U_h increased near the end of Ophelia's track, as the storm became extratropical and gained latitude. D26 values were 0 m in this region as SSTs dropped below 26°C.

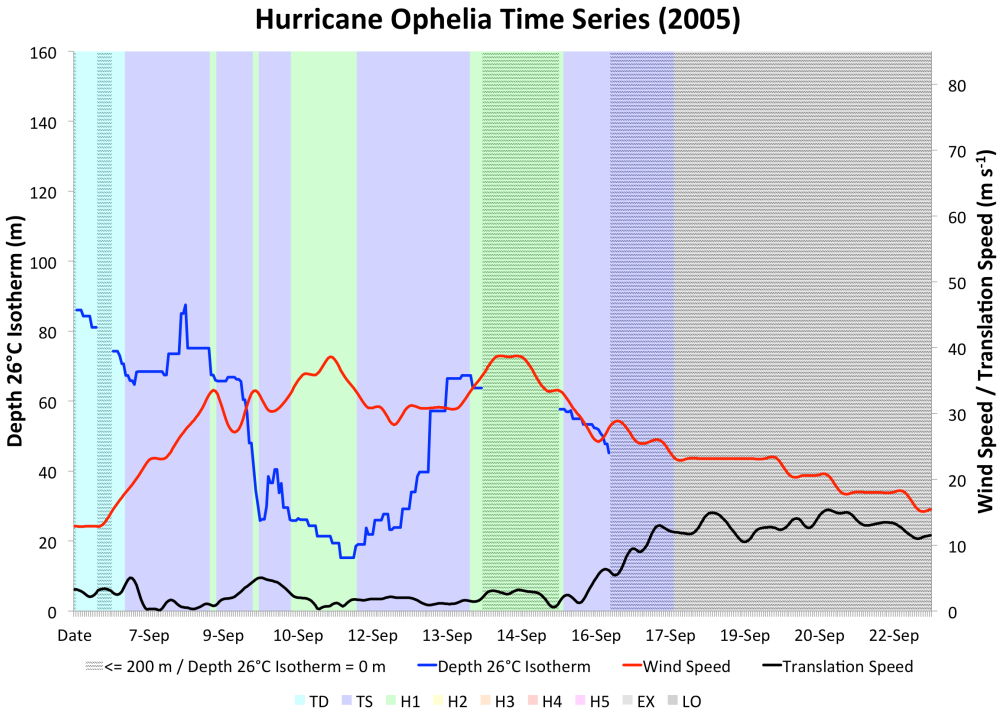

Figure 4.33: Hurricane Ophelia's time series of D26, U_{10}, U_h, and intensity category.

Given that Ophelia took an erratic path and had a very low U_h throughout most of its lifetime, a deeper analysis was conducted in an attempt to understand how these two factors affected intensity. Ophelia's first erratic movement occurred as a counterclockwise loop (loop 1) on 8 – 9 September. During the beginning of loop 1, D26 values averaged 74.8 m with an average U_h of 0.88 m s^{-1} on 8 September (Figure 4.34a). Near the end of 8 September, Ophelia became a category 1 with U_{10} of 33.3 m s^{-1}. This increased intensity could be explained by the slow U_h and modest D26 values in the mid-70s. However, near the end of loop 1, on 9 September, D26 values dropped to 54.9 m with a slight increase in U_h at 3 m s^{-1} (Figure 4.34b). It

appears possible that Ophelia's category 1 status only lasted for three hours during this loop because D26 values decreased on 9 September. Coupled with a U_h of 3 m s^{-1}, the slow motion over these decreasing D26 values led to a downgrade in intensity to tropical storm status.

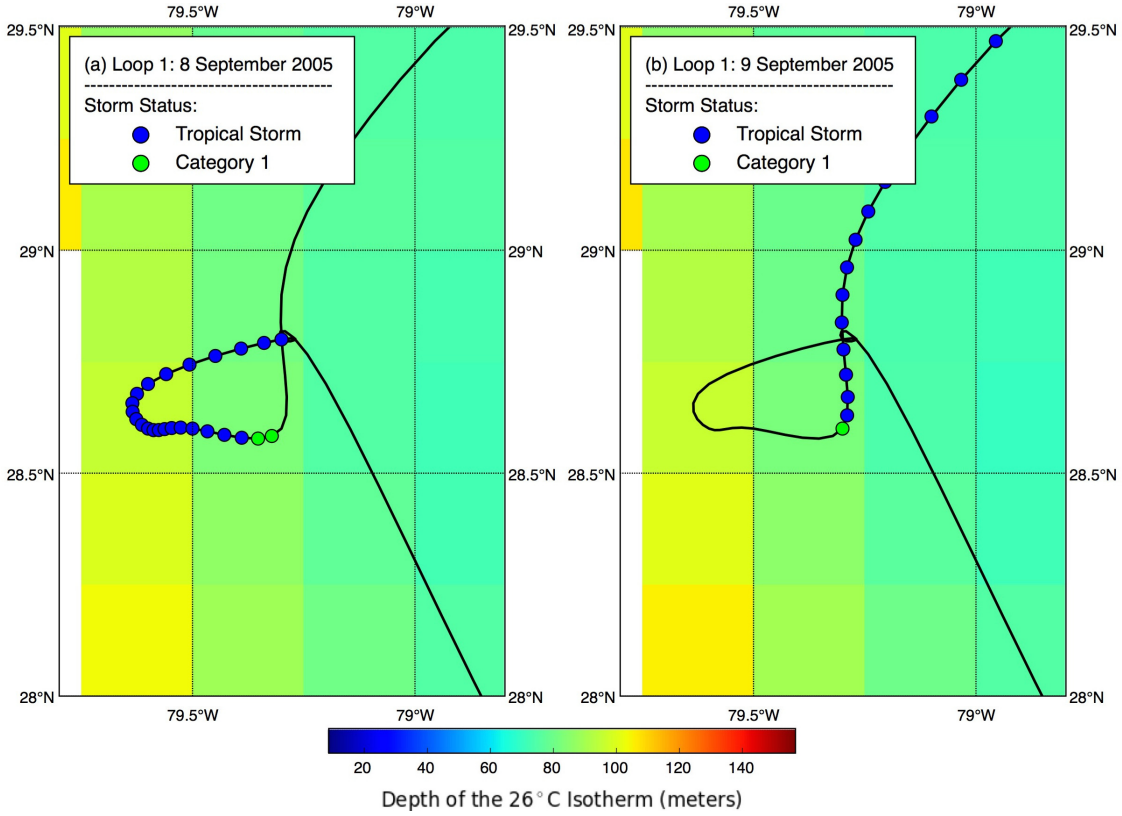

Figure 4.34: Hurricane Ophelia's first loop with D26 plotted for 8 – 9 September.

Hurricane Ophelia's second loop (loop 2), a clockwise loop which occurred on 11 – 12 September, reveals that the storm may have actually weakened over its own cool wake. As Ophelia entered loop 2 on 11 September, it was a category 1 hurricane. However, late on 11 September, Ophelia degenerated to a tropical storm. This degeneration may be explained by an average D26 of 18.9 m paired with an average U_h of 1.1 m s^{-1} (Figure 4.35a). It appears that Ophelia had caused a cooling of the sea surface as it traveled on the northern periphery of loop 2, thus causing D26 values to decrease substantially to the mid-teens. Ophelia then traveled over the cooled area late on 11 September and early on 12 September. By 12 September, Ophelia was

a tropical storm, while D26 values averaged a 27.2 m with an average U_h of 1.9 m s^{-1} (Figure 4.35b). Ophelia also appears to have caused substantial cooling of the waters beneath it as it reduced SSTs to less than 26°C on 12 September. These findings suggest that Ophelia may have directly caused its weakening when it traveled back over its own cool wake at a slow speed.

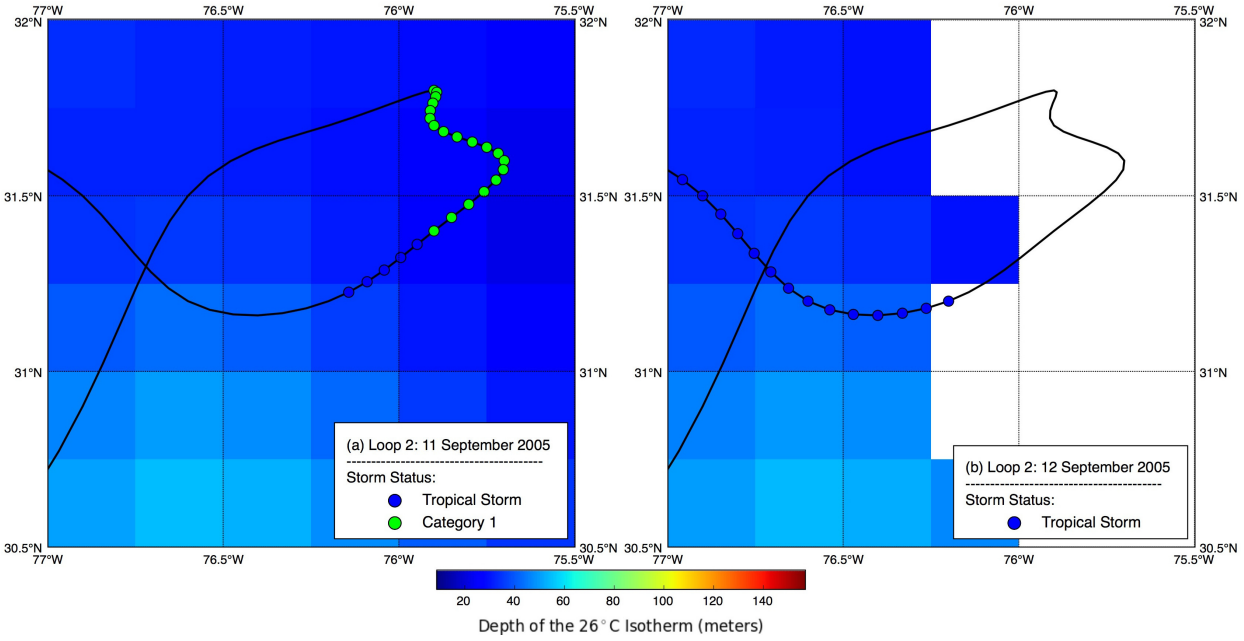

Figure 4.35: Hurricane Ophelia's second loop with D26 plotted for 11 – 12 September. Note the white area to the right of the track on panel b, indicating a surfacing of the D26 due to cooling of sea surface temperatures.

4.1.16 Hurricane Philippe

Hurricane Philippe formed from a tropical wave that left the African coast on 9 September 2005. Moving westward in the southern portion of the Atlantic, the wave lost much of its convection. However, on 13 September, convection developed and maintained itself. Four days later, convection had become concentrated enough to designate the wave as a tropical depression on 17 September (Figure 4.36). Later on 17 September, the wave strengthened to Tropical Storm Philippe. Steering currents were very weak during this time but nevertheless,

Philippe was able to move northwestward into a weakness in the subtropical ridge located in the central Atlantic. Early on 19 September, Philippe became a category 1, with U_{10} of 33.4 m.

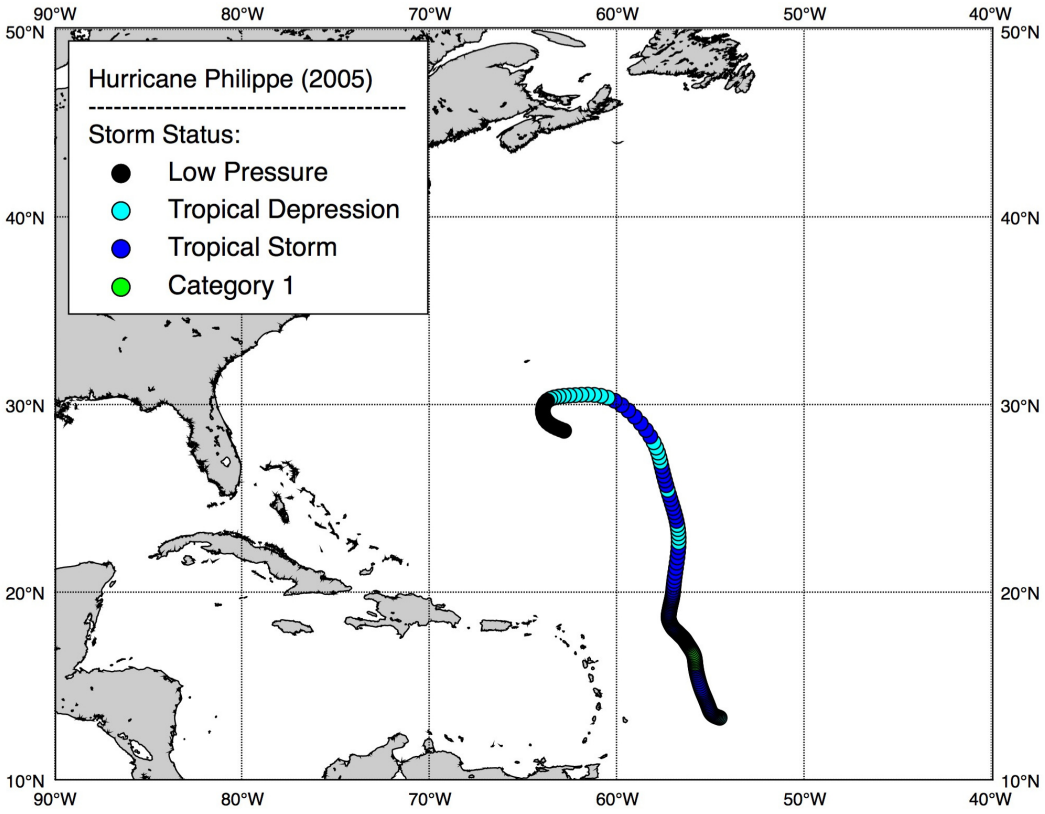

Figure 4.36: Hurricane Philippe's (17 – 24 September 2005) track.

On 20 September, Philippe reached its maximum intensity with U_{10} of 36 m s^{-1}. Philippe then weakened into a tropical storm due to strong westerly shear. Philippe continued to weaken to tropical storm strength late on 20 September and eventually weakened to a depression on 22 September. Intensity fluctuated between depression and tropical storm until Philippe eventually weakened to a low-pressure system on 23 September. Note that in Figure 4.36, category 1 status points are not seen on the track due to the brevity of their appearance. Also, early in the track, it appears that Philippe was a low-pressure system (appears black in Figure 4.36). However, this is due to the fact that the storm was moving very slowly, which caused the plotted status points to overlap and appear black. Hurricane Philippe's oceanic conditions appear to have been favorable

early in its track. Early in Philippe's lifetime, before it became a tropical storm, D26 values were in the mid-80s (Figure 4.37).

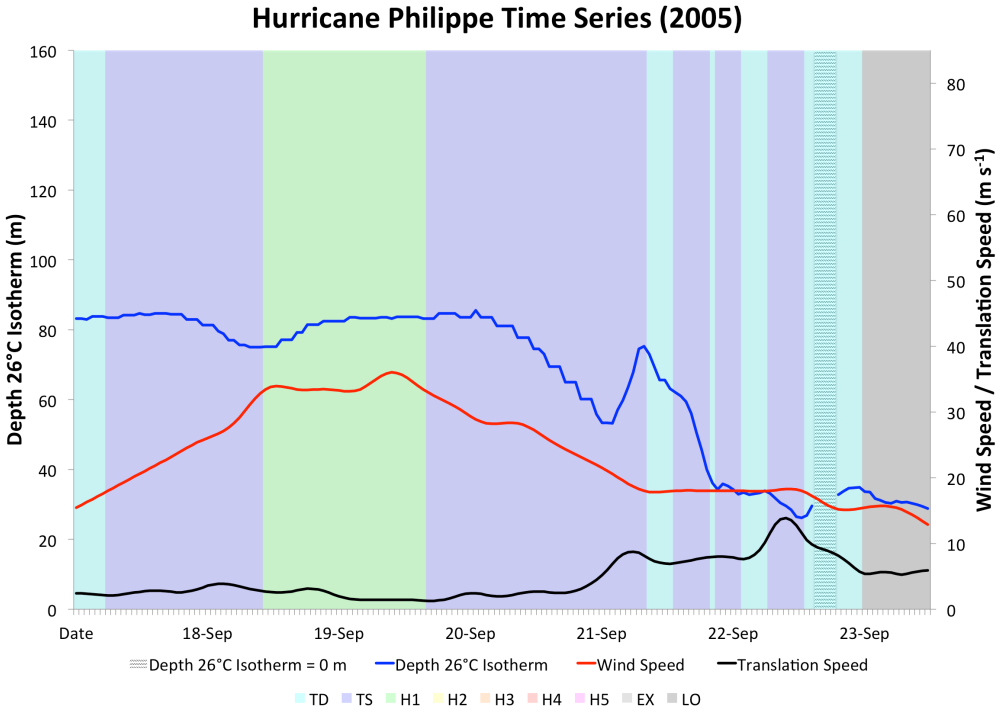

Figure 4.37: Hurricane Philippe's time series of D26, U_{10}, U_h, and intensity category.

U_h was also approximately 2 m s^{-1}, which suggests that the depression was over these high D26 values for a long period of time. This slow U_h over the deep warm pool likely led to the increase in intensity to tropical storm status on 17 September. As Philippe became a hurricane on 19 September, D26 values were in the mid-70s, with a D26 value of 75.2 m and a U_h of 2.7 m s^{-1} at category 1 status designation. These moderately large D26 values coupled with a slow U_h appear to have contributed to Philippe's increased intensity to a category 1 hurricane. D26 values remained in the mid-80s during Philippe's category 1 status. As Philippe weakened back into a tropical storm on 20 September, values remained in the mid-80s with a slow U_h. Despite these oceanic conditions and a slow U_h, Philippe still experienced a decrease in intensity. Beven *et al.* (2008) attributed the weakening to increased westerly wind shear, and the results herein support

this assertion, at least circumstantially. The warm pool thinned (*i.e.*, D26 values decreased) slowly northward with an increase in U_h. These smaller D26 values coupled with shear explained why Philippe eventually weakened to a depression, then to a low-pressure system.

4.1.17 Hurricane Rita

Hurricane Rita originated from the interaction of a tropical wave and a cold front that eventually merged (Figure 4.38).

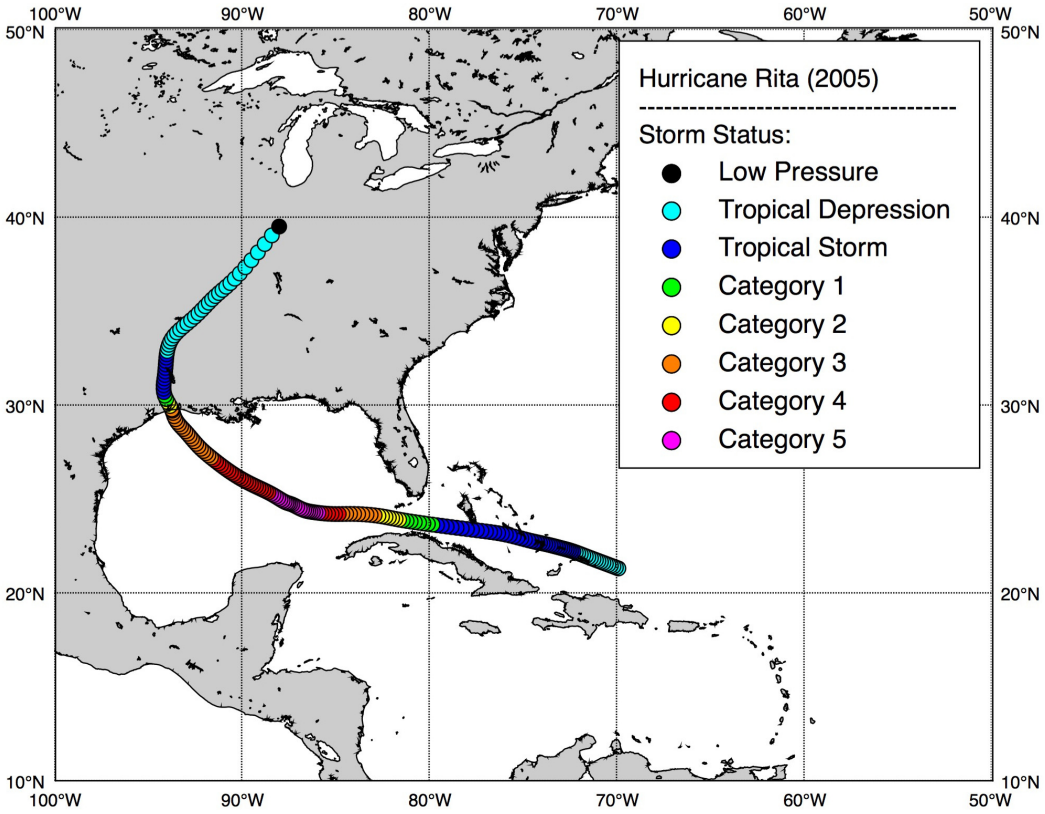

Figure 4.38: Hurricane Rita's (18 – 26 September 2005) track.

The cold front created a surface trough of low-pressure, which merged with the tropical wave on 17 September 2005. A tropical depression formed early on 18 September just east of the Turks and Caicos Islands. The depression moved toward the northwest and became Tropical Storm Rita late on 18 September near the southeastern Bahamas. Rita moved toward the northwest and then

west under the guidance of a strong ridge of high-pressure located the western Atlantic and Florida. On 20 September, Rita became a category 1 hurricane just southeast of Key West, Florida. Rita continued to strengthen and became a category 2 storm later on 20 September with U_{10} of 43.7 m s^{-1}. Rita continued to move westward in the southeastern Gulf of Mexico and became a category 3 storm early on 21 September while located over the very warm waters of the Loop Current. Rita then underwent an explosive intensification process (Beven *et al*. 2008) and became a category 4 and soon afterward a category 5 storm, all within a 16-hour period, by late on 21 September. Rita attained its maximum U_{10} of 80.1 m s^{-1} on 22 September while located in the central Gulf of Mexico. Rita then underwent an eyewall replacement cycle (Beven *et al*. 2008), which weakened the storm to a category 4 with U_{10} of 69 m s^{-1} late on 22 September. Rita also turned toward the northwest as it traveled around the periphery of a ridge located to its east. Rita did not re-intensify, but rather slowly weakened as a result of increased southerly shear and cooler waters. Rita made landfall on 24 September near the Texas-Louisiana border as a category 3 storm. Rita continued to move toward the northwest then north as it hugged the Texas-Louisiana border. Rita slowly weakened after landfall, and became a remnant low-pressure system on 26 September over central Illinois.

Hurricane Rita appears to have gained its intensity from a high oceanic heat content environment complemented by a slow U_h. Rita's along-track average D26 was 71.8 m with an average U_h of 5.6 m s^{-1} (Figure 4.39). Rita traveled over areas where D26 exceeded 100 m, with a maximum of 103 m. As Rita crossed over the Loop Current, it encountered D26 values in the low-90s. Rita also had a slow U_h throughout most of its track. In fact, U_h fell below 3 m s^{-1} at times, indicating that Rita had abundant time over these deep warm water pools, which may have intensified the storm.

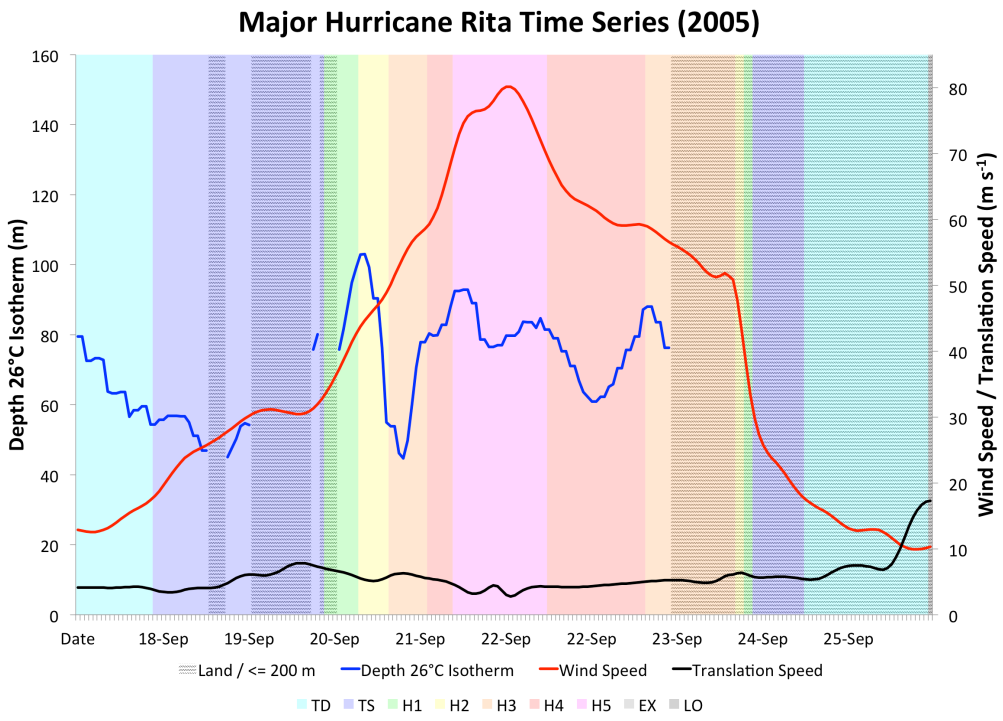

Figure 4.39: Hurricane Rita's time series of D26, U_{10}, U_h, and intensity category.

A detailed analysis of Hurricane Rita's along-track conditions reveals an interaction with the southern branch of the Florida Current in the Florida Straits, a possible CCE, the Loop Current, and another CCE. These features all likely contributed to its intensity fluctuations. Rita approached the first possible CCE on 20 September (Figure 4.40a), and appears to be the same CCE that Katrina had encountered on 27 August. As Rita neared this CCE on 20 September, D26 values were large, with an average of 89.1 m. During 20 September, Rita strengthened from a tropical storm to a category 2 hurricane in 18 hours. U_h averaged 6.6 m s^{-1}, which indicated that Rita spent a moderate amount of time over the deep warm water pool. This rapid increase in intensity may be the result of large D26 values and a moderate U_h prior to entering the CCE. On 21 September, Rita traveled directly over the first CCE (Figure 4.40b), during which D26 values decreased to the mid-50s and 40s. A minimum D26 value of 44.6 m occurred as Rita moved directly over the CCE. A U_h in the 5 – 6 m s^{-1} range indicates that Rita was moving at a constant

speed. Despite the presence of this CCE, Rita maintained its strength. Rita strengthened to a category 3 storm with U_{10} of 50 m s^{-1} while directly over the CCE. These findings suggest that Rita must have been in a highly favorable atmospheric environment during this time period. On 22 September, Rita encountered the Loop Current (Figure 4.40c), with an average D26 of 77.1 m. U_h also slowed to an average of 4 m s^{-1} on 22 September. D26 values reached the mid-80s as Rita traversed the Loop Current. Large D26 values and a slow U_h appear to contribute to Rita's category 5 status. However, on the 23 September, Rita appears to have approached a second CCE (Figure 4.40d), as D26 values rapidly decreased to the low-60s, with a minimum of 60.8 m. Rita also decreased in strength to a category 3. This CCE was noted by Jaimes and Shay (2009) as a cause for Rita's weakened state prior to landfall. Beven *et al.* (2008) also noted southerly wind shear and cooler waters as contributors to this weakening prior to landfall.

The detailed analysis of Hurricane Rita reveals that the storm likely encountered the southern branch of the Florida Current within the Florida Straits, two CCEs, and the Loop Current. Rita's initial intensification was found to be the result of large D26 values in the Florida Current, located just south of the Florida peninsula in the Straits of Florida. The first possible CCE that Rita encountered was found to have had minimal effect on the storm's intensity. In fact, Rita strengthened while over this feature, likely due to strongly favorable atmospheric conditions. Rita then passed over the Loop Current, where D26 values were large and U_h was slow. These features may explain why Rita experienced an explosive intensification while traveling over the Loop Current where D26 values were in the low 90s. Next, Rita passed over a CCE, where it weakened from a category 4 to a category 3 on 23 September. This CCE was found to corroborate Jaimes and Shay (2009)'s findings. Those authors noted that this CCE

contributed directly to Rita's weakening prior to landfall near the Texas-Louisiana border on 23 September.

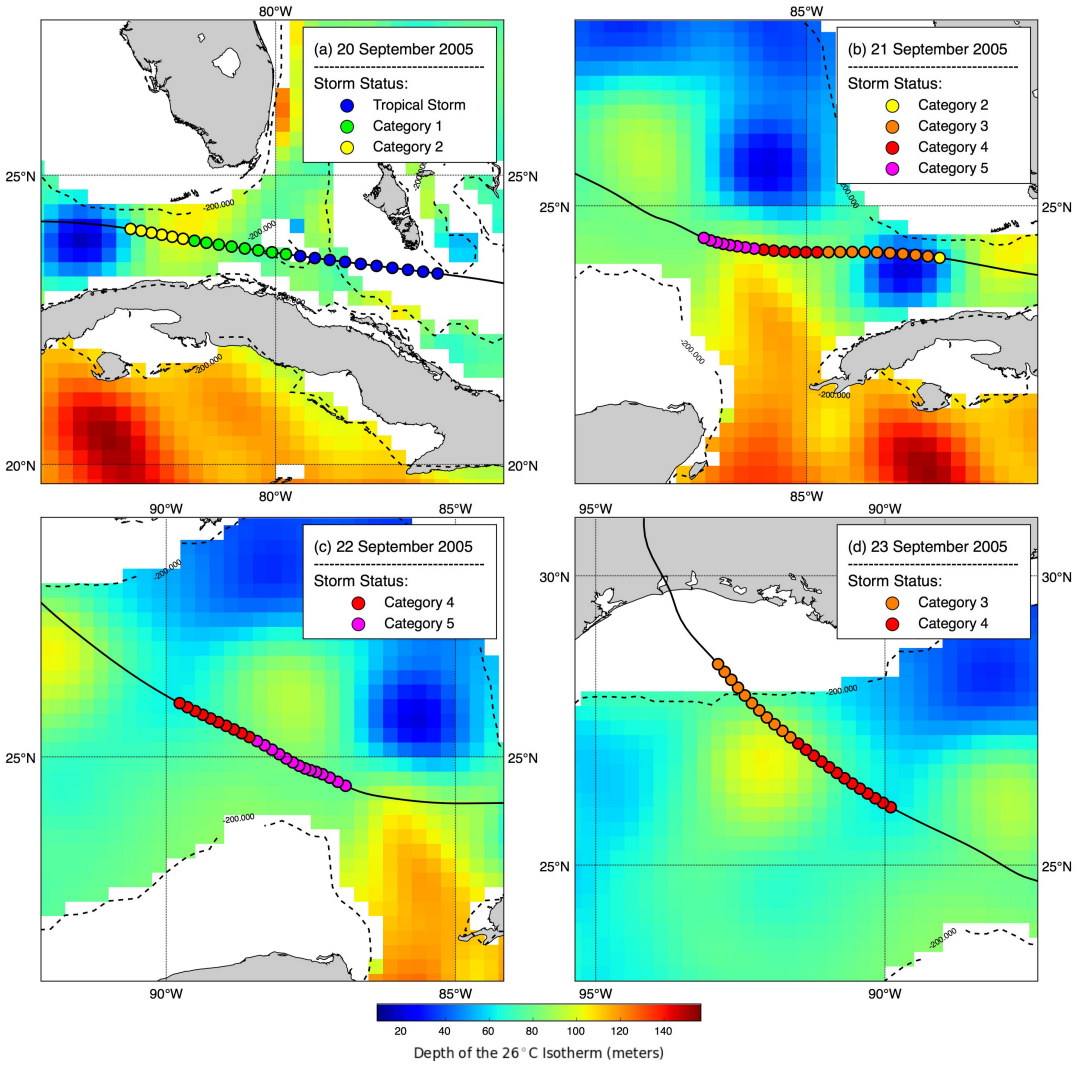

Figure 4.40: Hurricane Rita's panel showing D26 with track overlain for each day. Areas where ocean depth is $\leq$ 200 m are masked in white.

4.1.18 Hurricane Stan

Hurricane Stan originated from a tropical wave that exited the coast of Africa on 17 September 2005. This wave traveled over the Atlantic Ocean and eventually entered the Caribbean Sea on 27 September. Organization of the wave was slow as strong wind shear was present. However, on 1 October, convection increased and a tropical depression formed

southeast of Cozumel, Mexico (Figure 4.41). Early on 2 October, the system became sufficiently well-organized that the depression was named Tropical Storm Stan. Stan moved toward the north-northwest and made landfall on the east coast of the Yucatán peninsula on 2 October. As the system crossed the Yucatán peninsula, it weakened back into a tropical depression. However, once it emerged back over water, it quickly strengthened back into a tropical storm. Intensification continued and on 3 October, Stan became a tropical storm once again. On 4 October, Stan attained category 1 status, with U_{10} of 33.4 m s^{-1} and reached a peak intensity of 36.7 m s^{-1} late on 4 October. Stan made landfall late on 4 October to the south-southeast of Veracruz, Mexico. Stan weakened rapidly after landfall to tropical storm status late on 4 October then a depression early on 5 October.

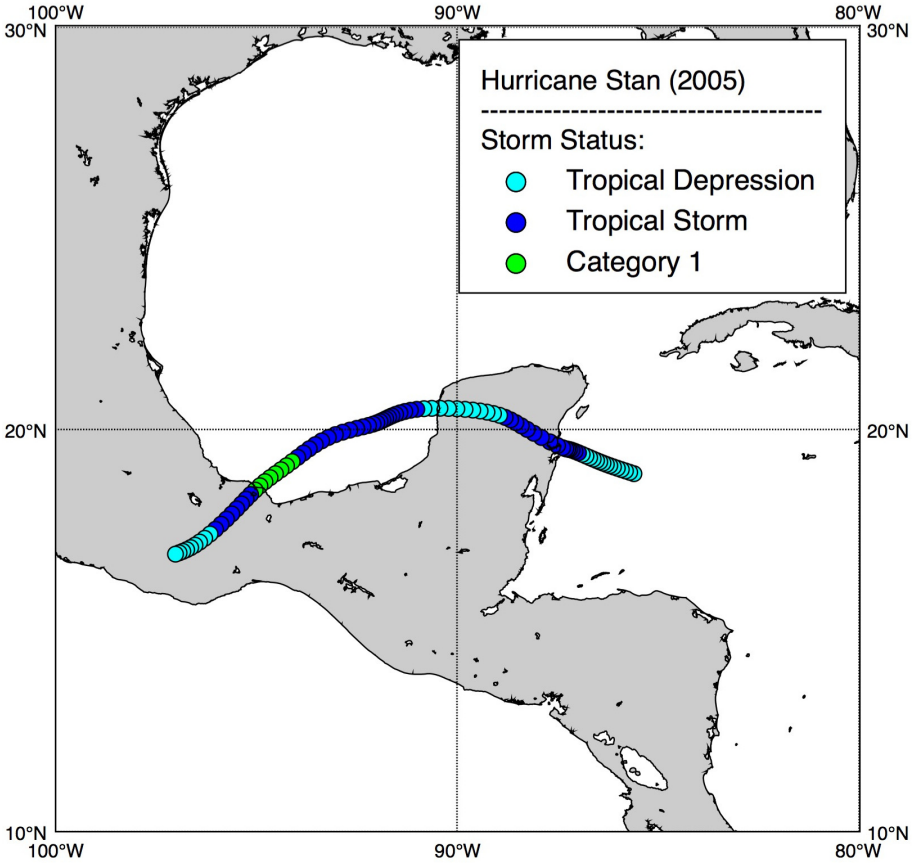

Figure 4.41: Hurricane Stan's (1 – 5 October 2005) track.

Hurricane Stan's strengthening coincided with abundant oceanic heat content while it was located in the western Caribbean Sea and weakening coincided with the relative lack of oceanic heat content while in the Bay of Campeche (Figure 4.42).

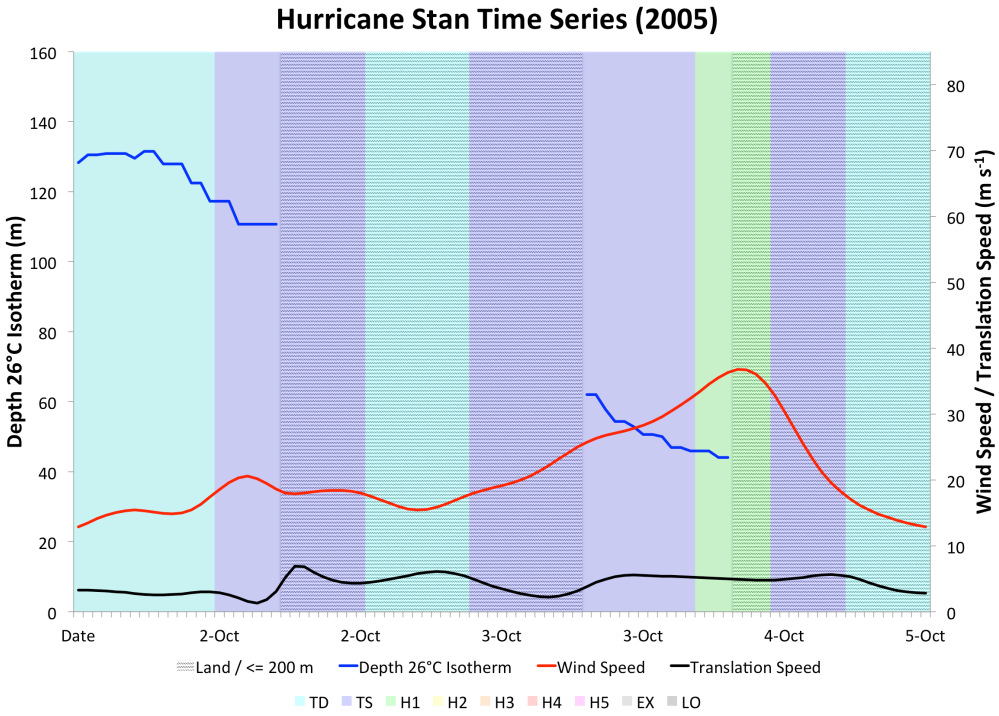

Figure 4.42: Hurricane Stan's time series of D26, U_{10}, U_h, and intensity category.

When Stan was first declared a tropical depression, D26 values averaged well over 100 m. A maximum of 131.5 m occurred as the storm was located in the Caribbean Sea and at tropical depression status. Once the depression was upgraded to Tropical Storm Stan on 2 October, D26 was at 117.3 m, with a U_h of 2.9 m s^{-1}. These very high D26 values and slow U_h seem to have contributed to Stan's intensity increase to a tropical storm before landfall in the Yucatán. In fact, D26 values averaged 123.1 m while Stan was located in the Caribbean Sea with an average U_h in the 2 – 3 m s^{-1} range. Once Stan crossed the peninsula and entered the Bay of Campeche, D26 values decreased, with an average of 50.9 m. Despite these drastically lower D26 values and a slightly faster U_h, Stan still managed to increase in intensity to a category 1 hurricane. This

finding implies that favorable atmospheric conditions played a more important role in the intensification over the Bay of Campeche.

4.1.19 Tropical Storm Tammy

Tropical Storm Tammy (Figure 4.43) appears to have formed from the interaction of a tropical wave and a large mid- to upper-tropospheric trough located in the central Atlantic. The wave, which moved off the coast of Africa on 24 September 2005, bifurcated with the northern portion merging with the large mid- to upper-tropospheric trough. This merge was accompanied by a strong pressure gradient which caused gale force winds to develop east of the Bahamas.

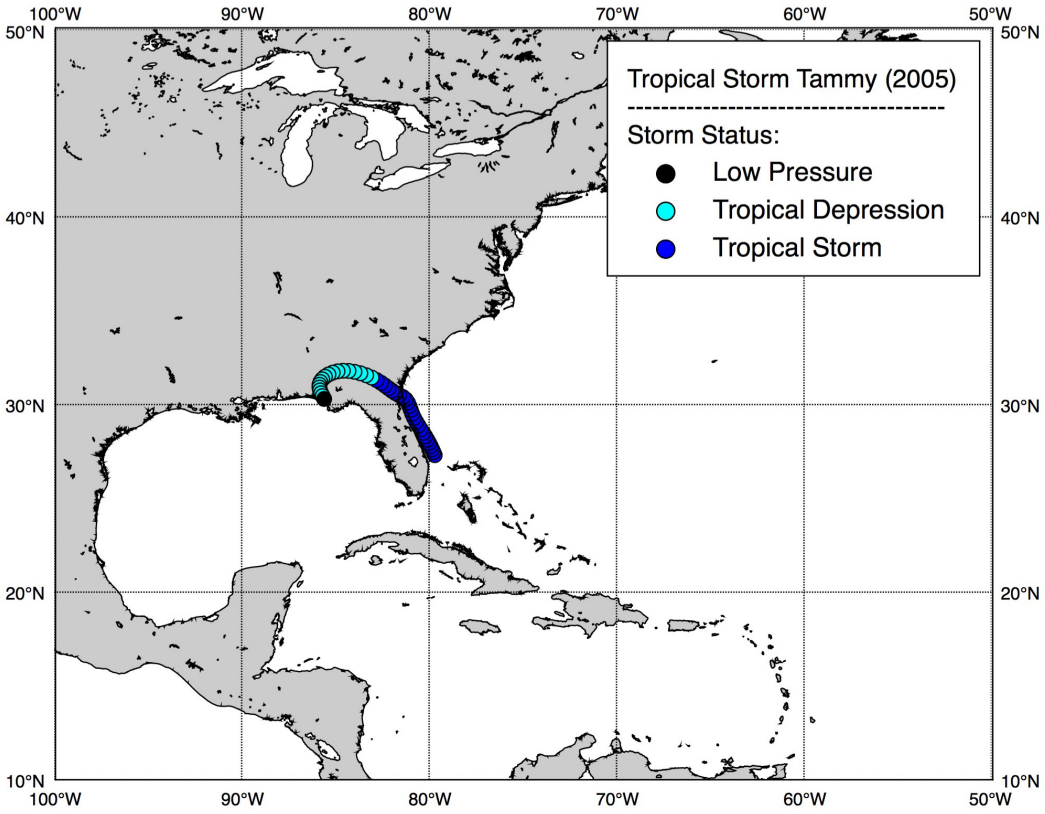

Figure 4.43: Tropical Storm Tammy's (5 – 7 October 2005) track.

On 5 October, as the trough moved closer to the Bahamas, an area of convection developed. As winds in the areas were already tropical storm force, Tammy became a tropical storm on 5

October just off the east coast of Florida, skipping the depression stage. Tammy moved to the northwest, paralleling the coast of Florida, and attained a peak U_{10} of 23.3 m s^{-1} before landfall near Atlantic Beach, Florida, on 5 October. Tammy moved toward the northwest, then curved to the southeast and became a low-pressure system on 7 October while over the Florida panhandle.

Tropical Storm Tammy's along-track analysis revealed that the storm was only over valid D26 data for three hours on 5 October. After that period, Tammy was traveling along the Florida coast in areas shallower than 200 m. The analysis of Tammy was limited to these three hours of valid data (Figure 4.44). However, for the three hours on 5 October, Tammy encountered an average D26 of 97.9 m, indicating that the system had sufficient oceanic heat content to support intensification. Little else could be determined after this time period, as Tammy entered an invalid data region.

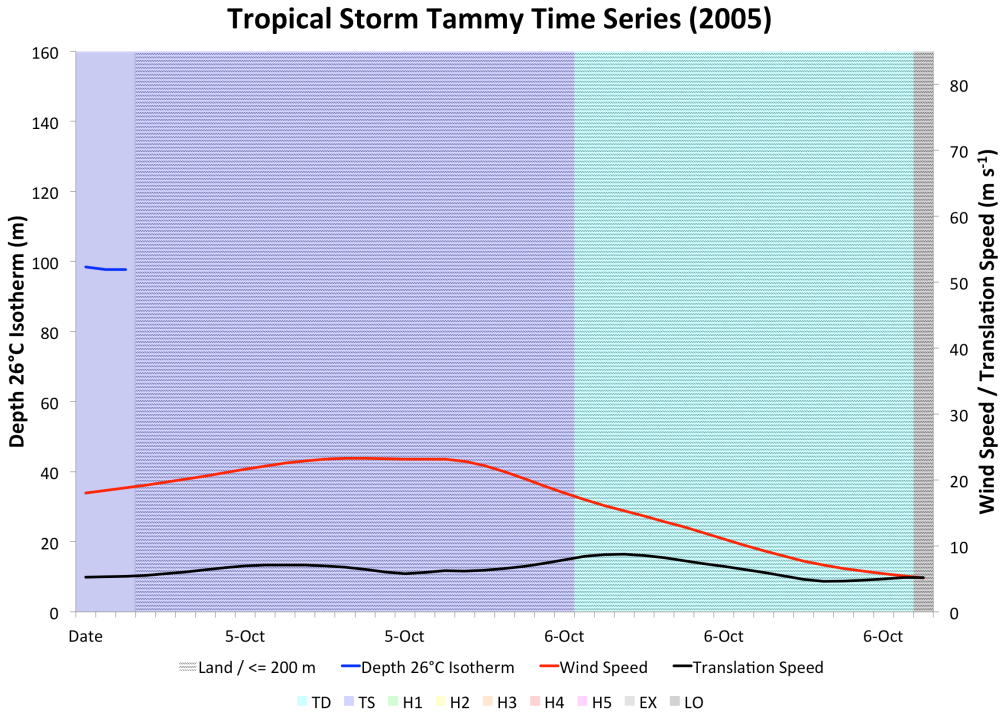

Figure 4.44: Tropical Storm Tammy's time series of D26, U_{10}, U_h, and intensity category.

4.1.20 Hurricane Wilma

Hurricane Wilma was an extremely powerful hurricane with the lowest central pressure in the Atlantic basin in recorded history. Wilma formed from the complex interaction of a large area of disturbed weather and two tropical waves that moved into the Caribbean Sea. By 15 October 2005, this area of disturbed weather developed a well-defined surface circulation, and a tropical depression was designated west-southwest of Grand Cayman (Figure 4.45).

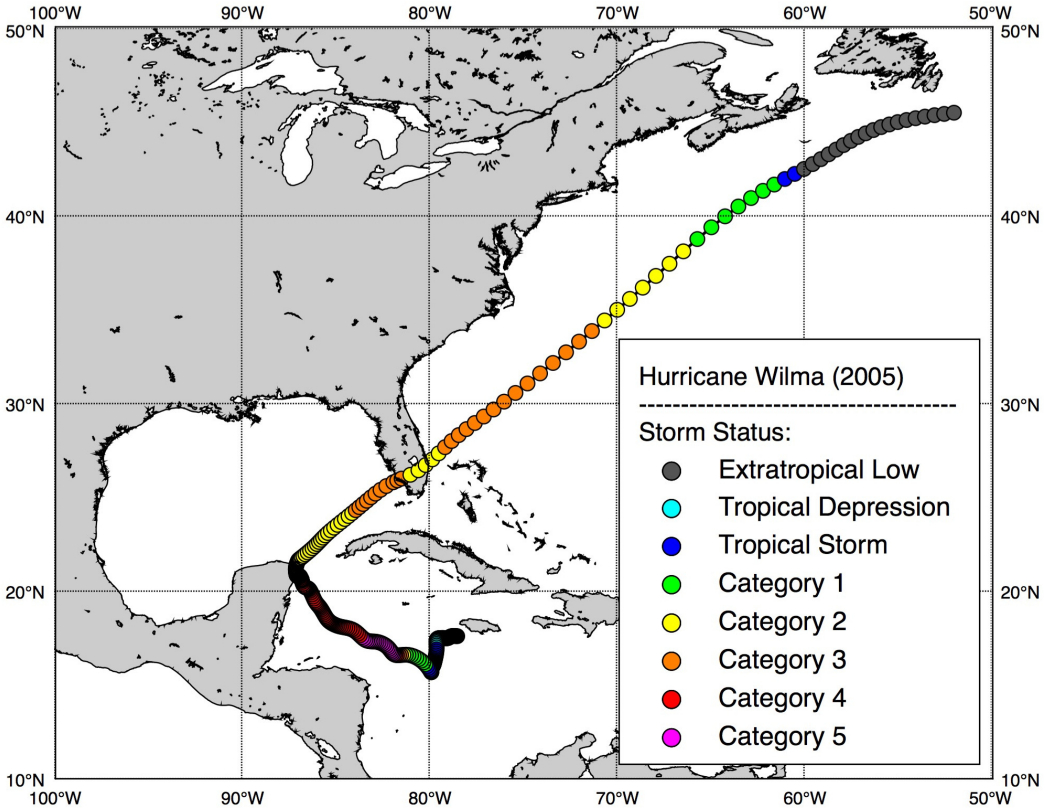

Figure 4.45: Hurricane Wilma's (15 – 26 October 2005) track.

The depression moved generally south-southwestward due to weak steering currents. Early on 17 October, the depression became Tropical Storm Wilma and began to move toward the west-northwest, strengthening to a category 1 hurricane on 18 October. Later on 18 October, explosive and unprecedented intensification occurred. Wilma strengthened from a category 1 hurricane with U_{10} of 33.3 m s^{-1} to a category 5 storm with U_{10} of 82.5 m s^{-1} in a 25-hour period. During

this period of rapid intensification, Wilma's eye had contracted to 2 nautical miles. This eye size was also noted to be the smallest ever recorded by the National Hurricane Center's staff. On 19 October, Wilma weakened to category 4 strength but maintained category 4 status as it turned toward the northwest, aimed directly at the Yucatán peninsula and Cozumel, Mexico. As Wilma moved over the Yucatán peninsula on 21 – 22 October, it weakened to a category 2 storm. A strong mid-tropospheric trough to Wilma's northeast provided strong steering currents throughout the rest of its track. This trough accelerated Wilma toward the northeast, which allowed the storm to make landfall in southern Florida near Cape Romano on 24 October as a category 3 hurricane. Wilma crossed the Florida peninsula in just 4.5 hours, with slight weakening to a category 2 hurricane. It emerged into the Atlantic Ocean later on 24 October and strengthened back to a category 3 with U_{10} of 57.7 m s^{-1}. This strengthening occurred despite the presence of cooler and drier air located behind the mid-tropospheric trough, as it was unable to penetrate Wilma's core. Wilma then slowly weakened due to unfavorable atmospheric conditions and became extratropical on 26 October. Due to Wilma's initially slow and erratic movement, plotted status points overlap and appear black in Figure 4.45.

Hurricane Wilma's analysis sheds some light onto why this storm was able to obtain record strength. Oceanic conditions throughout almost the entirety of Wilma's track were highly favorable (Figure 4.46), with an average D26 of 89.4 m, the highest of any storm thus far in this analysis. D26 values frequently exceeded 100 m, with a maximum of 117.4 m on 22 October. An average U_h of 5.9 m s^{-1} indicates Wilma's modest speed. However, during its time in the Caribbean Sea and southern Gulf of Mexico when D26 values were large, U_h was often below 3 m s^{-1}. The warm water pool was shallowest on 24 – 25 October as Wilma entered the Atlantic

Ocean and gained latitude. The minimum D26 of 24.5 m occurred during this time period as the storm was located off the east coast of Florida on 25 October.

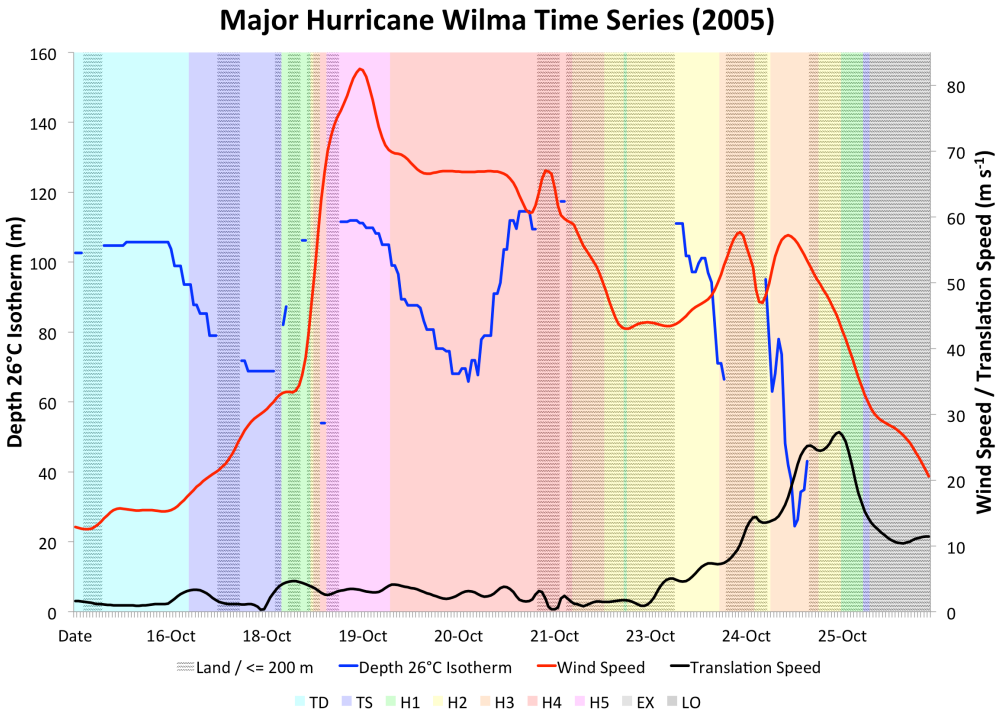

Figure 4.46: Hurricane Wilma's time series of D26, U_{10}, U_h, and intensity category.

The detailed analysis of Hurricane Wilma's along-track data indicates that it traveled over a thick warm layer of water on almost every day (Figure 4.47). Given this, the analysis did reveal why Wilma's rapid intensification process began and ended. On 18 October, the start date of Wilma's explosive intensification, it strengthened from a tropical storm with U_{10} of 28.3 m s^{-1} to a category 4 hurricane with U_{10} of 62.6 m s^{-1}. D26 values averaged 75.4 m on 18 October (Figure 4.47a), and U_h averaged 3 m s^{-1}. A maximum D26 value of 106.2 m occurred approximately four hours before Wilma strengthened into a category 4 hurricane. These large D26 values coupled with a slow U_h appear to explain the initiation of the rapid intensification process. On 19 October, Wilma reached category 5 status and maintained such strength for approximately 20 hours. D26 values averaged 105.1 m (Figure 4.47b) during this period, which

suggest the presence of a very large amount of oceanic heat content. U_h averaged only 3.3 m s^{-1} on 19 October. High D26 values and slow U_h on 18 – 19 October partially explained the cause of this unprecedented rapid intensification process.

The intensification process was slowed on 20 October, perhaps by Wilma's movement over either a weak CCE, or simply by encountering smaller D26 values (Figure 4.47c). D26 values averaged 78 m on 20 October, but values slowly decreased as Wilma traveled over this possible feature. The surface warm water pool was over 80 m deep and slowly decreased to the lower 60s, with a minimum thickness of 68 m. U_h averaged 2.9 m s^{-1} throughout the day, dropping to 2 m s^{-1} at times. Although this area of decreased D26 values did not cause Wilma to weaken suddenly, it did appear to cause slight weakening, as Wilma decreased to a category 4 status with U_{10} of 69.4 m s^{-1}, with a decrease in U_{10} to approximately 66 m s^{-1} late on 20 October. On 21 October, as Wilma neared Cozumel, Mexico, and the Yucatán peninsula, it maintained category 4 strength. D26 values averaged 98.8 m (Figure 4.47d). Decreasing D26 values continued into early on 20 October, with a minimum of 67.7 m early in the day. U_h averaged a slow 2.4 m s^{-1}, which again illustrates that Wilma had plenty of time to tap the high oceanic heat content present.

Closer analysis of Wilma's oceanic conditions reveals that the storm had very high D26 values available along with a slow U_h throughout most of the time. Wilma's rapid intensification process was aided by high D26 values on the 18 – 19 October. A slow U_h also likely increased Wilma's intensification as it allowed abundant time over these D26 values. Wilma was then found to travel over a possible weak CCE or simply an area of lower D26 values, which halted the rapid strengthening process. Later on 21 October, D26 values were again very high and U_h

slowed to a crawl. These results, along with favorable atmospheric conditions, explain how and why Wilma underwent intensification to an unprecedented extent.

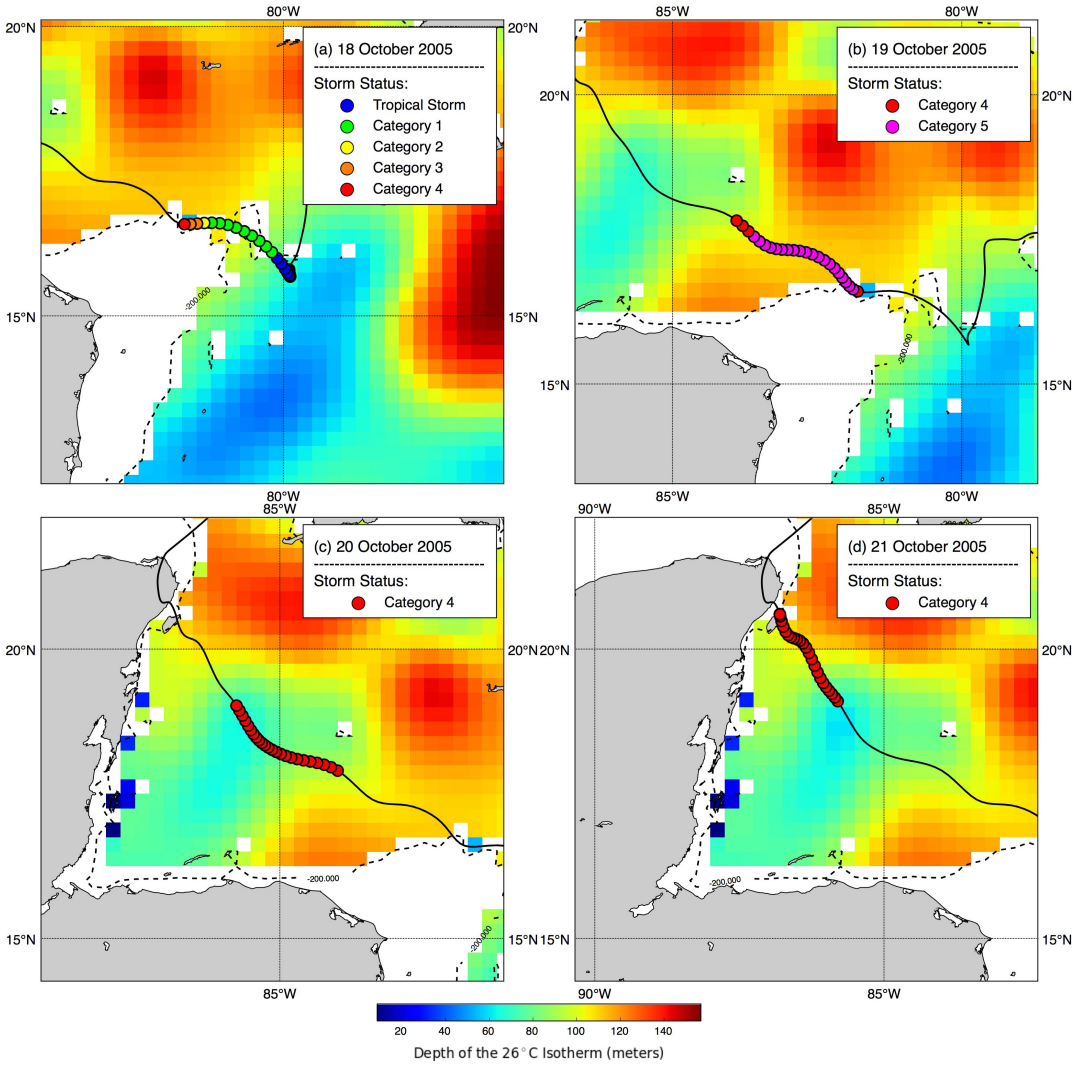

Figure 4.47: Hurricane Wilma's panel showing D26 with track overlain for each day. Areas where ocean depth is $\leq$ 200 m are masked in white.

4.1.21 Tropical Storm Alpha

Tropical Storm Alpha, the season's first Greek alphabet storm, formed from a tropical wave that reached the Windward Islands on 19 October 2005. This wave became better organized and on 22 October a tropical depression formed just to the southwest of Puerto Rico (Figure 4.48). The depression strengthened and became Tropical Storm Alpha later on 22

October. Alpha continued to move to the northwest and made landfall in the Dominican Republic on 23 October and weakened rapidly due to the high terrain. Alpha then moved toward the north-northwest and then northward near the eastern Bahamas. Alpha did not regain tropical storm intensity and was eventually absorbed by the circulation of Hurricane Wilma on 25 October.

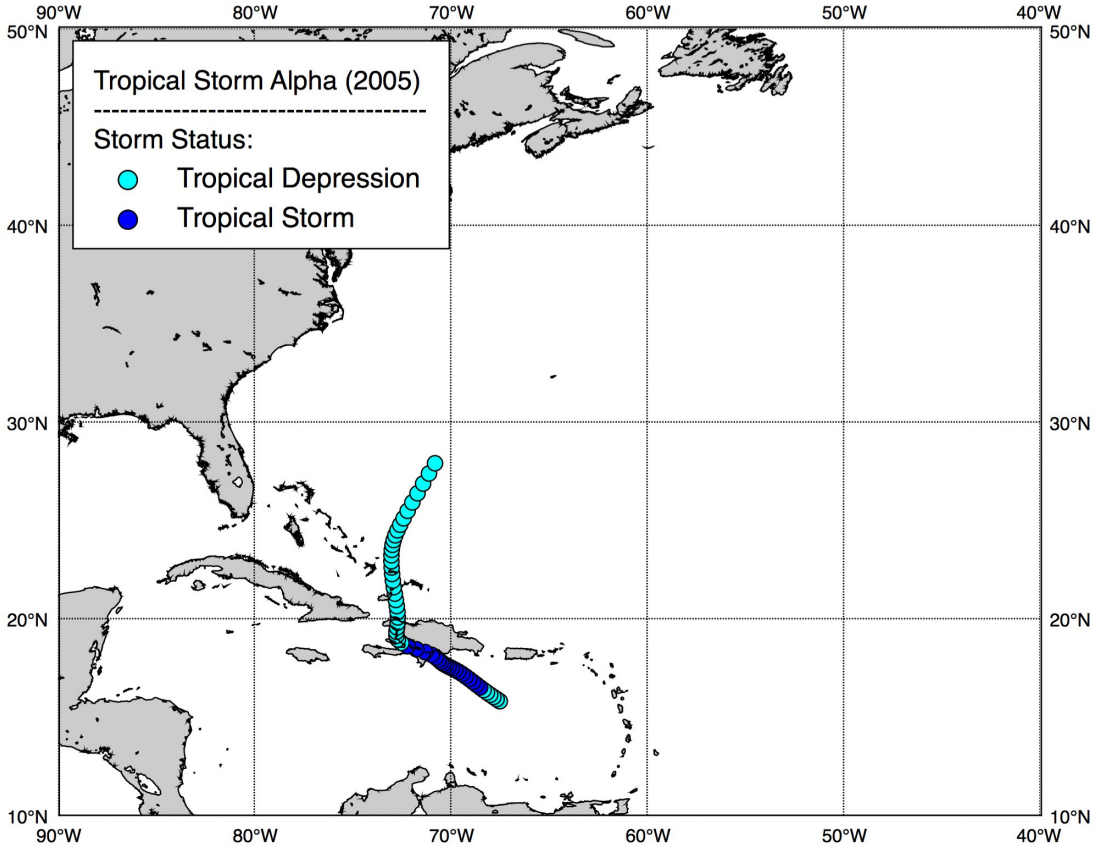

Figure 4.48: Tropical Storm Alpha's (22 – 24 October 2005) track.

Although Alpha only attained tropical storm status, with a maximum U_h of 24.3 m s^{-1}, it did have large D26 values at its disposal, especially before it made landfall in the Dominican Republic on 23 October (Figure 4.49). In fact, D26 values averaged 95.9 m prior to landfall. U_h was in the 5 – 7 m s^{-1} range. These D26 values likely led to Alpha's intensification into a tropical storm, and had it experienced these values for a longer period of time, it is possible that the storm

would have reached greater intensity. As Alpha entered the Atlantic Ocean after landfall, it experienced reduced D26 values, with an average of 57.2 m. A minimum of 36.2 indicates that oceanic conditions gradually became less conducive for Alpha to re-intensify. Another factor that likely contributed to Alpha's lack of intensification once in the Atlantic was Wilma's presence in the area. Wilma absorbed Alpha before it could intensify.

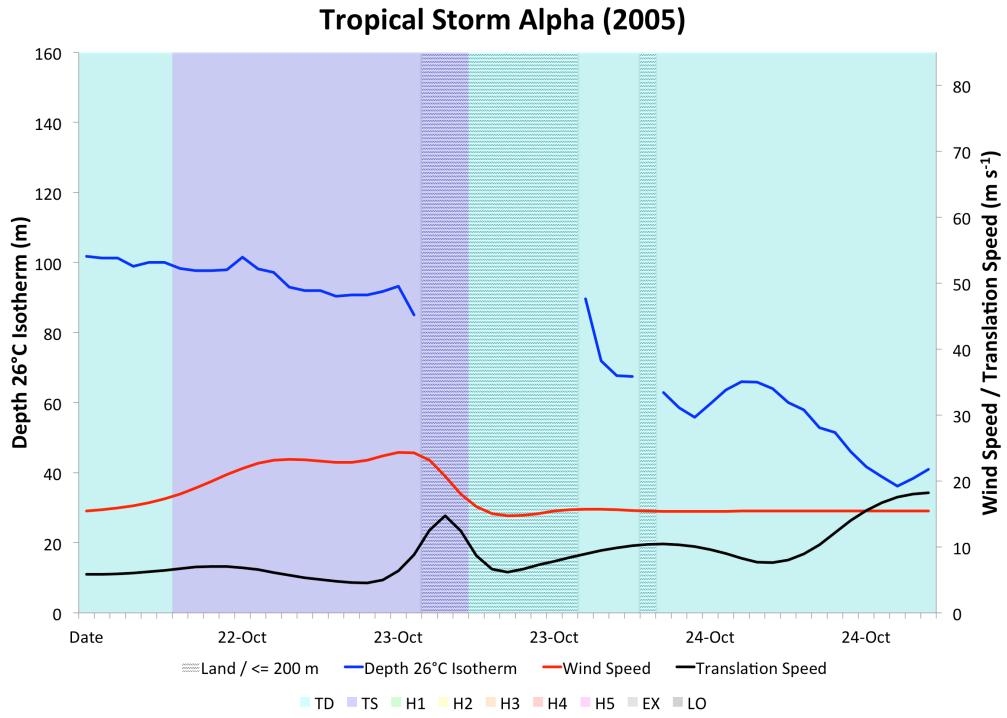

Figure 4.49: Tropical Storm Alpha's time series of D26, U_{10}, U_h, and intensity category.

4.1.22 Hurricane Beta

Hurricane Beta, the final hurricane of the 2005 North Atlantic basin hurricane season, formed from the same tropical wave that formed Tropical Storm Alpha days earlier. This wave continued westward and entered the Caribbean Sea. On 25 October 2005, this wave developed increased convection. On 26 October, organization was sufficient enough to designate the wave a tropical depression. The depression moved toward the northwest then to the north (Figure 4.50). On 27 October, the depression became Tropical Storm Beta while located in an environment of

low shear and high SSTs. Beta continued to move toward the north with development slowed by strong northeasterly wind shear. However, Beta slowly intensified into a category 1 hurricane on 29 October. Beta then began to move toward the west-southwest as a ridge of high-pressure became established to the north and northeast. Beta's intensification continued and it reached category 3 status, with U_h of 51.5 m s^{-1} on 30 October. Later that same day, Beta made landfall on the Nicaraguan coast as a category 2 on 30 October. Beta weakened rapidly over Nicaragua and dissipated on 31 October.

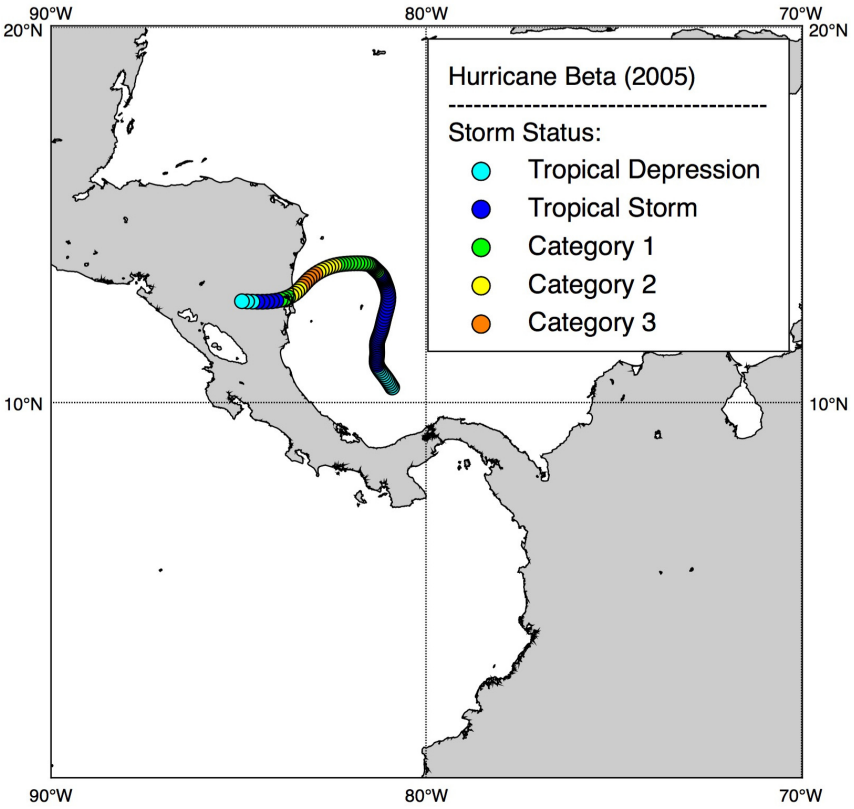

Figure 4.50: Hurricane Beta's (26 – 31 October 2005) track.

Hurricane Beta's oceanic conditions along-track were marginal, with an average D26 of 57.5 m (Figure 4.51). Values began in the upper-60s, and dropped to the low-40s. Beta was a very slow-moving storm, with an average U_h of 2.2 m s^{-1}. D26 values in the upper-60 m range and a U_h of less than 2 m s^{-1} on 26 October explain why Beta strengthened from a depression to a

tropical storm. However, as Beta increased in intensity to hurricane status, it had moved into areas where ocean depth was less than 200 m. Therefore, no valid D26 data were obtained during and after the point at which Beta became a hurricane. Therefore, no conclusions can be reached regarding oceanic conditions as Beta attained hurricane intensity on 29 October.

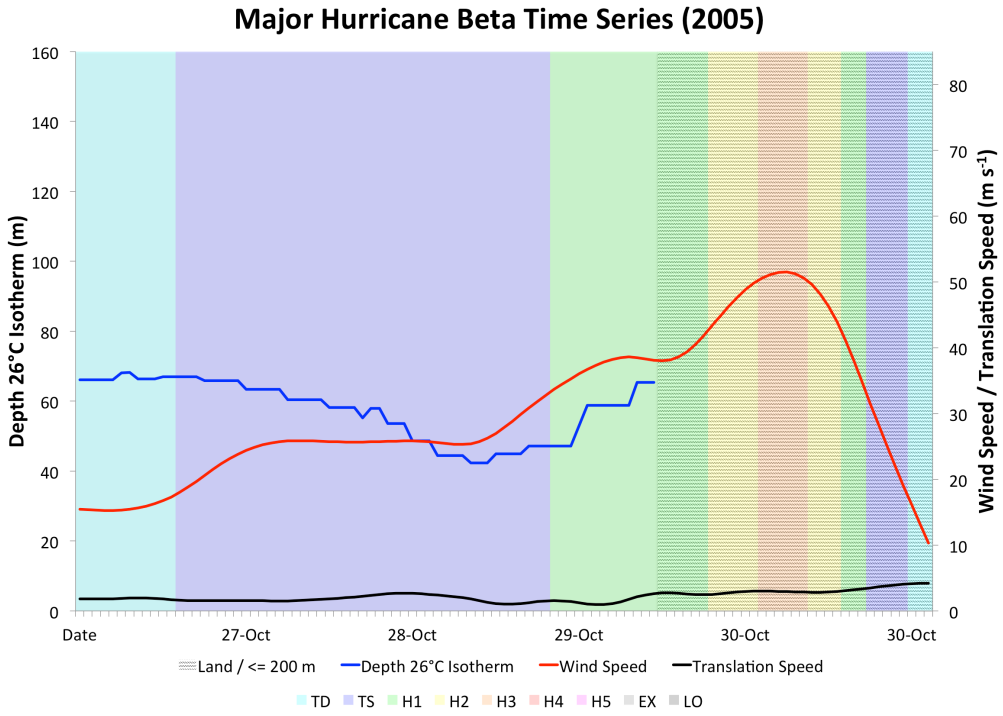

Figure 4.51: Hurricane Beta's time series of D26, U_{10}, U_h, and intensity category.

4.1.23 Tropical Storm Gamma

Tropical Storm Gamma formed from a tropical wave that exited the coast of Africa on 3 November 2005. This wave moved toward the west and convection maintained itself well enough for the system to be labeled a tropical depression on 14 November. The depression moved toward the west and became Tropical Storm Gamma on 15 November (Figure 4.52). However, this tropical storm status lasted only seven hours, as strong westerly wind shear demoted Gamma back into a depression later on 15 November. Gamma was further weakened on 16 November back into a tropical wave near Jamaica. This wave moved toward the west and

reached the western Caribbean Sea, where it interacted with a surface low-pressure system located over Panama.

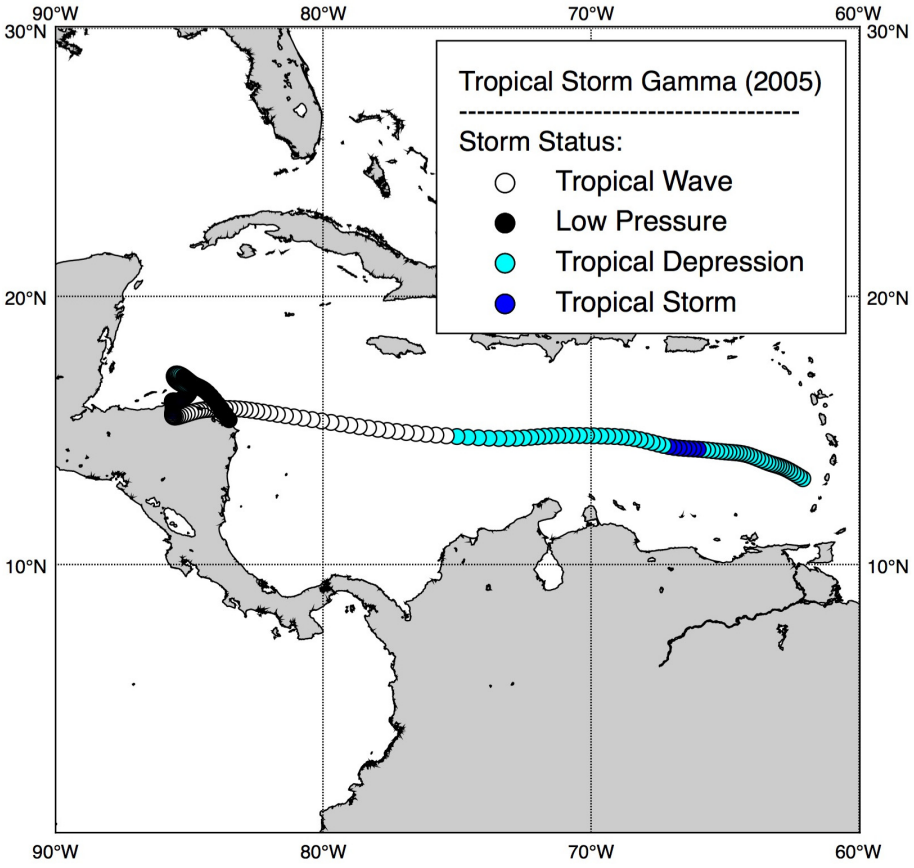

Figure 4.52: Tropical Storm Gamma's (14 – 22 November 2005) track.

Gamma re-intensified into a tropical storm once again while located along the northern coast of Honduras on 18 November. Gamma moved toward the north over the Caribbean Sea and reached a peak intensity of 23.1 m s^{-1} on 19 November. Gamma eventually moved toward the southeast and weakened to a depression on 20 November, a result of strong southerly shear. Weakening continued and Gamma became a remnant low on 21 November. Note in Figure 4.52 that the second tropical storm status points appear black, as the storm was moving very slowly.

Further analysis of Gamma reveals that the storm had an average D26 of 90 m. Gamma experienced very large D26 values as it moved through the Caribbean Sea, as values exceeded 100 m often, with a maximum D26 of 141.5 m (Figure 4.53).

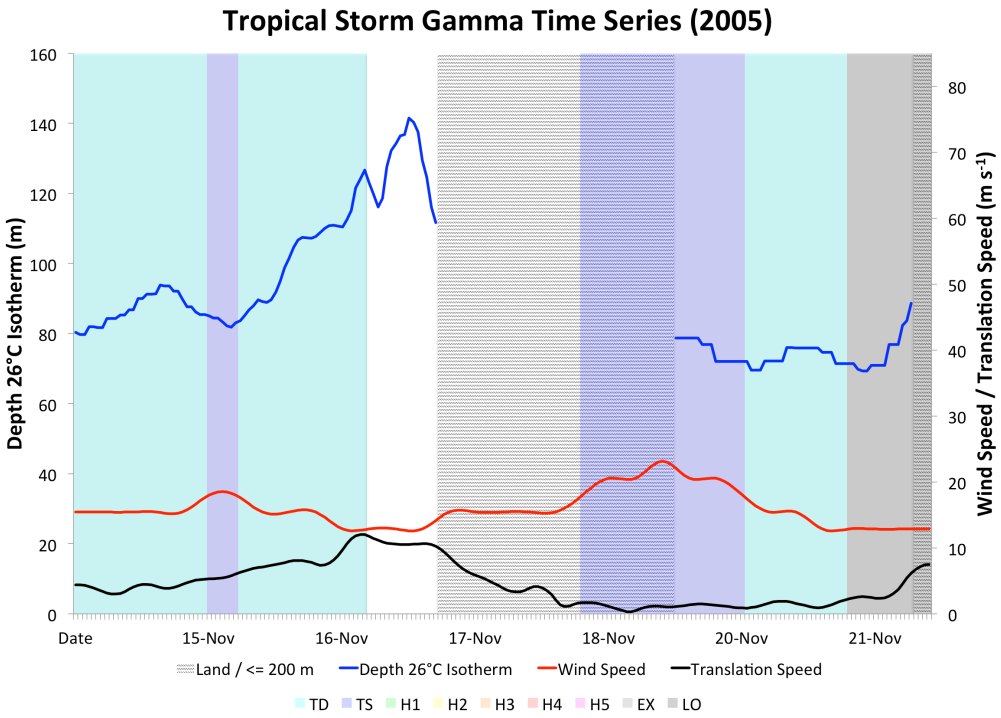

Figure 4.53: Tropical Storm Gamma's time series of D26, U_{10}, U_h, and intensity category. The white area in the foreground indicates the time period when Gamma was a tropical wave.

As Gamma became a tropical storm on 15 November, D26 was at 85.1 m. As Gamma continued through the Caribbean Sea, values steadily increased to over 100 m. U_h averaged 4.5 m s^{-1} along-track, while speeds decreased substantially to less than 2 m s^{-1} near the end of Gamma's track. These large D26 values presumably provided excess oceanic heat content. However, Gamma weakened back to a tropical wave on 16 November despite these values. A possible explanation lies in the fact that Gamma experienced strong westerly wind shear while in the Caribbean Sea (Beven *et al.*, 2008). As Gamma reached Central America, D26 values were smaller, with values

in the 70 – 90 m range. U_h also slowed substantially, below 2 m s^{-1}. This slow U_h, coupled with the moderately large D26 values, appear to have contributed to Gamma's re-intensification.

4.2 Threshold Analysis

The threshold analysis was completed to understand the required D26 value for the cyclogenesis of tropical storms and hurricanes (category 1)(Table 4.1). Results suggest that the threshold D26 value for tropical storm formation in 2005 was 23.5 m (Nate) and that for hurricane formation was 36.8 m (Maria). Collectively, these results demonstrate that storms are indeed able to form under shallow D26 values if atmospheric conditions are favorable.

Table 4.1: Summary of genesis D26 values at tropical storm (TS) and category 1 (H1) status. Invalid data indicates that a storm reached H1 status while located over ocean depths ≤ 200 m. Asterisks (*) demarcate storms that reached major status (category 3 +).

Storm #:	Storm Name:	TS D26 (m):	H1 D26 (m):
1	Arlene	106.4	-
2	Bret	37.4	-
3	Cindy	73.6	Invalid data
4	Dennis*	81.9	107.4
5	Emily*	73.8	73.4
6	Franklin	49.4	-
7	Gert	45.6	-
8	Harvey	30.1	-
9	Irene	62.8	39.2
10	Jose	34.1	-
11	Katrina*	75.8	86.2
12	Lee	35.1	-
13	Maria*	69.2	36.8
14	Nate	23.5	-
15	Ophelia	67.3	67.5
16	Philippe	83.4	75.2
17	Rita*	54.3	Invalid data
18	Stan	110.6	45.9
20	Tammy	98.4	-
21	Wilma*	93.7	82.1
22	Alpha	98.3	-
23	Beta*	67.0	Invalid data
24	Gamma	85.1	-

4.2.1 June

The contoured tropical storm and category 1 hurricane D26 thresholds reveal that in June 2005 the spatial extent of "tropical cyclogenesis" areas of the Atlantic basin gradually expanded in size as the month proceeded. This expansion was northward to include the central Atlantic by 30 June (Figure 4.54c).

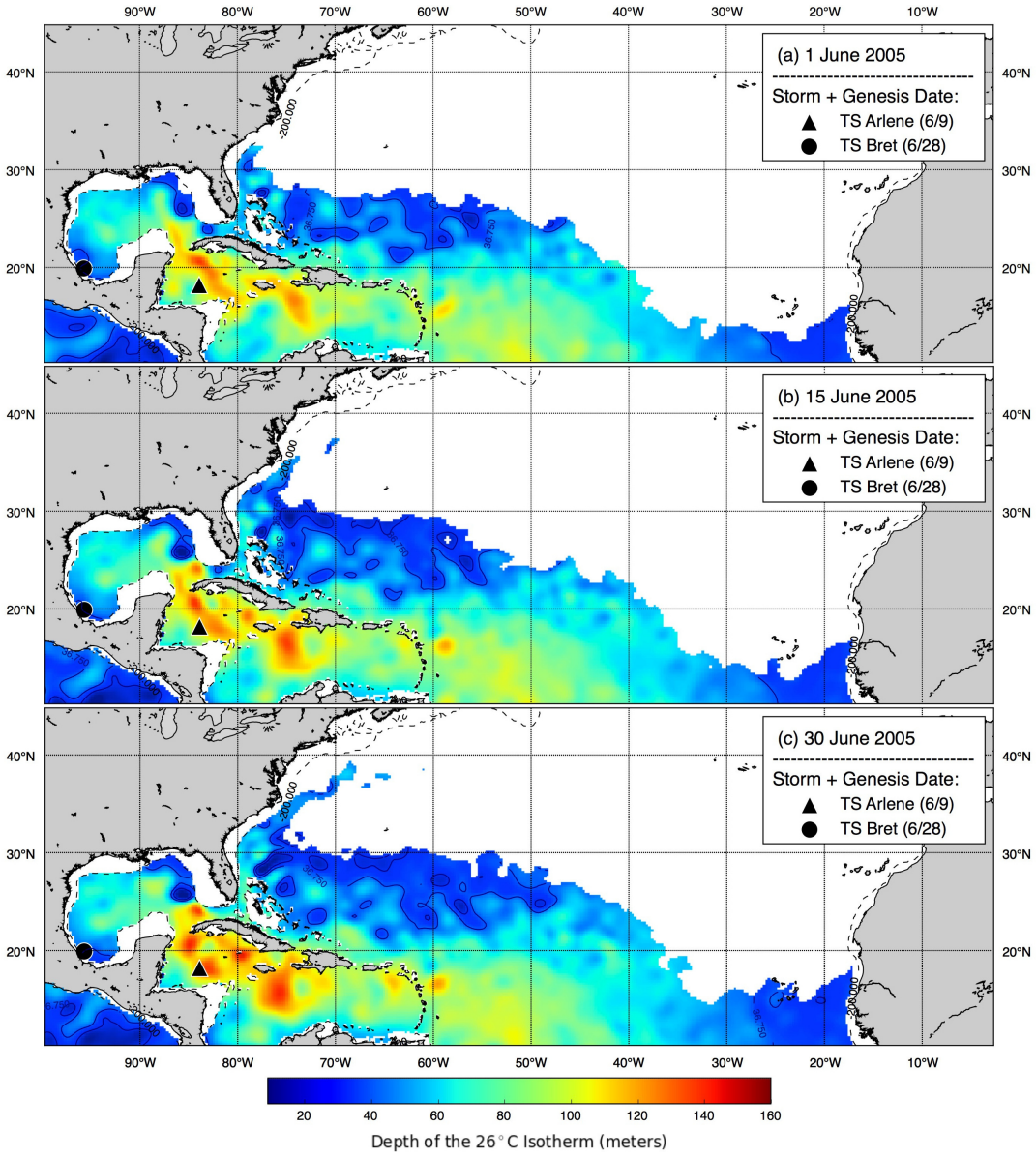

Figure 4.54: June D26 plotted for the 1st, 15th, and 30th with storm genesis locations overlain. Tropical storm (23.5 m) and category 1 (36.8 m) D26 thresholds are contoured.

Two tropical storms formed in June (Arlene and Bret). Arlene's tropical storm genesis D26 of 106.4 m in the western Caribbean Sea was well over the threshold of 23.5 m. Tropical Storm Bret's genesis value of 37.4 m was slightly above the threshold. Both storms formed in the western portion of the basin, as is common in June. The results also reveal that the area with the greatest oceanic heat content was located in the Caribbean Sea, where Tropical Storm Arlene formed. Tropical Storm Bret's genesis location in the far western Gulf of Mexico appears to have been an area with small oceanic heat content throughout the entire month.

4.2.2 July

The area susceptible to tropical storm and category 1 cyclogenesis based on D26 thresholds continued to expand substantially during July 2005. Through 31 July, a northward expansion of the thresholds into the central and northern Atlantic occurred (Figure 4.55c). Another interesting finding from the July threshold analysis was the presence of the Gulf Stream on 1 July (Figure 4.55a). The zone of abundant oceanic heat content in the Caribbean Sea and Gulf of Mexico also appears to have expanded spatially. In terms of storm formation, five systems were active in July. The first, Hurricane Cindy, began its tropical storm genesis over a D26 of 73.6 m while its hurricane genesis D26 was removed from analysis due to its location in ocean depths less than 200 m. Cindy's genesis location was the Gulf of Mexico, which appears to harbor high D26 values due to the presence of the Loop Current. This heat content appears to increase slightly in intensity throughout the month. Hurricane Dennis, a major storm, began in the eastern Caribbean Sea, an area that stored abundant oceanic heat content. Dennis had a tropical storm genesis D26 of 81.9 m and a hurricane genesis D26 of 107.4 m. Hurricane Emily, the season's first category 5 storm, formed in the south central Atlantic, where D26 values were

large, as apparent by Emily's 73.8 and 73.8 m D26 values at tropical storm and hurricane genesis.

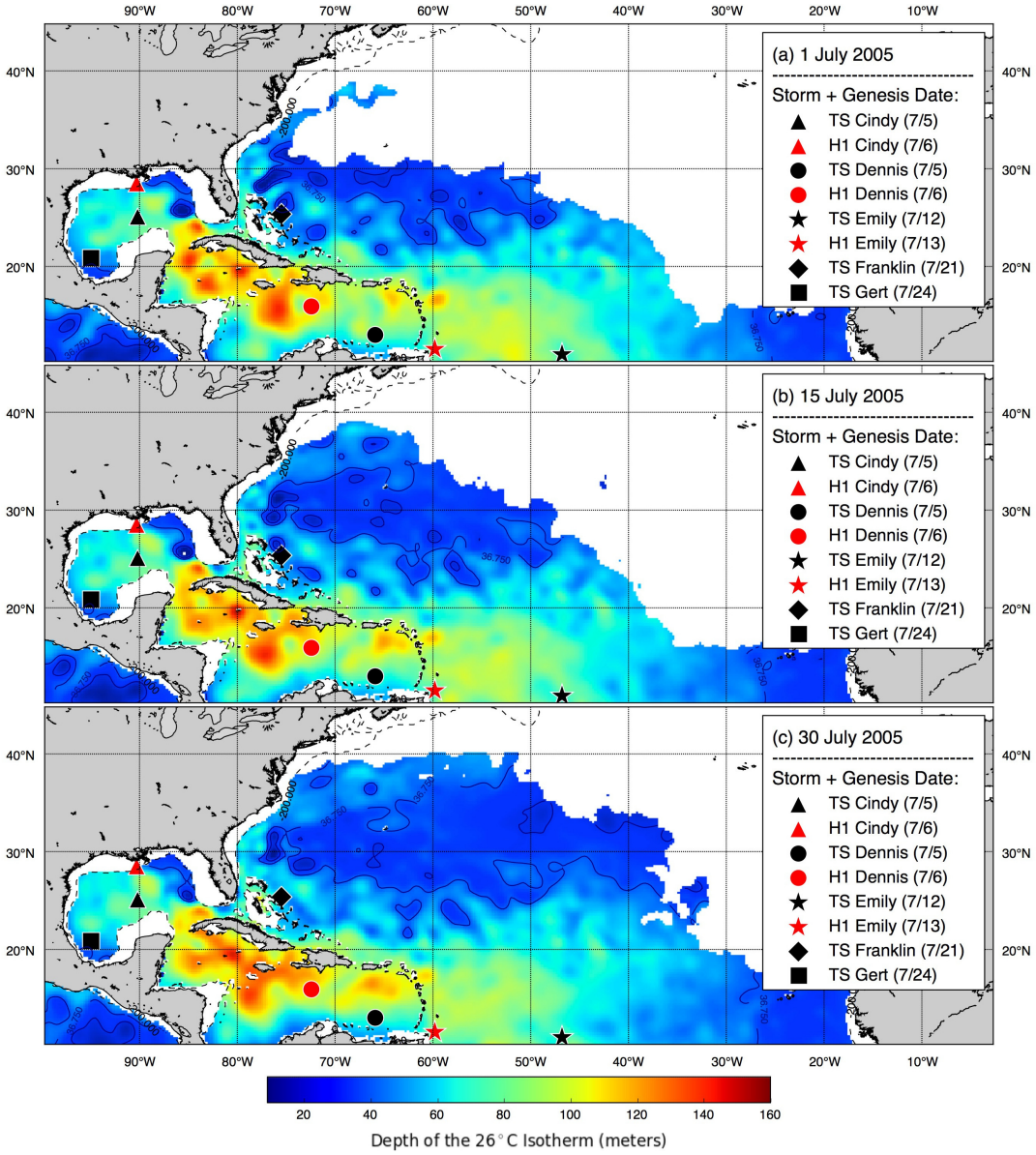

Figure 4.55: July D26 plotted for the 1st, 15th, and 30th with storm genesis locations overlain. Tropical storm (23.5 m) and category 1 (36.8 m) D26 thresholds are contoured.

The last two tropical systems, Franklin and Gert, formed in areas where D26 was small, in the 40s. Franklin's formation zone near the Bahamas appears to have experienced little change in D26 throughout July. Gert's genesis in the southwestern Gulf of Mexico, like Bert's in June, was

in an area with small D26 values. This area appears to remain with small D26 values throughout July 2005. Overall, similar to June, the Caribbean Sea stored the most volumetric heat.

4.2.3 August

As expected, the spatial extent of the tropical storm and hurricane-capable thresholds greatly increased during August 2005. A protrusion northward into the northern sections of the Atlantic Ocean was apparent by 15 and 30 August (Figure 4.56b, 4.56c). Like July, a total of five storms formed during the month of August. Harvey, the first storm of the month, became a tropical storm in the open Atlantic Ocean, with a genesis value of 30.1 m. Hurricane Irene also formed in the open Atlantic, with genesis values of 62.8 and 32.9 at tropical storm and category 1 designation, respectively. The smaller category 1 genesis value was present because Irene became a hurricane in the northwest Atlantic, poleward of 30° N. Tropical Storm Jose, similar to Bert and Gert, formed in the southwestern Gulf of Mexico. A genesis value at 34.1 m again provided support to the conclusion that the southwestern Gulf of Mexico contained only shallow warm water pools consistently from June through August 2005. Hurricane Katrina, the season's second category 5 storm, formed just off the coast of Florida with genesis values of 75.8 and 86.2 at tropical storm and category 1 designation, respectively. Katrina's genesis values were well above the threshold values. The area where Katrina formed (just east of Florida in the Atlantic Ocean) appears to have contained relatively high D26 values throughout the month. The last storm of the season, Tropical Storm Lee, had a low genesis value of 35.1 m. This was not surprising given the location of genesis (29° N) in the north central Atlantic where values tended to be lower. The August analysis revealed no specific preferred genesis location, as storms formed throughout the entire basin. This spread in genesis locations for the month of August was likely a result of the increased spatial extent of the threshold values along with an increase in

values in the Caribbean Sea and Gulf of Mexico. This increase in values in the Caribbean Sea reached a peak in spatial extent just south of Cuba (Figure 4.56c).

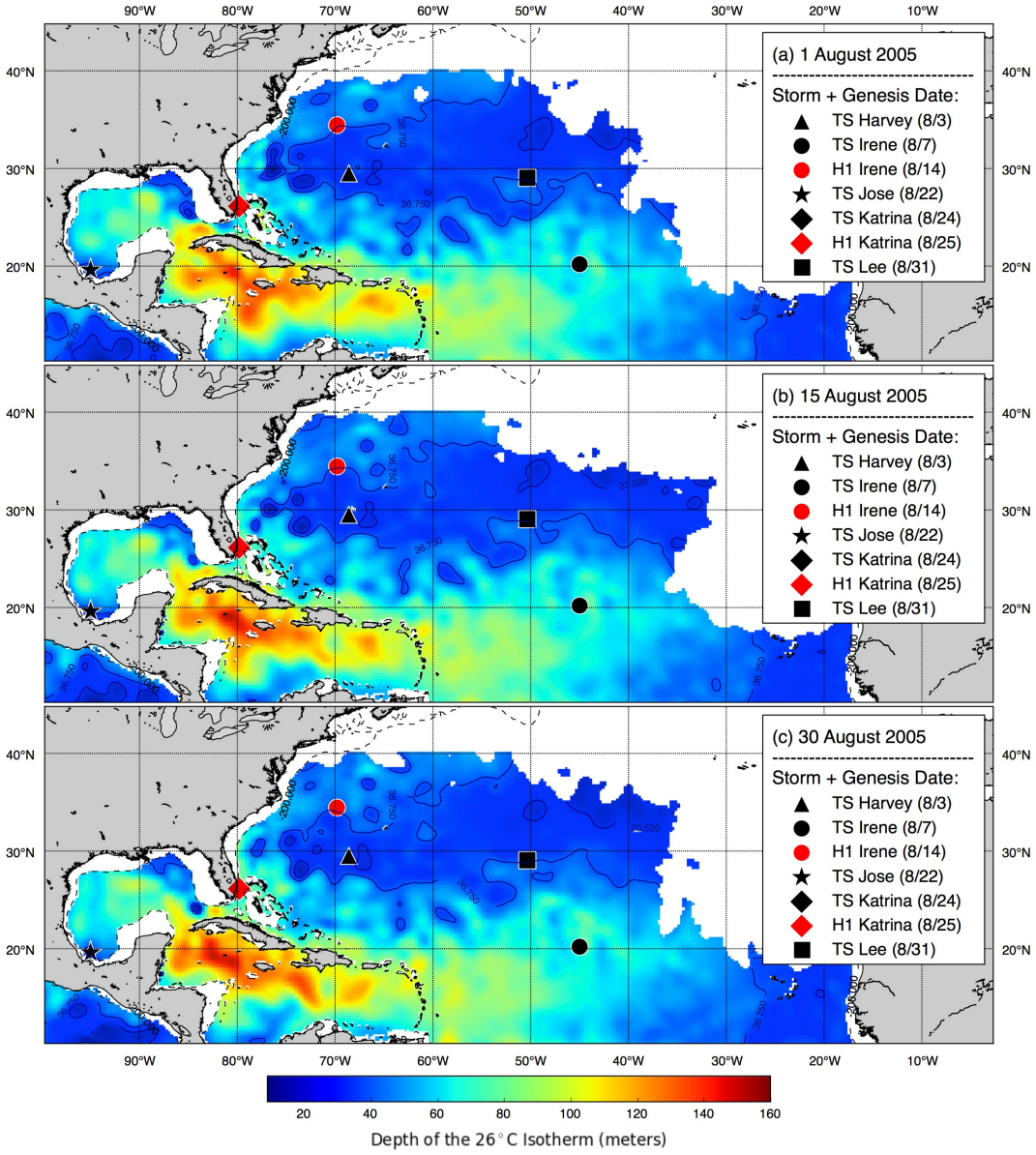

Figure 4.56: August D26 plotted for the 1st, 15th, and 30th with storm genesis locations overlain. Tropical storm (23.5 m) and category 1 (36.8 m) D26 thresholds are contoured.

4.2.4 September

The September 2005 threshold analysis reveals that, unlike August, a slight contraction of threshold areas occurred as the month progressed. This contraction was especially apparent in the

northern and eastern Atlantic Ocean on 30 September, as the threshold areas generally retreated equatorward of 30° N latitude (Figure 4.57c). Again, five storms formed during September, with genesis locations spread throughout the basin. Hurricane Maria formed in the south central Atlantic with genesis values at 69.2 and 36.8, respectively. In fact, Hurricane Maria's category 1 genesis value of 36.8 was the source of the threshold used in this research, as it was the lowest value in which a category 1 hurricane formed. Tropical Storm Nate's genesis value of 23.5 m in the western Atlantic was the lowest value in which a tropical storm formed during the season, and thus the threshold. Hurricane Ophelia, which formed just off the east coast of Florida near the Gulf Stream, had values of 67.3 and 67.5 at tropical storm and category 1 genesis, respectively. Ophelia's genesis location near the Gulf Stream appears to have facilitated its formation and eventual strengthening to a category 1 storm. Hurricane Philippe formed in the eastern Caribbean Sea, which contained very large D26 values in September, with Philippe's genesis values of 83.4 and 75.2. Hurricane Rita, the season's third category 5 storm, had a tropical storm genesis value of 54.2 m. Its category 1 genesis value was not obtainable, given the fact that it achieved hurricane status in a location where ocean depths were less than 200 m. However, a look at D26 values just before Rita entered depths of less than 200 m revealed a value of 80.1 m. Rita encountered this depth a mere two hours before entering the invalid D26 data area. In general, the September analysis revealed no specific genesis location for storms. There were genesis locations in the central Atlantic Ocean and in the eastern Caribbean Sea. Storm genesis also occurred just off the east coast of the United States. These findings were as expected for the month of September, given that the peak of hurricane season takes place in September and conditions typically become optimal over a large part of the basin during this time period.

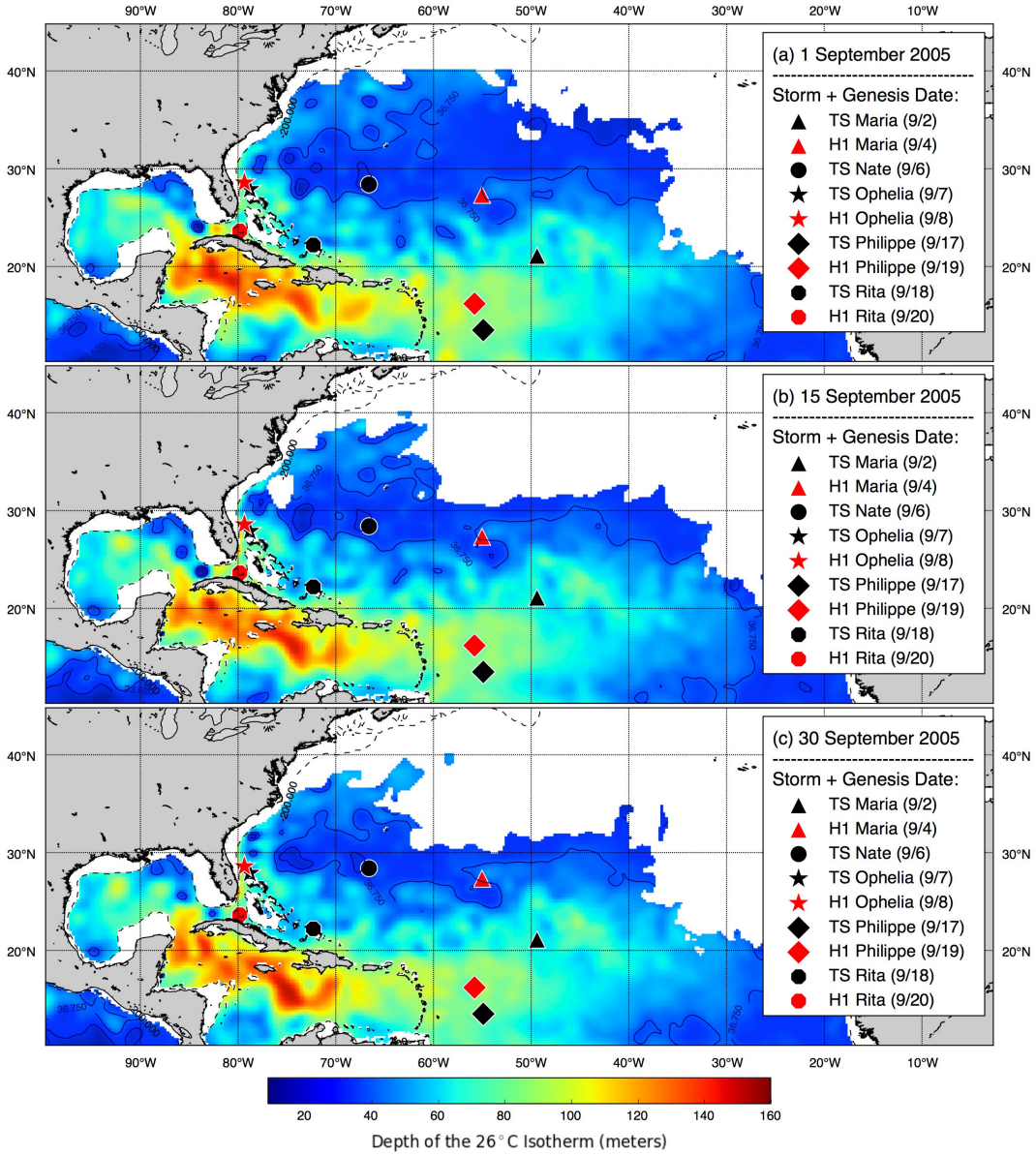

Figure 4.57: September D26 plotted for the 1st, 15th, and 30th with storm genesis locations overlain. Tropical storm (23.5 m) and category 1 (36.8 m) D26 thresholds are contoured.

4.2.5 October

The October 2005 threshold analysis revealed an abrupt contraction in total threshold areas, specifically near the east coast of the United States. This contraction was especially apparent on 30 October (Figure 4.58c), when values fell to 0 m just off the east coast of the United States. However, the Gulf Stream seems to have harbored substantial oceanic heat

content (Figure 4.58c). Once again, the Caribbean Sea contained some of the largest D26 values in the entire basin (Figure 4.58a, 4.58b, 4.58c). A total of five named storms formed during the month, all west of 60° W longitude. All except one storm formed in the Caribbean Sea, where D26 values were very large. The first storm of the month, Hurricane Stan, formed near the Yucatán peninsula with a genesis value of 110.6 m at tropical storm status. This tropical storm genesis value was the highest value recorded in this research. As Stan became a hurricane in the southwestern Gulf of Mexico, its genesis value actually decreased to 45.9 m. Stan was the fourth storm of the season to form in this area, despite consistently low D26 values for June – October. Tropical Storm Tammy, the lone October storm to form in the Caribbean Sea, underwent cyclogenesis with a D26 value of 98.4 m just off the east coast of Florida. This area appears to consistently store significant heat, with its large D26 values, as Katrina (August) and Ophelia (September) also formed there. Hurricane Wilma, which was the strongest storm of the season, formed in the western Caribbean Sea where D26 values were very large. Wilma's genesis values were 93.7 m and 82.1 m at attainment of tropical storm and category 1 strength. Tropical Storm Alpha's genesis value of 98.3 m again supports the conclusion that the Caribbean Sea contained the highest values, even during the end of the season. Hurricane Beta, which formed in the southern Caribbean Sea late in October, had a genesis value of 67.0 m when it gained tropical storm status. Its genesis value at category 1 status was invalid due to its proximity to the coast of Honduras where ocean depths were less than 200 m. The October analysis reveals a shift in storm genesis location to the west with all but one storm forming in the Caribbean Sea. This westward shift could be explained by the slow thinning of the surface warm layer in the eastern and northern Atlantic Ocean.

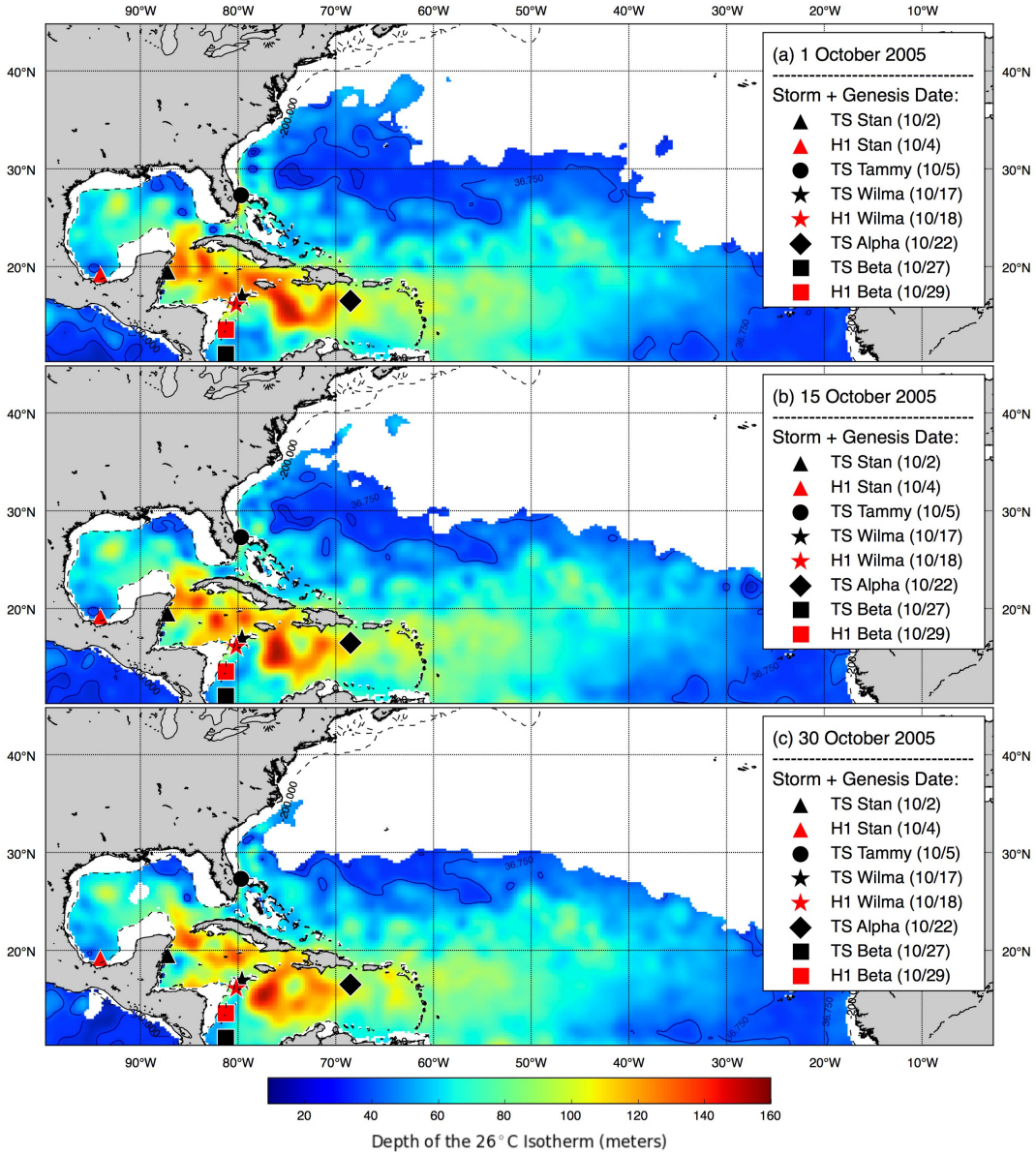

Figure 4.58: October D26 plotted for the 1st, 15th, and 30th with storm genesis locations overlain. Tropical storm (23.5 m) and category 1 (36.8 m) D26 thresholds are contoured.

4.2.6 November

The November 2005 threshold analysis revealed no surprises, with the smallest threshold areas of any month analyzed. The smallest area with warm layers exceeding the threshold thickness was present on 30 November (Figure 4.59c). These areas retreated to equatorward of 30° N. The Gulf of Mexico was too cold for tropical cyclogenesis. However, the Loop Current

did appear to maintain its heat content, even on 30 November. The Caribbean Sea finally displayed reductions in D26 values, although it still contained high values even as of 30 November. Only one storm formed during the month of November. Tropical Storm Gamma's genesis occurred in the central Caribbean Sea, with a value of 85.1 m. In summary, the analysis demonstrated a noticeable shrinking in the threshold areas throughout November 2005.

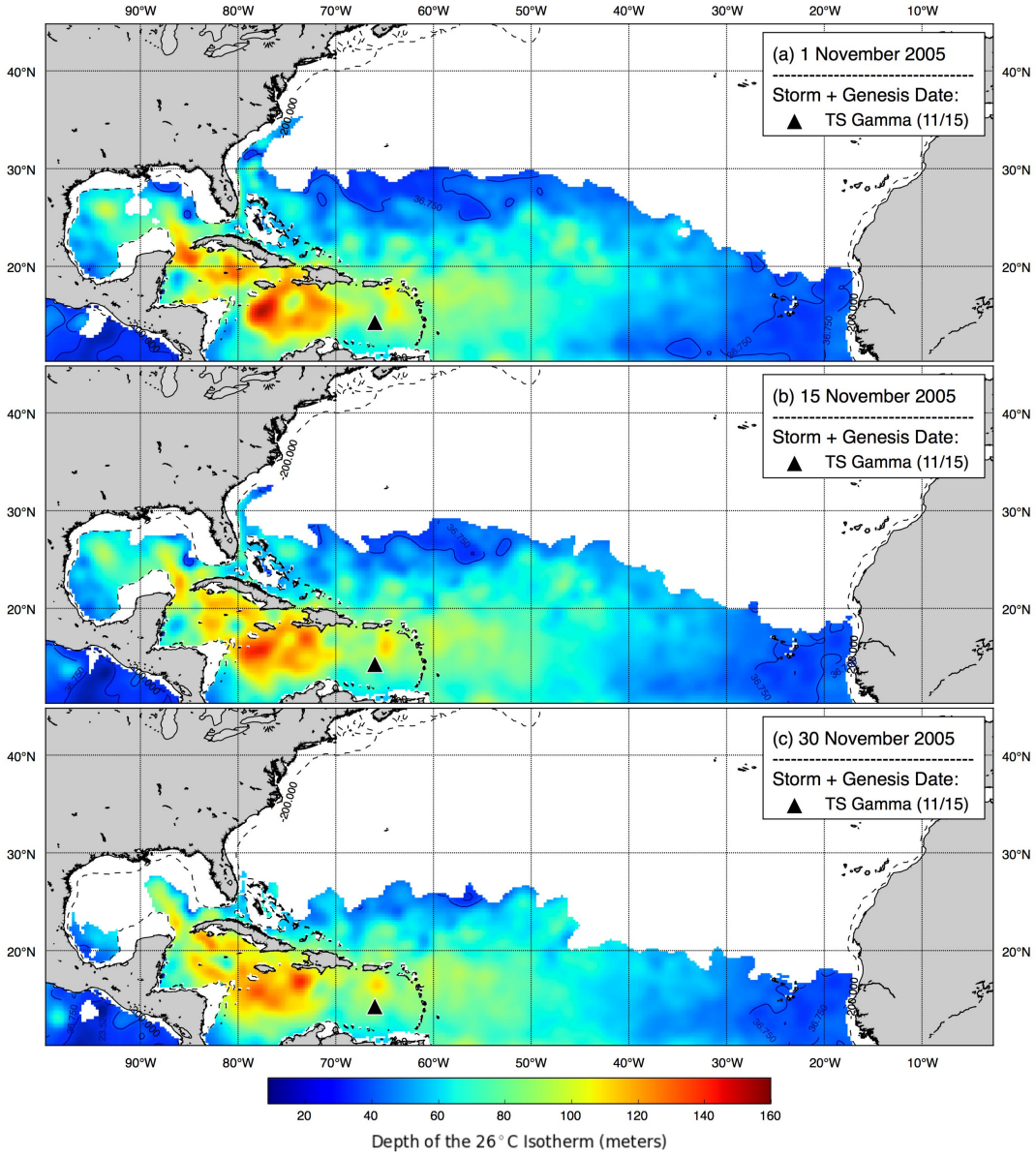

Figure 4.59: November D26 plotted for the 1st, 15th, and 30th with storm genesis locations overlain. Tropical storm (23.5 m) and category 1 (36.8 m) D26 thresholds are contoured.

4.3 Regression Analysis

A set of regression models (1 simple, 7 multiple; labeled A – H) were run on various subsets of the data in an attempt to explain the variability of along-track U_{10} using U_h and D26 as the explanatory variables. More specific models that were used to analyze a subset of the tropical cyclones were also developed, in an attempt to determine whether the explanatory power of the model increases for storms with certain common features. Each regression model was analyzed to confirm that it did not violate the assumption of normality of residuals, multicollinearity, and homoscedasticity. If a model was found to violate one of these assumptions, it was noted in the model subsection and interpreted with caution. Each subsection contains specifics of each model, including which variables were used and on which data sets. In addition, the regression equation for category 5 storms (Emily, Katrina, Rita, and Wilma) is included for reference. A more detailed overview of the regression models run in the following subsections can be found in Chapter 3 (subsection 3.5.6).

4.3.1 Regression A – All Data

Regression A (n = 2,430) – all data – is a simple linear regression model that includes all data (U_{10} and D26) from the 23 named stormed analyzed in this research. This model performed poorly in explaining the variation in along-track U_{10}, as apparent by an adjusted r-squared value of 0.0435, meaning that approximately 4% of the variation in U_{10} could be explained by D26. This model also violated a key regression assumption; a plot of the residuals shows signs of non-normality. Therefore, the results of this model should be taken with extreme caution. However, this model was useful in that it provided evidence that not all storms can easily be explained by one single explanatory variable.

4.3.2 Regression B – All Data

Regression B (n = 2,430) – all data, is a multiple regression model that includes U_h as a second explanatory variable along with D26 to explain the variation in along-track U_{10}. This model, like Regression A – all data, performed unsatisfactorily in explaining the variation in along-track U_{10} for the 23 storms analyzed in this research. The adjusted r-squared value of 0.0439, almost identical to Regression A – all data, reveals that including another explanatory variable only increased the model's explanatory power by 0.0004. This improvement was very miniscule and therefore demonstrated that including U_h into the model provided no real improvement. Regression B – all data also violated the normality of residual assumption. The plot of residuals shows a deviation from normality. Once again, the results of this model should be interpreted with caution because of the violation.

4.3.3 Regression C – Majors

Regression C (n = 333) – major hurricanes is a multiple regression model run only on the major storms of the season (*i.e.*, $\geq$ 50 m s^{-1}; Dennis, Emily, Katrina, Rita, and Wilma). Hurricanes Maria and Beta were discarded even though they briefly reached major status. This model performed well at explaining the variation in along-track U_{10} for the majors, with an adjusted r-squared of 0.1982. This indicates that approximately 20% of the variation in U_{10} for the majors could be explained by D26 and U_h. The plotted residual plot for Regression C – majors also appears to follow a normal distribution for the most part. There was a slight plateauing of residuals near the tails of the data set, but there were no extreme outliers. This model provided strong evidence that major storms are more influenced by D26 and U_h than weaker storms.

4.3.4 Regression D – Dennis

Regression D (n = 48) – Dennis is another multiple regression model, run on Hurricane Dennis, the first major storm of the season. D26 and U_h were used to predict the variation in along-track U_h of Dennis. Regression D – Dennis revealed a very low adjusted r-squared value of 0.0145. The residual plot for this regression model showed some deviations from normality, thus violating the normality of residuals assumption required. This model showed that D26 and U_h explained little of the variance in U_{10} along-track, indicating that atmospheric parameters may have played a much larger role in its intensity.

4.3.5 Regression E – Emily

Regression E (n = 92) – Emily is similar to the previous model, except that it includes Hurricane Emily, the season's first category 5 storm. This model produced the highest adjusted r-squared value yet, at 0.5560. This model, with its moderately high adjusted r-squared value, provided evidence that for Hurricane Emily D26 and U_h played an important role in modulating along-track U_{10}. Regression assumptions were met, with a moderate skewness in residuals and a few outliers. Despite the skewness and outliers, the model appears useful. Overall, this model run on Emily successfully showed that D26 and U_h do play an important role in controlling along-track U_{10}. The regression equation this model utilized was given as the following:

$$\hat{U}_{10} = 43.31 + 0.22\ (D26;\ m) + (-0.45)\ (U_h;\ m\ s^{-1})$$

where 43.31 represents the intercept and 0.22 and –0.45 both represent the coefficients of D26 and U_h.

4.3.6 Regression F – Katrina

Hurricane Katrina's multiple regression model (n = 49) which incorporated D26 and U_h as the explanatory variables produces a very high adjusted r-squared value of 0.7493. This

provided some evidence, coupled with Emily, that these two explanatory variables may be important for modeling category 5 storms. Katrina's regression seems to satisfy all assumptions of a multiple regression model, including the normality of residuals. There was some slight deviation from normality, but nothing of concern. The regression equation this model utilized was given as the following:

$$\hat{U}_{10} = 21.79 + 0.11\ (D26;\ m) + 7.52\ (U_h;\ m\ s^{-1})$$

where 21.79 represents the intercept and 0.11 and 7.52 both represent the coefficients of D26 and U_h.

4.3.7 Regression G – Rita

Hurricane Rita's multiple regression model (n = 67), like that of Katrina, produced a high adjusted r-squared value at 0.7427. Hurricane Rita was also a category 5 storm for a time during its track. Most assumptions were met, except for the normal distribution of residuals. A slight plateauing of the residuals was noted near the beginning of the data set. However, this model was still considered useful as it provided further support to the hypothesis that major storms that reach category 5 status are more influenced by D26 and U_h. The regression equation this model utilized was given as the following:

$$\hat{U}_{10} = 89.03 + 0.15\ (D26;\ m) + (-7.63)\ (U_h;\ m\ s^{-1})$$

where 89.03 represents the intercept and 0.15 and –7.63 both represent the coefficients of D26 and U_h.

4.3.8 Regression H – Wilma

The last multiple regression model was run on Hurricane Wilma (n = 81), the last category 5 storm of the season. It was expected that Hurricane Wilma would produce a high adjusted r-squared value, similar to the three previous category 5 storms (Emily, Katrina, and

Rita). However, a surprisingly low value of 0.4139 was produced. The plot of residuals does reveal a highly non-normal appearance. The regression equation this model utilized was given as the following:

$$\hat{U}_{10} = 59.02 + 0.11\ (D26;\ m) + (-0.43)\ (U_h;\ m\ s^{-1})$$

where 59.02 represents the intercept and 0.11 and –0.43 both represent the coefficients of D26 and U_h.

4.4 Summary

In addition to providing a summary of overviews by Beven *et al*. (2008) of the life cycles of the 28 named storms in 2005, this chapter has examined the role of U_h and D26 on tropical cyclogenesis. Overall, the results presented in this chapter suggest that U_h and D26 influence the along-track intensity fluctuations of tropical cyclones, in at least some instances. However, each storm had its own unique oceanic and atmospheric interactions that explained some of the variability in U_{10}. Major storms (Emily, Dennis, Katrina, Rita, and Wilma) analyzed in this research were found to be largely influenced by the along-track three-dimensional oceanic thermal structure, including oceanic mesoscale features (*i.e.*, Florida Current, Loop Current, WCEs, and CCEs). In addition, U_h appears to play a crucial role in the intensification and weakening of tropical cyclones by affecting the amount of time a cyclone spent over the underlying oceanic thermal structure. The threshold analysis reveals a threshold D26 value for tropical storm and hurricane (category 1) cyclogenesis of 23.5 m and 36.8 m. These thresholds were found to reach a peak spatial extent in August and September. Cyclogenesis locations shift intra-seasonally from the Gulf of Mexico to the Atlantic Ocean and Caribbean Sea, then back to the Caribbean Sea. The Caribbean Sea contains the greatest oceanic heat content throughout the entirety of the season, with no decrease until mid- to late November. Regression models run on

various subsets of the data reveal that U_h and D26 are able to explain a large portion of the variability in along-track U_{10} for category 5 storms Emily, Katrina, and Rita. These results provided further support to the conclusion that category 5 storms appeared to be more influenced by U_h and D26 than other storms. Table 5.1 presents a review of the regression models and their corresponding results.

Table 5.1: Summary of regression models with results. Asterisks (*) demarcate storms that reached category 5 status.

Name:	Observations (n):	Independent Variable(s):	Dependent Variable:	Adjusted r-squared:
A – all named storms in 2005	2,430	D26	U_{10}	0.0435
B – all named storms in 2005	2,430	D26, U_h	U_{10}	0.0004
C – Major hurricanes	333	D26, U_h	U_{10}	0.1982
D – Dennis	48	D26, U_h	U_{10}	0.0145
E – Emily*	92	D26, U_h	U_{10}	**0.5560**
F – Katrina*	49	D26, U_h	U_{10}	**0.7493**
G – Rita*	67	D26, U_h	U_{10}	**0.7427**
H – Wilma*	81	D26, U_h	U_{10}	**0.4139**

CHAPTER 5: SUMMARY AND CONCLUSIONS

5.1 Summary and Conclusions

This research represents the first major attempt to increase understanding of tropical cyclones in the North Atlantic basin by investigating the role of the three-dimensional oceanic thermal structure and translation speed (U_h) on the cyclogenesis and intensification processes. It was found through an along-track analysis of the 23 named storms that the oceanic thermal structure, as represented by the depth of the surface layer with temperatures exceeding 26°C (D26), coupled with U_h, did in fact have an influence on intensity fluctuations. Specifically, storms were found to be largely influenced by oceanic mesoscale features such as warm-core eddies and cold-core eddies (WCEs and CCEs) as well as the Loop Current. These features were shown to either increase or decrease the intensity of the tropical cyclone by modulating the amount of oceanic heat content to fuel the storms. Specifically, Hurricanes Dennis, Emily, Katrina, Rita, and Wilma were found to be largely influenced by these WCEs and CCEs as intensification or weakening took place. U_h along-track also played a substantial role by governing the amount of time the cyclone spent over the oceanic thermal structure. A threshold analysis revealed that the minimum D26 for the formation of tropical storms (23.5 m) and hurricanes (category 1) (36.8 m). These observed minimum D26 values revealed that tropical systems can and do form within a shallow warm layer given favorable atmospheric conditions. However, the threshold analysis did reveal that most major storms (*i.e.*, winds $\geq$ 50 m s^{-1}) formed over waters with much thicker warm (*i.e.*, $\geq$ 26°C) layers. Spatially, the extent of the ocean basin with depths exceeding these threshold D26 values was found to expand in size from the beginning of the season (1 June) to September. A contraction of the area with depths exceeding the minimum threshold was observed beginning in October, until the end of the season (30 November). The area with the most consistently abundant oceanic heat content was the

Caribbean Sea, where the area of sufficient D26 for tropical cyclone development did not decrease until mid- to late November. In June and July, storms were able to form in the Caribbean Sea and Gulf of Mexico, with no formation in the Atlantic Ocean. This result seems to be related to the spatial distribution of the D26 threshold depths. By August and September, these genesis locations migrated eastward to include the Central Atlantic and eastern Caribbean Sea. Formation then began to move back toward the Gulf of Mexico and western Caribbean Sea by October and November.

Linear regression models performed using wind speed (U_{10}) as the dependent variable and D26 and U_h as the independent (explanatory variables) revealed varying results. A simple linear regression model performed on all 23 storms using only D26 as the explanatory variable revealed low explained variance in along-track U_{10}. A multiple linear regression model that incorporated U_h as a secondary explanatory variable showed a low but significant amount of explained variability. Several storm-specific multiple linear regression models were then run and revealed that category 5 storms were more likely to be influenced by along-track D26 and U_h. These results demonstrate that major storms, specifically ones that reach category 5, were more likely to be impacted by the three-dimensional oceanic thermal structure and U_h with subsequent responses in U_{10}.

This research emphasizes the importance of including the three-dimensional oceanic thermal structure in the study of tropical cyclones. While the sea surface temperature plays a significant role in the cyclogenesis and intensification of cyclones, the characteristics of the subsurface ocean are also important. In addition, U_h was found to be extremely important in modulating the intensity changes along-track, as it determines the residence time of tropical cyclones over distinct oceanic thermal conditions. Also, U_h directly affects the oceanic thermal

structure itself, by enhancing turbulent mixing and upwelling. Overall, this research provided strong evidence for the currently accepted (but largely untested) importance of the three-dimensional oceanic thermal structure and U_h on the behavior of tropical cyclones.

The broader impacts of this research are to increase the accuracy of coupled oceanic-atmospheric models in an attempt to better tropical cyclone intensity forecasts. Model-predicted intensity forecasts have been improving at a slower rate compared to track prediction. DeMaria *et al.* (2014) noted that there has been very little improvement in intensity forecasts, in particular at the shorter time periods (24 – 48 hours). Given this finding, the need to improve these models via the inclusion of oceanic thermal conditions is of high priority. Accurate intensity forecasts are of vital importance not only the scientific community, but also to public officials and coastal residents.

5.2 Research Limitations and Future Research

This research provided valuable results in the understanding of tropical cyclone interaction with the underlying ocean. However, one major limitation of this research is its inclusion of only one hurricane season. Although this season did provide numerous storms to analyze, the inclusion of additional seasons would strengthen the results. The spatial and temporal resolution of the D26 data was also not ideal, although it was the best data set available. Finally, this research focused mainly on the oceanic aspect of cyclogenesis and intensity fluctuations and did not directly utilize atmospheric data. The incorporation of along-track atmospheric variables such as upper-level winds and dry air advection could be of use to explain the cyclogenesis and intensity fluctuations more fully. In addition to these atmospheric parameters, the inclusion of storm size could also be of use. The utilization of radius of maximum winds (RMW) data, in an attempt to sample D26 data not only at the storm's center,

could provide a more accurate picture of the state of the oceanic thermal structure. The RMW data could also aid in the understanding of the effect of D26 and U_h on cyclogenesis and intensity fluctuations. Future research on this topic could include other ocean basins, particularly the East Pacific and Western North Pacific. However, despite the limitations, this research was still powerful enough to demonstrate the important role of the three-dimensional oceanic thermal structure along with U_h on tropical cyclone behavior. These results may benefit tropical cyclone modelers as they seek to improve forecasting that will protect lives and property.

REFERENCES

Ali, M. M., G. J. Goni & V. Jayaraman (2010): Satellite-derived ocean heat content improves cyclone predictions: Utilization of satellite-derived oceanic heat content for cyclone studies: Hyderabad, India, 25–26 March 2010. *EOS, Transactions American Geophysical Union*, **91**, 396–396.

Amante, C. & B.W. Eakins (2009): ETOPO1 1 Arc-Minute Global Relief Model: Procedures, Data Sources and Analysis. *NOAA Technical Memorandum NESDIS NGDC-24*. National Geophysical Data Center, NOAA.

Beven, J. L., L. A. Avila, E. S. Blake, D. P. Brown, J. L. Franklin, R. D. Knabb, R. J. Pasch, J. R. Rhome & S. R. Stewart (2008): Atlantic hurricane season of 2005. *Monthly Weather Review*, **136**, 1109–1173.

Boyd, E. C. K. (2011): *Fatalities Due to Hurricane Katrina's Impacts in Louisiana* (Doctoral Dissertation). Louisiana State University.

Byers, H. R. (1974): *General Meteorology*. McGraw-Hill, New York, 314 pp.

Dare, R. A. & J. L. McBride (2011): The threshold sea surface temperature condition for tropical cyclogenesis. *Journal of Climate*, **24**, 4570–4576.

DeMaria, M., C. R. Sampson, J. A. Knaff & K. D. Musgrave (2014): Is tropical cyclone intensity guidance improving? *Bulletin of the American Meteorological Society*, **95**, 387–398.

Elsner, J. B. & A. B. Kara (1999): *Hurricanes of the North Atlantic: Climate and Society*. Oxford University Press, New York, 488 pp.

Elsner, J. B. & T. H. Jagger (2012): *Hurricane Climatology: A Modern Statistical Guide Using R*. Oxford University Press, New York. 150–153 pp.

Elsner, J. B., S. E. Strazzo, T. H. Jagger & T. LaRow (2013): Sensitivity of limiting hurricane intensity to SST in the Atlantic from observations and GCMs. *Journal of Climate*, **26**, 5949–5957.

Emanuel, K. A. (1986): An air-sea interaction theory for tropical cyclones. Part I: Steady-state maintenance. *Journal of the Atmospheric Sciences*, **43**, 585–604.

Emanuel, K. A. (2003): Tropical cyclones. *Annual Review of Earth and Planetary Sciences*, **31**, 75–104.

Falkovich, A. I., A. P. Khain & I. Ginis (1995): The influence of air-sea interaction on the development and motion of a tropical cyclone - numerical experiments with a triply nested model. *Meteorology and Atmospheric Physics*, **55**, 167–184.

Fisher, E. L. (1958): Hurricanes and the sea-surface temperature field. *Journal of Meteorology*, **15**, 328–331.

Foltz, G. R. & M. J. McPhaden (2006): Unusually warm sea surface temperatures in the tropical North Atlantic during 2005. *Geophysical Research Letters*, **33**, L19703.

Goni, G. J. Kamholz, S. Garzoli & D. Olson (1996): Dynamics of the Brazil-Malvinas Confluence based on inverted echo sounders and altimetry. *Journal of Geophysical Research: Oceans*, **101**, 16273–16289.

Goni, G. J. & J. A. Trinanes (2003): Ocean thermal structure monitoring could aid in the intensity forecast of tropical cyclones. *EOS, Transactions American Geophysical Union*, **84**, 573–578.

Gray, W. M. (1968): Global view of the origin of tropical disturbances and storms. *Monthly Weather Review*, **96**, 669–700.

Holliday, C. R. & A. H. Thompson (1979): Climatological characteristics of rapidly intensifying typhoons. *Monthly Weather Review*, **107**, 1022–1034.

Hong, X. D., S. W. Chang, S. Raman, L. K. Shay & R. Hodur (2000): The interaction between Hurricane Opal (1995) and a warm core ring in the Gulf of Mexico. *Monthly Weather Review*, **128**, 1347–1365.

Jacob, S. D. & L. K. Shay (2003): The Role of oceanic mesoscale features on the tropical cyclone–induced mixed layer response: A case study. *Journal of Physical Oceanography*, **33**, 649–676.

Jaimes, B. & L. K. Shay (2009): Mixed layer cooling in mesoscale oceanic eddies during Hurricanes Katrina and Rita. *Monthly Weather Review*, **137**, 4188–4207.

Lea, A. S. & M. A. Saunders (2006): How well forecast were the 2004 and 2005 Atlantic and US hurricane seasons? Weather, **61**, 245–249.

Leipper, D. F. & D. Volgenau (1972): Hurricane heat potential of the Gulf of Mexico. *Journal of Physical Oceanography*, **2**, 218–224.

Lin, I. I., C. C. Wu, K. A. Emanuel, I. H. Lee, C. R. Wu & I. F. Pun (2005): The interaction of Supertyphoon Maemi (2003) with a warm ocean eddy. *Monthly Weather Review*, **133**, 2635–2649.

Lin, I. I., C. C. Wu, I. F. Pun & D. S. Ko (2008): Upper-ocean thermal structure and the western North Pacific Category 5 typhoons. Part I: Ocean features and the category 5 typhoons' intensification. *Monthly Weather Review*, **136**, 3288–3306.

Lin, I. I., I. F. Pun & C. C. Wu (2009): Upper-ocean thermal structure and the western North Pacific Category 5 typhoons. Part II: Dependence on translation speed. *Monthly Weather Review*, **137**, 3744–3757.

Lin, I. I., G. J. Goni, J. A. Knaff, C. Forbes & M. M. Ali (2013): Ocean heat content for tropical cyclone intensity forecasting and its impact on storm surge. *Natural Hazards*, **66**, 1481–1500.

Mainelli, M., M. DeMaria, L. K. Shay & G. Goni (2008): Application of oceanic heat content estimation to operational forecasting of recent Atlantic category 5 hurricanes. *Weather and Forecasting*, **23**, 3–16.

Mei, W., C. Pasquero & F. Primeau (2012): The effect of translation speed upon the intensity of tropical cyclones over the tropical ocean. *Geophysical Research Letters*, **39**, L07801.

Ooyama, K. (1969): Numerical simulation of the life cycle of tropical cyclones. *Journal of the Atmospheric Sciences*, **26**, 3–40.

Palmén, E. H. (1948): On the formation and structure of tropical cyclones. *Geophysica*, **3**, 26–38.

Perlroth, I. (1967): Hurricane behavior as related to oceanographic environmental conditions. Tellus, **19**, 258–&.

— (1969): Effects of oceanographic media on equatorial Atlantic hurricanes. *Bulletin of the American Meteorological Society*, **48**, 614–&.

Price, J. F. (1981): Upper ocean response to a hurricane. *Journal of Physical Oceanography*, **11**, 153–175.

Price, J. F., T. B. Sanford & G. Z. Forristall (1994): Forced stage response to a moving hurricane. *Journal of Physical Oceanography*, **24**, 233–260.

Price, J. F., R. A. Weller & R. Pinkel (1986): Diurnal cycling: Observations and models of the upper ocean response to diurnal heating, cooling, and wind mixing. *Journal of Geophysical Research: Oceans*, **91**, 8411–8427.

Sanford, T. B., P. G. Black, J. R. Haustein, J. W. Feeney, G. Z. Forristall & J. F. Price (1987): Ocean response to a hurricane. Part I: observations. *Journal of Physical Oceanography*, **17**, 2065–2083.

Seo, H. & S. P. Xie (2013): Impact of ocean warm layer thickness on the intensity of Hurricane Katrina in a regional coupled model. *Meteorology and Atmospheric Physics*, **122**, 19–32.

Shay, L. K., P. G. Black, A. J. Mariano, J. D. Hawkins & R. L. Elsberry (1992): Upper ocean response to Hurricane Gilbert. *Journal of Geophysical Research-Oceans*, **97**, 20227–20248.

Shay, L. K., G. J. Goni & P. G. Black (2000): Effects of a warm oceanic feature on Hurricane Opal. *Monthly Weather Review*, **128**, 1366–1383.

Shay, L. K. & E. W. Uhlhorn (2008): Loop Current response to Hurricanes Isidore and Lili. *Monthly Weather Review*, **136**, 3248–3274.

Strazzo, S., J. B. Elsner, J. C. Trepanier & K. A. Emanuel (2013): Frequency, intensity, and sensitivity to sea surface temperature of North Atlantic tropical cyclones in best-track and simulated data. *Journal of Advances in Modeling Earth Systems*, **5**, 500–509.

Trenberth, K. E. & D. J. Shea (2006): Atlantic hurricanes and natural variability in 2005. *Geophysical Research Letters*, **33**, 4.

Uhlhorn, E. W. & L. K. Shay (2012): Loop Current mixed layer energy response to Hurricane Lili (2002). Part I: Observations. *Journal of Physical Oceanography*, **42**, 400–419.

Virmani, J. I. & R. H. Weisberg (2006): The 2005 hurricane season: An echo of the past or a harbinger of the future? *Geophysical Research Letters*, **33**, 4.

Walker, N. D., R. R. Leben & S. Balasubramanian (2005): Hurricane-forced upwelling and chlorophyll a enhancement within cold-core cyclones in the Gulf of Mexico. *Geophysical Research Letters*, **32**, L18610.

Walker, N.D., A. Haag, S. Balasubramanian, R. R. Leben, I. V. Heerden, P. Kemp & H. Mashriqui (2006): Hurricane prediction: A century of advances. *Oceanography* **19**, 24–36.

Walker, N. D., R. R. Leben, C. T. Pilley, M. Shannon, D. C. Herndon, I. F. Pun, I. I. Lin & C. L. Gentemann (2014): Slow translation speed causes rapid collapse of northeast Pacific Hurricane Kenneth over cold core eddy. *Geophysical Research Letters*, **41**, 7595–7601.

Wentz, F. J., C. Gentemann, D. Smith & D. Chelton (2000): Satellite measurements of sea surface temperature through clouds. *Science,* **288**, 847–850.

Williams, M. N., C. A. G. Grajales & D. Kurkiewicz (2013): Assumptions of multiple regression: correcting two assumptions. *Practical Assessment, Research & Evaluation,* **18**, 11.

Wu, C. C., C. Y. Lee & I. I. Lin (2007): The effect of the ocean eddy on tropical cyclone intensity. *Journal of the Atmospheric Sciences*, **64**, 3562–3578.

Yoo, J., J. M. Collins & R. V. Rohli (2014): Tropical cyclogenesis in the Intra-Americas Sea: Hurricane Cindy (2005). *Professional Geographer,* **66**, 511–524.

— (2015): An investigation of the tropical cyclogenesis of Arlene (2005) using ERA-interim reanalysis and the WRF model simulation. *Professional Geographer,* **67**, 396–411.

APPENDIX A: WIND SPEED DATA COMPARISON

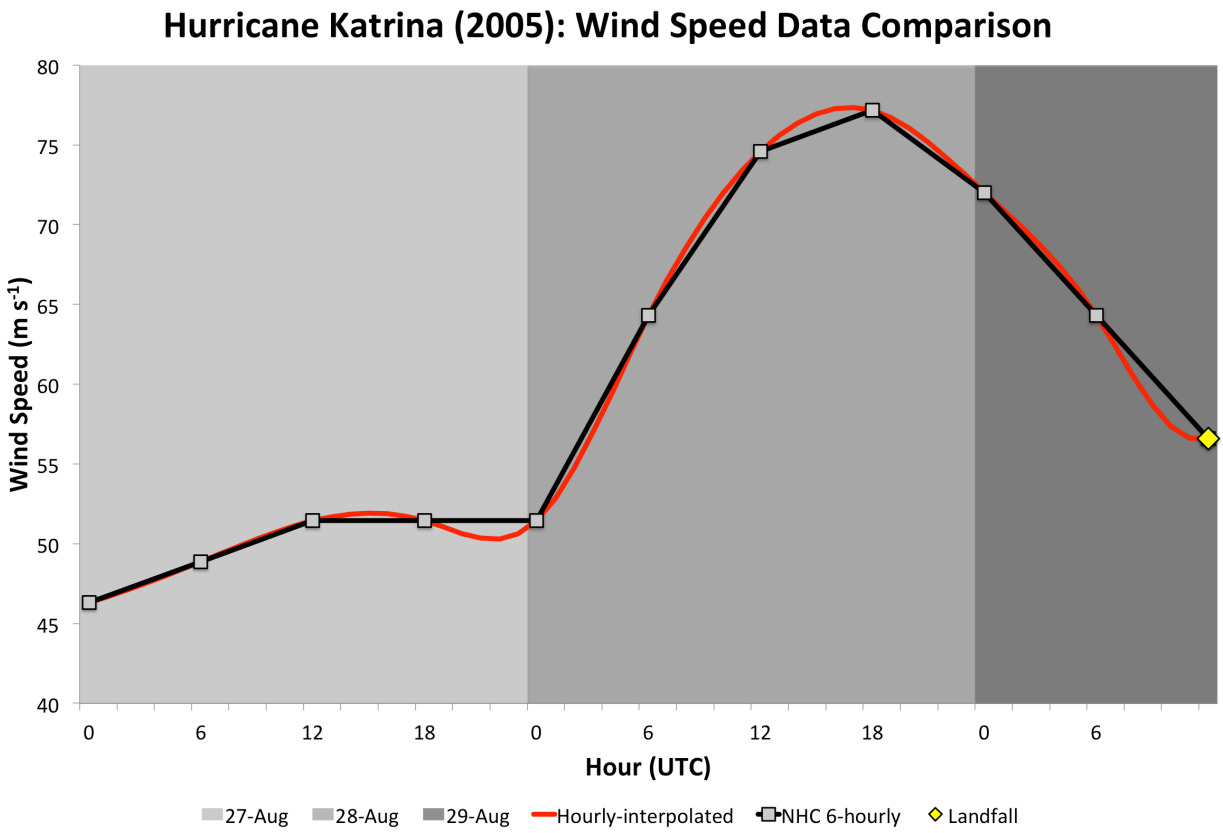

Figure A.1: Wind speed comparison between the hourly-interpolated dataset and NHC's 6-hourly dataset for 27 August – 29 August (landfall). Note the hourly-interpolated dataset appears smoothed.

APPENDIX B: MAJOR STORM INSET MASTER FIGURES

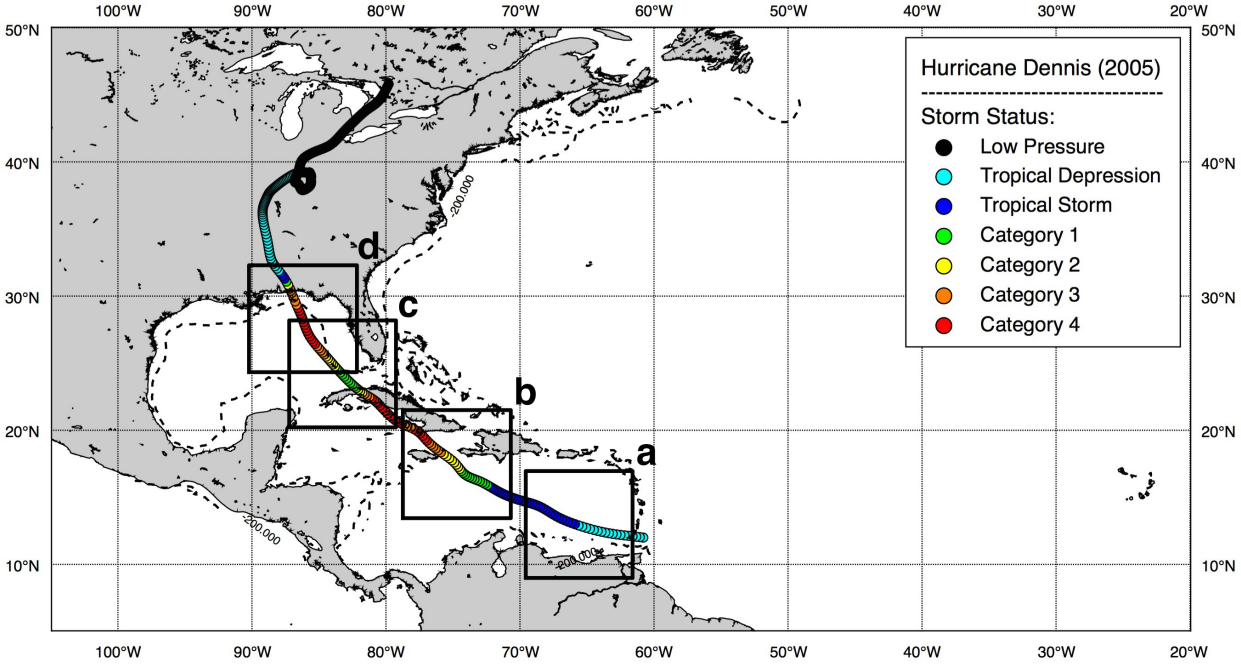

Figure B.1: Hurricane Dennis' complete track, showing inset locations corresponding to Figure 4.9.

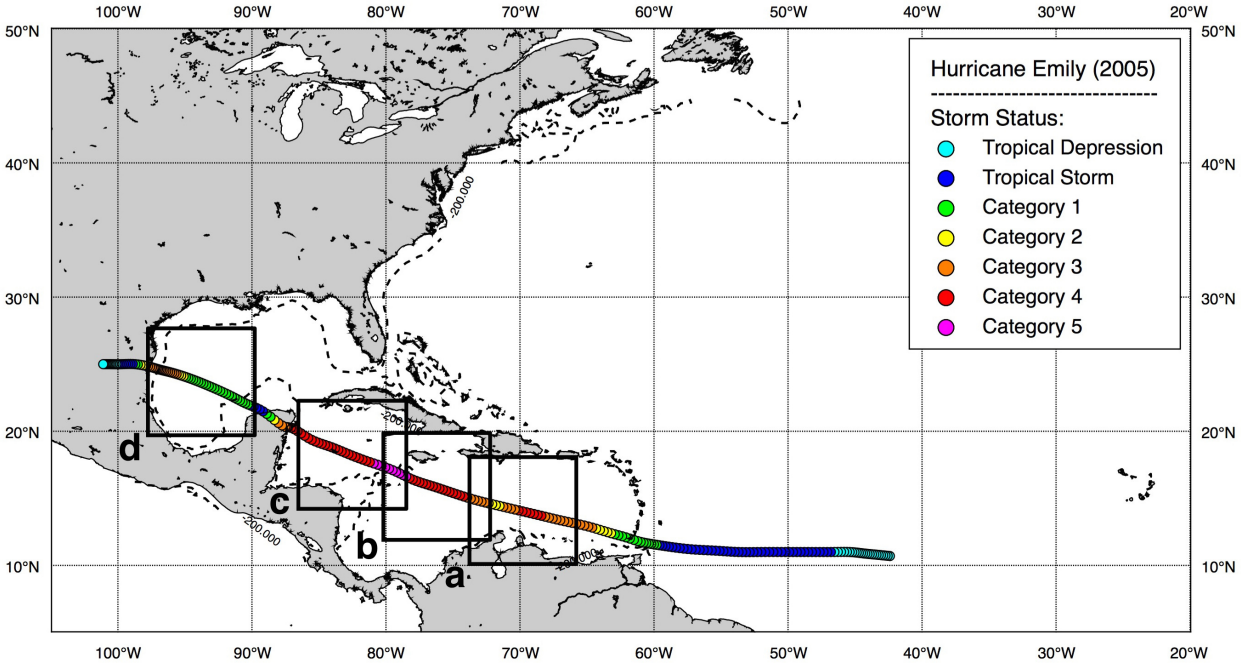

Figure B.2: Hurricane Emily's complete track, showing inset locations corresponding to Figure 4.12.

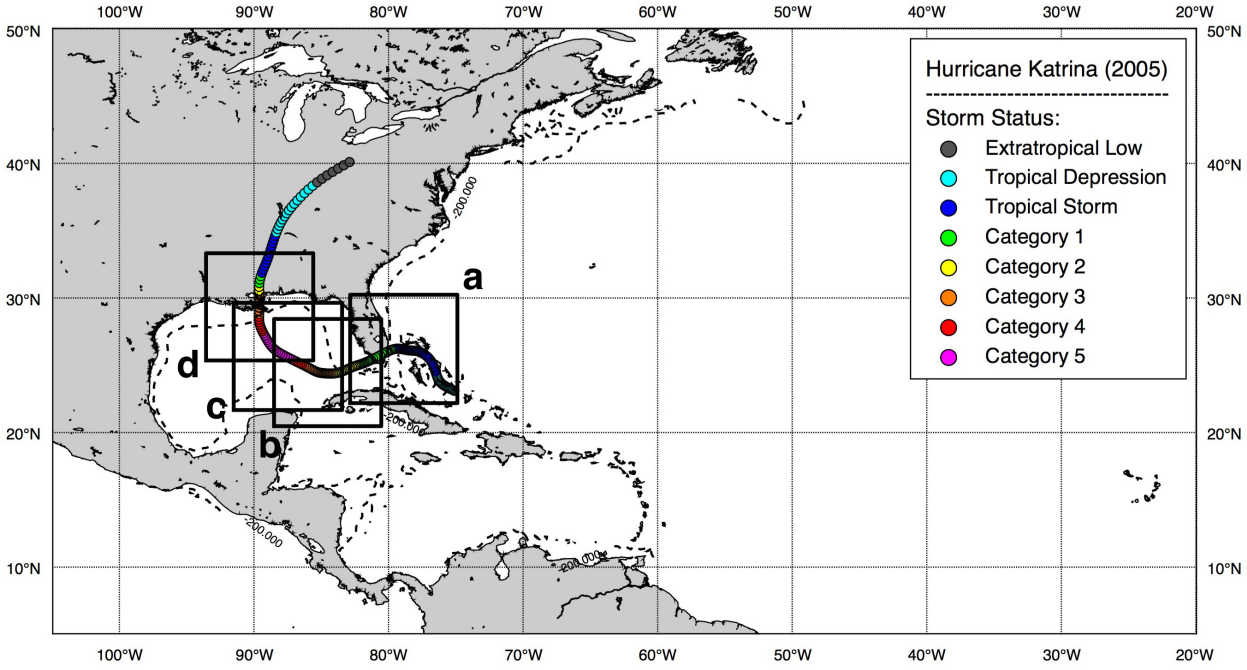

Figure B.3: Hurricane Katrina's complete track, showing inset locations corresponding to Figure 4.25.

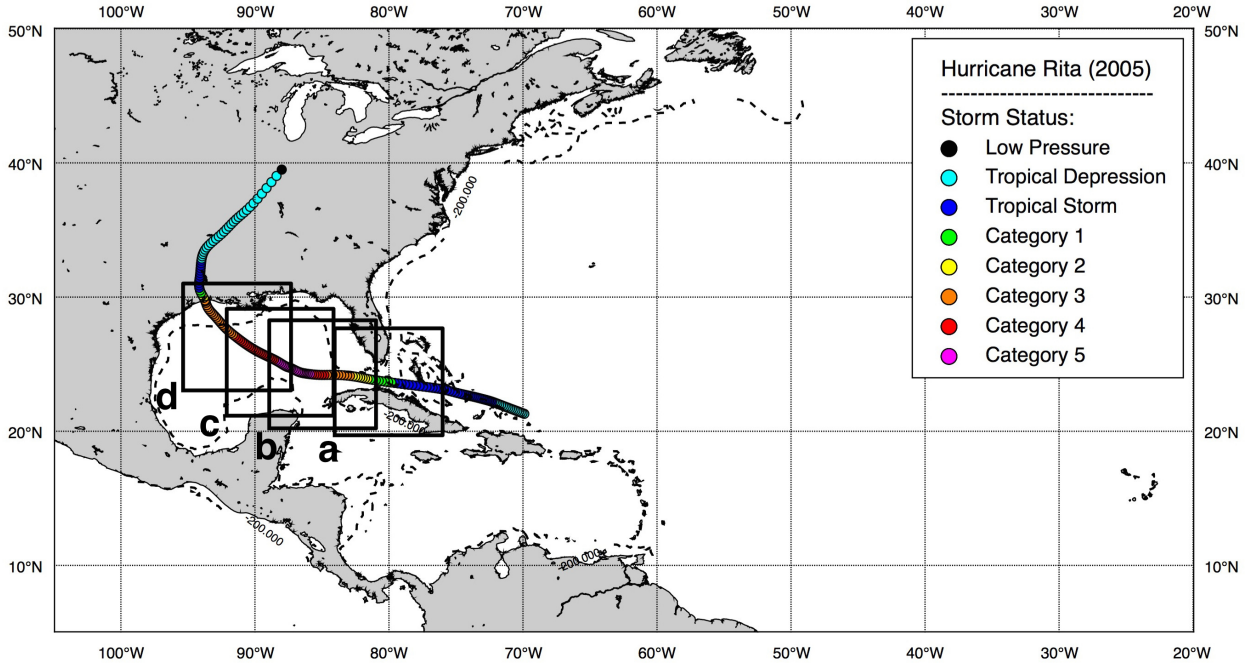

Figure B.4: Hurricane Rita's complete track, showing inset locations corresponding to Figure 4.40.

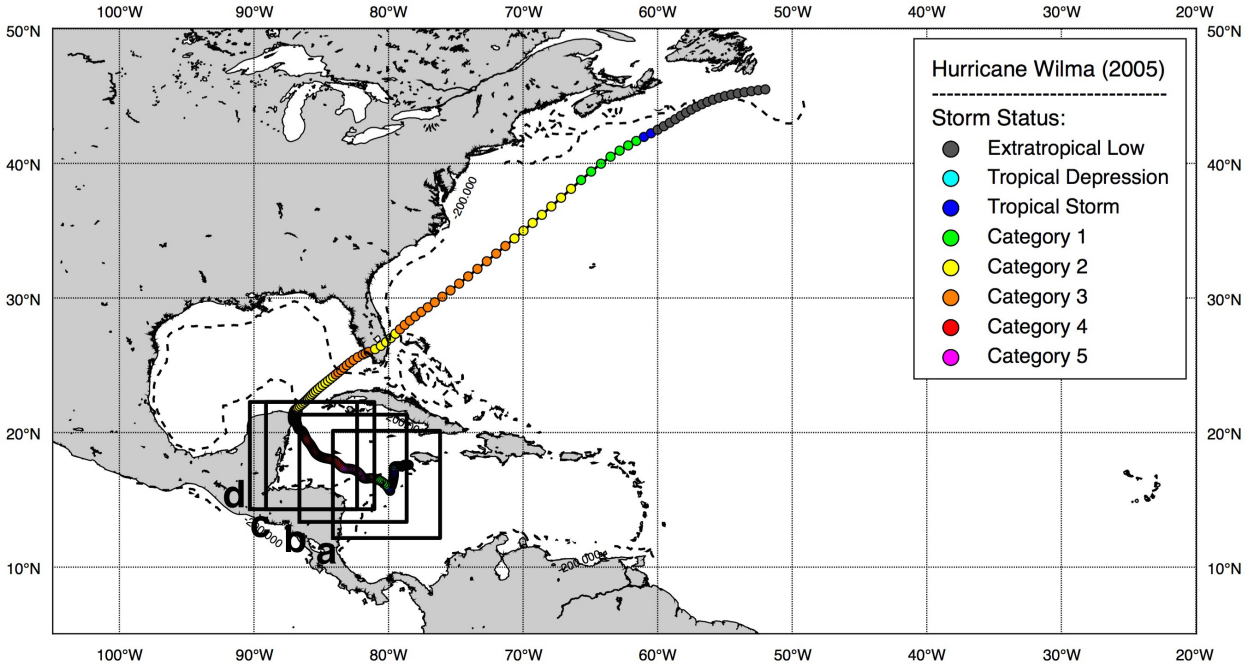

Figure B.5: Hurricane Wilma's complete track, showing inset locations corresponding to Figure 4.47.

VITA

Jordan Vick Pino was born in Baton Rouge, Louisiana, in 1991, and graduated from Catholic High School in May of 2010. He then enrolled at Louisiana State University in the Fall of 2010 in pursuit of a Bachelor of Science (B.S.) degree in the Department of Geography and Anthropology. While a sophomore, he obtained a position at the Earth Scan Laboratory on campus, where he gained research and technical skills that further enhanced his passion for weather and climate. Finishing his bachelor's degree in only three and a half years, he started his graduate studies in the Spring of 2014 in the Department of Geography and Anthropology, while continuing to work in the Earth Scan Laboratory. His research focused on air-sea interaction of tropical cyclones. He expects to graduate in December of 2015 with a Master of Science (M.S.) degree in Geography. He will then begin a Doctor of Philosophy (Ph.D.) program in Geography at Texas A&M University starting in the Spring of 2016.